

**Novel rare earth metal doped one dimensional TiO₂ nanostructures:
Fundamentals and multifunctional applications**

**Jai Prakash^{1*}, Samriti¹, Ajay Kumar², Hongliu Dai³, Bruno C. Janegitz⁴, Venkata
Krishnan², Hendrik C. Swart⁵, Shuhui Sun³**

¹Department of Chemistry, National Institute of Technology Hamirpur, Hamirpur-177005, Himachal Pradesh, India.

²School of Basic Sciences and Advanced Materials Research Center, Indian Institute of Technology Mandi, Kamand, Mandi-175075, Himachal Pradesh, India.

³Department of Energy, Materials and Telecommunications, INRS-EMT, Quebec J3X 1S2, Canada

⁴Department of Nature Sciences, Mathematics, and Education, Federal University of São Carlos, 13600-970, Araras, São Paulo, Brazil.

⁵Department of Physics, University of the Free State, Bloemfontein, ZA 9300, South Africa.

***Corresponding author:** Dr. Jai Prakash, National Institute of Technology Hamirpur, Hamirpur-177005, India. Email: jaip@nith.ac.in, Mob: +91-9910533582

Abstract

In the last few years, titanium dioxide (TiO_2) based various dimensional (0D, 1D, 2D, and 3D) nanostructures (NSs) have been extensively investigated due to their outstanding physio-chemical properties and multifunctional applications in a variety of fields, including energy, environment, biomedicine, etc. Particularly, one-dimensional (1D) TiO_2 NSs have gained much attention among researchers as these nanomaterials can be explored in various morphologies, such as nanorods, nanotubes, nanofibers, nanowires, etc. In addition to their unique 1D shape and large specific surface area, these 1D NSs show confinement in the radial direction making them more valuable as compared to other dimensional NSs. However, due to their large band gap, these NSs show inability of exploiting visible light and lower charge recombination rate becoming less efficient materials for practical applications in society. To achieve the high efficiency of these materials and to improve their visible light activity, considerable efforts have been made by narrowing the band gap through doping or nanocomposite formation with other functional nanomaterials. This review article is mainly focused on the rare-earth metal-doped 1D TiO_2 NSs with the detailed mechanism of action, improved optoelectronic properties, and their multifunctional applications in the energy and environmental fields. It includes photocatalytic (photodegradation/surface-enhanced Raman scattering detection of organic pollutants, photocatalytic CO_2 reduction, photocatalytic water splitting and upconversion based photocatalytic activities), environmental gas sensing, solar cells, supercapacitors, lithium-ion batteries applications with an emphasis on their fundamental working principles. Also, synthesis methods of rare earth metal doped 1D TiO_2 NSs, the doping effect on the microstructural and optical properties, recent advances in these directions followed by challenges and future opportunities, have been discussed.

Keywords: Rare-earth metals, 1D TiO_2 nanostructures, band gap engineering, multifunctional applications.

1. Introduction

The field of nanotechnology that deals with nanostructures (NSs) and their interfacial interaction with materials of different functionalities have encouraged the scientific community to develop nanomaterials with multifunctional applications [1-8]. To produce multifunctional nanomaterials, a great deal of research has been focused on the development of novel synthesis strategies [9-14] for controlling dimensions (size and shape) of nanomaterials which not only improve the various properties but also tailor the various surface functionalities [1, 6, 15-18]. Furthermore, recent technological advancements provide various aspects of materials modifications i.e. structural, surface, transport properties, etc. to improve their functional properties [19-27]. After the discovery of carbon nanotubes (NTs) [28], one dimensional (1D) NSs in different shapes and sizes such as nanorods (NRs), nanofibers (NFs), nanobelts (NBs), nanoribbons (NRBs), and nanowires (NWs) have gained considerable attention in various fields for basic research as well as for their potential technological applications in industries [29-35]. Particularly, 1D NSs are very promising for fabricating nanodevices due to their unique physio-chemical properties [15, 32, 34, 36, 37]. These 1D NSs are mainly preferred due to their specific geometries, shape, tunable, and large aspect ratios which are promising and provide ample opportunities to tune various properties such as morphological, electrical, structural, magnetic, optical etc. [29, 32, 35, 38, 39]. Furthermore, in addition to all these properties, due to the high surface area to volume ratio and the confinement in the radial direction, these 1D NSs exhibit attractive properties [1, 2, 34, 40].

Titanium dioxide (TiO_2) is one of the semiconductor photocatalysts which is being used in almost all fields of sciences [41-44]. It exhibits tremendous properties such as higher chemical stability, lower toxicity, better chemical resistance etc. and follows cost-effective preparation strategies for mass productions [4, 42, 45-47]. TiO_2 is the most efficient metal oxide semiconductor being used as multifunctional nanomaterials due to its unique properties including good recycle ability and high energy conversion efficiency [48-51]. However, TiO_2 is widely used as a photocatalyst and shows potential applications in other fields such as sensor, antibacterial agent, solar cell component etc. [2, 4, 38, 39, 41, 52-55]. Various TiO_2 NSs such as 0D, 1D, 2D, and 3D have been extensively studied on account of their outstanding physical and chemical properties in the last decades. Out of these 0-3D NSs, 1D TiO_2 NSs have gained considerable attention as these

can be explored in various morphologies such as NRs, NFs, NBs, NWs, NRbs, NTs etc. and have been implemented in many fields including energy, environmental remediation and biomedical etc. [34, 38, 39, 56-59]. In addition to the unique 1D geometry, large specific surface area and high crystallinity, these 1D NSs show confinement in the radial direction which makes them more valuable as compared to other dimensional NSs [39, 60, 61]. These different morphologies of 1D TiO₂ NSs have different abilities for a particular application. For example, TiO₂ NFs are promising for photocatalytic degradation of dye molecules [62]. Shao et al. [63] studied the effect of arrays of various 1D TiO₂ NSs such as NRs, NBs and other kinds of rod-like NSs on the performance of dye-sensitized solar cells (DSSCs). It was found that maximum power conversion efficiency (PCE) was achieved for NRs based DSSCs devices. Similarly, TiO₂ NBs are very promising for multifunctional applications such as photoelectric, photocatalytic and sensing applications [35, 64].

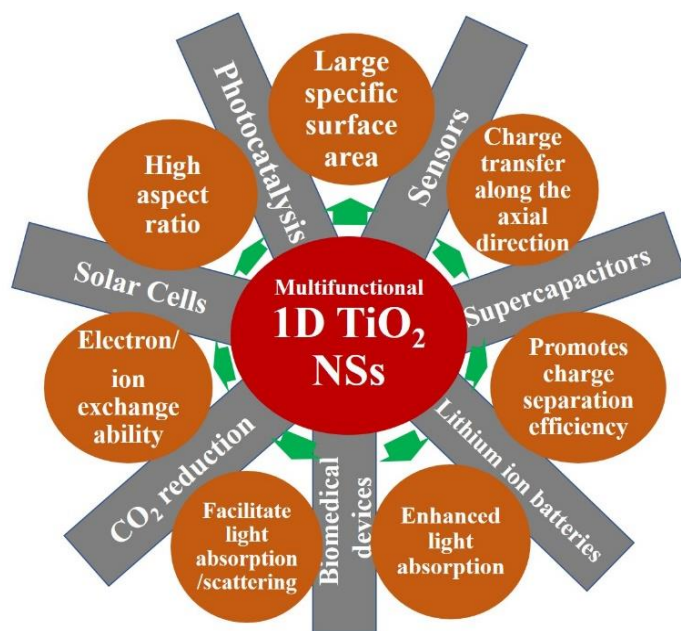


Figure 1. Properties and multifunctional applications of 1D TiO₂ NSs.

Several research papers reveal that tailoring morphology, size, and shape of 1D TiO₂ NSs, their optoelectronic as well as surface properties, and hence multifunctionality can be tuned into several directions. 1D TiO₂ NSs show many fascinating properties and enhanced functional activities as compared to the pure TiO₂ nanoparticles with a potential to be applied in several fields shown in **Figure 1**. However, these 1D TiO₂ NSs still show some disadvantages such as wide band

gap, higher electrons, and holes combination rate, slow charge carrier transfer, visible light inactivity, etc. which restrict their proper implementation as visible light active and multifunctional materials in the field of solar energy technology [42, 65, 66] and environment remediation [15, 43, 48, 56]. The reason is that TiO_2 has a wide band gap of 3.2 eV and can be activated by UV radiation only while remains inactive under visible light radiation [4, 43, 46, 51, 67]. TiO_2 gives low quantum yield as a result of the fast recombination of electrons and holes in its normal form. Also, the sunlight contains hardly 5% of UV radiation that makes TiO_2 based nanomaterials less efficient under solar radiation [4, 15, 68]. These characteristics of TiO_2 NSs need to be improved for the proper utilization of 1D TiO_2 NSs for their real practical application. It could provide better performance to the functional properties of these NSs in addition to their novel properties due to their special 1D geometry and different morphologies [7].

In recent years, extensive research has been carried out to overcome the drawbacks of TiO_2 which make it unsuitable for solar energy harnessing through the development of novel preparation techniques and materials modifications using several physical and chemical routes. The modifications which have been carried out to improve the functional properties of 1D TiO_2 NSs for several applications include surface functionalization, doping, composite formation with metals, semiconductors, 2D functional materials, dye sensitization etc. [4, 38, 68-76]. These modifications not only enhance their optoelectronic properties by absorption of visible light radiation but also reduce the recombination of photo-generated charge carriers along with improvement in their structural, electrical, surface and intrinsic properties suitable for various applications in the field of energy and environmental applications.

Among these various strategies, doping is one of the most studied and simple way to modify the structural, intrinsic and surface properties of TiO_2 NSs for such applications [77-82]. For example, Li et al. [78] performed a systematic study on doping TiO_2 with metal and non-metal ions using Gd, F and N ions for high-performance photocatalytic activities. It was reported that there was an excellent enhancement in the photodegradation of dye molecules that was attributed to the doping-induced higher surface area, narrowing of band gap and creation of defects and oxygen vacancies. Gd co-doping played a major role in the improvement of structural and optoelectronic properties and achieving higher photocatalytic efficiency. Doping of rare-earth (RE) metal ions into TiO_2 shows great potential to improve the photocatalytic activity by efficiently utilizing the broad region of the solar spectrum (UV to NIR) in addition to their activity

under UV light [48, 83, 84]. For example, Song et al. [85] demonstrated the excellent and enhanced photocatalytic activities of RE doped TiO₂ NRs as compared to the undoped TiO₂ NRs and commercial TiO₂ nanoparticles. Similarly, RE doped TiO₂ based methanol sensor has also been developed which showed better optoelectronic properties and selective response due to RE doping [86]. Keskin et al. [84] performed the comparative study of morphological, structural and optical properties of Ce and N doped 1D TiO₂ based NSs and found that Ce doping is more prominent for the improvement of optical and photocatalytic properties. Similarly, RE doped TiO₂ NSs were studied for various photocatalytic applications such as photocatalytic CO₂ reduction [87, 88], photocatalytic water splitting [67, 89] and upconversion based photocatalyst activities [90]. Furthermore, doping with RE metal ions into TiO₂ provides better transport properties useful in solar cell devices [58, 91-94]. Akman et al. [91] studied the RE doped TiO₂ and its role in improving photovoltaic properties of dye-sensitized solar cells (DSSCs). They synthesized Eu and Tb co-doped TiO₂ and studied interfacial charge transfer which was found to be superior providing higher efficiency as compared to individual RE doped TiO₂ as well as undoped TiO₂. Similarly, Wang et al. [94] studied the Er and Yb RE co-doped TiO₂ NRs as an electron transport layer in perovskite solar cells. The solar cell device exhibited enhanced conversion efficiency as compared to the device made of only NRs due to doping induced visible and infrared light driven activities along with improved current density. Similarly, various RE metals have been used for doping TiO₂ NSs for improved photovoltaic properties and harnessing solar energy for various energy applications. RE doping in metal oxides has also been used for improving the luminescence properties of these materials. The f-f electronic transitions within the partially filled 4f orbitals of RE metal ions result in luminescence properties [95, 96]. The shielding of 4f orbitals by the filled 5s and 5p orbitals results in narrow transition emission bands without any perturbation [48, 91, 97]. Due to this unique phenomenon of RE metal ions, they are also useful for various other potential energy applications.

Although researched extensively, TiO₂ nanomaterials with short and long-term multifunctional activities in various fields of energy and environment have rarely been reviewed because of the synergic effect including their 1D geometry and doping effect using RE metals. In this review article, the synthesis, modification, and engineering of 1D TiO₂ NSs through RE metal ion doping along with their enhanced properties and multifunctional applications in various fields of energy and environment have been addressed. A brief introduction of various 1D TiO₂ NSs and

their properties/characteristics are followed by the introduction of RE metals and their doping mechanism. Various synthesis methods along with the recent advancement in the synthesis processes of 1D TiO₂ NSs have been discussed in detail. Various applications of RE metal ions doped 1D TiO₂ NSs in the field of energy and environment such as photocatalytic degradation/ultrasensitive detection of organic pollutants, photocatalytic CO₂ reduction, photocatalytic water splitting, solar cells, supercapacitors, environmental gas sensing, lithium-ion batteries, etc. have been discussed with an emphasis on their fundamental mechanisms. Furthermore, recent advances in these directions followed by challenges and future opportunities, have been discussed.

2. Characteristics of 1D TiO₂ NSs

TiO₂ is mainly found in three different forms i.e. anatase, rutile, and brookite. Anatase and rutile forms both have tetragonal crystal structures whereas brookite has orthorhombic crystal structures (**Figure 2 A**) [98]. In all these forms of TiO₂, Ti cations are coordinated to six O anions and form a distorted TiO₆ octahedron with the different spatial arrangement of these building blocks. The research shows that rutile form is most thermodynamically stable in bulk whereas, at nanoscale both anatase and brookite are known to be more stable. Out of these different forms, anatase is mainly used in photocatalysis, and rutile form is mainly used in the paint industry [1, 4, 29, 98]. The wide band gap this semiconductor restricts its functional activities beyond the UV region [4]. TiO₂ in nanoscale shows better functionality as compared to the bulk TiO₂ material due to its enhanced surface area and broadened band gap which leads to improved functionality as a result of enhanced active sites on the surface [38, 98]. It has also been reported that at the nanoscale, 0D spherical TiO₂ nanoparticles are not much influenced in terms of their multifunctional applications due to large interfacial area slowing down the transport of the charge carriers, wide band gap limiting their applications under sun light radiation and also resulting in fast recombination of photo-generated charge carriers. Furthermore, these nanoparticles are difficult to recycle especially during the photocatalytic applications in water treatment and give rise to water pollution indirectly [1, 52, 98, 99].

Among various TiO₂ NSs, 1D TiO₂ NSs have a high aspect ratio, large specific surface area, the shorter distance for electrons and holes diffusion, enhanced light adsorption, enhanced light scattering properties, specific interface effect excellent electronic or ionic charge transport

properties, etc. [56, 61, 100]. 1D TiO₂ NSs exist in different morphologies which results in different properties of the material. 1D TiO₂ exists majorly in the form of NRs, NTs, NFs, NBs, NRbs, NWs, etc. as shown in **Figure 2B**. **Figure 2B** shows the secondary electron microscopy (SEM) images of various 1D TiO₂ NSs. Most commonly used 1D NSs are solid except NTs which are hollow structures. NFs are the kind of NSs which possess two dimensions in the nm range with another as a longer dimension. If we look at the geometry of all the solid 1D NSs, all these are types of NFs and only the difference is that of their aspect ratio [87]. NRs are with length sizes ranging between 1-100 nm and an aspect ratio of around 3-4. NRs are found to be thermally stable and are similar to NTs except for not having an internal surface [65, 101]. This is true for all the solid 1D NSs that these are lacking hollow-core [102]. NRs have a smaller length than NWs which are of micron lengths with an aspect ratio of 1000 or more [103]. Apart from these NSs, NBs, and NRbs are similar to NWs but these are wide with a width of 30-500 nm. They show a high aspect ratio and their ends are rolled and are thinner [103].

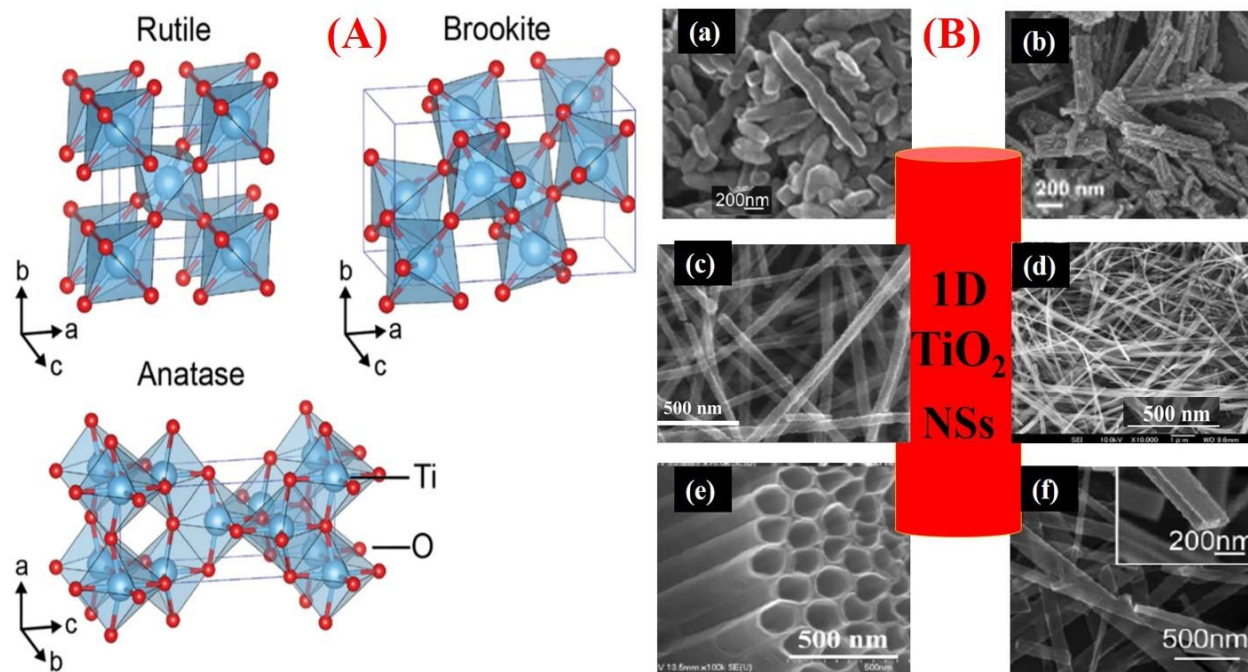


Figure 2. (A) Crystal structures of different forms of TiO₂: rutile and anatase (tetragonal, P4₂/mmm), and brookite (orthorhombic) polymorphs. **Permission is required from [98].** (B) SEM images of various 1D TiO₂ NSs: (a) NRs **Permission is required from [104]** (b) NRbs **Permission is required from [105]** (c) NFs [2] (d) NWs **Permission is required from [106]** (e) NTs **Permission is required from [107]** (f) NBs **Permission is required from [108]**.

1D TiO₂ NSs have shown to be very advantageous for the photocatalytic and other functional activities as a result of larger surface area due to the 1D geometry as compared to their bulk providing more reaction sites, reduced electrons, and holes recombination rate [62]. Furthermore, the 1D geometry facilitates a high interfacial charge carrier transfer rate and promotes charge separation efficiency due to the shorter distance for the diffusion of these carriers [29, 62]. Rosales et al. [62] demonstrated the photochemical performances of various 1D TiO₂ NSs and reported that TiO₂ NFs showed a better response in terms of reactive oxygen species (ROS) generation and also observed the following trend, NFs > NT s > NRs > NWs. Similarly, 2D NSs have a high aspect ratio, high adhesion to substrates, smooth surfaces and show low turbidity and exhibit great potential as self-cleaning surfaces and surface functionality. However, the synthesis of 2D NSs is complex and requires harsh experimental conditions [99]. 1D TiO₂ NSs are promising as energy transport nanomaterials due to their ability to conduct the quantum particles (photons, phonons, and electrons) as a result of their large aspect ratio and this transportation is very much influenced by the 1D geometry [1, 40, 60]. Similarly, 1D TiO₂ NSs are promising in several fields as multifunctional nanomaterials.

As discussed in the last sections, despite having several good characteristics, some factors limit the wider and potential applications of 1D TiO₂ NSs in several fields. Literature indicates that for making these 1D TiO₂ NSs more promising for various applications and further improvement of their properties, several kinds of modifications, particularly rare-earth metal doping strategy have extensively been carried out resulting in improved properties and functionality. For example, Zeng et al. [109] performed a comparative study of La-doped 0D TiO₂ nanospheres and 1D TiO₂ NBs for their structural and sensing properties and found that these properties could be improved by tailoring the shape of the NSs by introducing TiO₂ NBs and further by doping with La. Similarly, Singh et al. [2] studied Ta doped TiO₂ NFs to demonstrate that doping improves the dual functional properties of photocatalytic degradation and ultrasensitive detection of organic dye molecules as compared to undoped TiO₂ NFs. Also, Hassan et al. [110] performed the effect of doping of La, Ce, and Nd in 1D TiO₂ NSs for photocatalytic dye degradation and found that doping prevented the phase transformation at a higher temperature from anatase to rutile. This could be beneficial for photocatalytic activities as it is eminent that the anatase phase is more active than the rutile phase. RE metal doping also decreased the band gap along with the recombination rate of charge carriers leading to enhanced photocatalytic activity

particularly with Nd-doped TiO₂ as compared to undoped one. This review article is mainly focused on such doping effects with RE metals into 1D TiO₂ NSs and their multifunctional applications. The details of doping and its mechanism have been discussed in detail in the next section.

3. RE metal doping of 1D TiO₂ NSs: Fundamentals and mechanism

As discussed above, TiO₂ based NSs are required to modify due to their wide band gap energy, fast recombination of photo-generated charge carriers, and low efficiency of their separation because of their potential applications in a variety of fields. There have been many efforts including coupling with functional materials, sensitization, and doping to reduce the band gap and to increase the charge carrier separation efficiency of TiO₂ NSs. Interestingly, doping is one of the most extensively used methods to achieve these goals among others using several metals (transition or noble or RE metals) or non-metals [29, 41, 111-115]. Extensive research has been carried out in the last few years to improve or modify the optical, electrical, structural, surface, and interface properties of 1D TiO₂ NSs by doping with RE metals.

(A)

1																	18				
1																	2				
H																	He				
1.01																	4.00				
3	2															13	14	15	16	17	18
Li	Be															B	C	N	O	F	Ne
6.94	9.01															10.81	12.01	14.01	16.00	19.00	20.18
11	12															13	14	15	16	17	18
Na	Mg															Al	Si	P	S	Cl	Ar
22.99	24.31															26.98	28.09	30.97	32.07	35.45	39.95
19	20	3	4	5	6	7	8	9	10	11	12	12	31	32	33	34	35	36			
K	Ca	Sc	Ti	V	Cr	Mn	Fe	Co	Ni	Cu	Zn	Ga	Ge	As	Se	Br	Kr				
39.10	40.08	44.96	47.87	50.94	51.99	54.94	55.85	58.93	58.69	63.55	65.38	69.72	72.63	74.92	78.97	79.90	84.00				
37	38	39	40	41	42	43	44	45	46	47	48	49	50	51	52	53	54				
Rb	Sr	Y	Zr	Nb	Mo	Tc	Ru	Rh	Pd	Ag	Cd	In	Sn	Sb	Te	I	Xe				
84.47	87.62	88.91	91.22	92.91	95.95	98.91	101.07	102.91	106.42	107.87	112.41	114.82	118.71	121.76	127.6	126.90	131.25				
55	56	57-71	72	73	74	75	76	77	78	79	80	81	82	83	84	85	86				
Cs	Ba		Hf	Ta	W	Re	Os	Ir	Pt	Au	Hg	Tl	Pb	Bi	Po	At	Rn				
132.91	137.33		178.49	180.95	183.84	186.21	190.23	192.22	195.09	196.97	200.59	204.38	207.2	208.98	[208.98]	209.99	222.02				
87	88	89-103	104	105	106	107	108	109	110	111	112	113	114	115	116	117	118				
Fr	Ra		Rf	Db	Sg	Bh	Hs	Mt	Ds	Rg	Cn	Uut	Fl	Uup	Lv	Uus	Uuo				
223.02	226.03		[261]	[262]	[266]	[264]	[269]	[268]	[269]	[272]	[277]	unknown	[289]	unknown	[298]	unknown	unknown				

Lanthanide series														
57	58	59	60	61	62	63	64	65	66	67	68	69	70	71
La	Ce	Pr	Nd	Pm	Sm	Eu	Gd	Tb	Dy	Ho	Er	Tm	Yb	Lu
138.91	140.12	140.91	144.24	144.91	150.36	151.96	157.25	158.93	162.50	164.93	167.26	168.93	173.06	174.97
89	90	91	92	93	94	95	96	97	98	99	100	101	102	103
Ac	Th	Pa	U	Np	Pu	Am	Cm	Bk	Cf	Es	Fm	Md	No	Lr
227.03	232.04	231.04	238.03	237.05	244.06	243.06	247.07	247.07	251.08	[254]	257.10	258.1	259.10	[262]

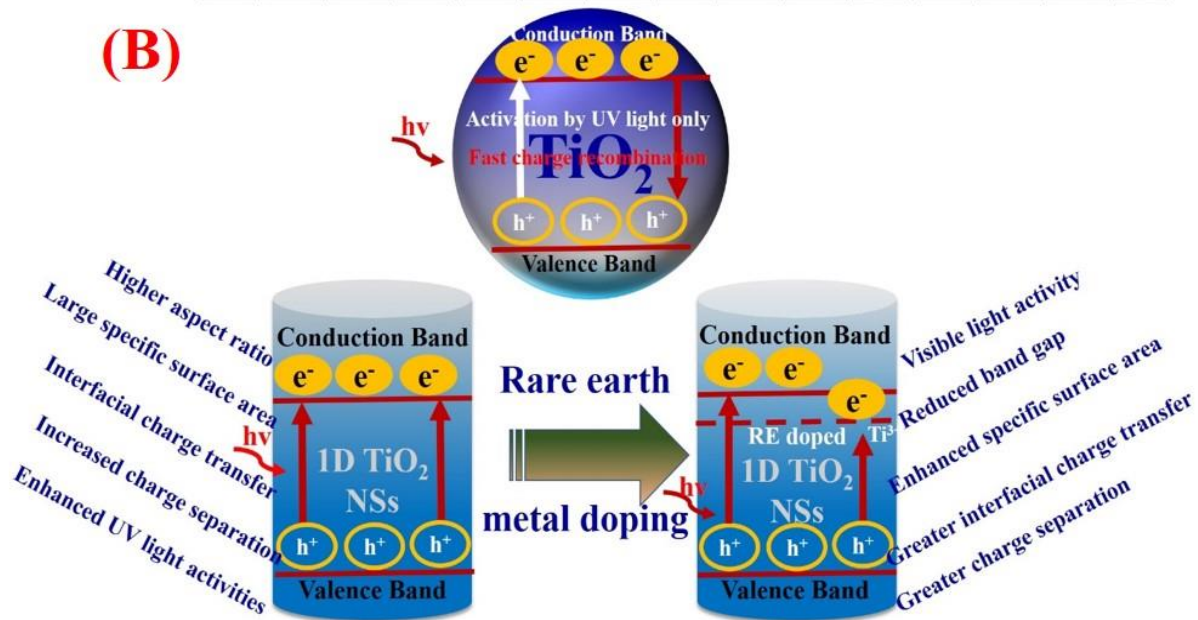


Figure 3. (A) Position of RE elements (in blue color) in periodic table. Titanium and oxygen are shown in green color. (B) Improved properties of 1D TiO₂ NSs as compared to 0D TiO₂ NSs and RE doping mechanism with further improvements in the properties of TiO₂ 1D NSs.

There are 15 lanthanide elements ranging from atomic number 57 (lanthanum) to 71 (lutetium) as shown in **Figure 3A**. Since scandium and yttrium are showing similar chemical behavior as lanthanides, thus they may also be considered under RE elements. Here, we have

discussed the fundamentals and mechanism of doping TiO₂ nanocrystals with RE metals leading to the improved optoelectronic and photocatalytic properties for multifunctional applications. **Figure 3B** shows modifications and improvements of various properties of TiO₂ NSs due to RE metal ions doping. The RE metals have the involvement of 4f, 5d, and 6s states and these are the ideal dopants for the modification of the optical, electrical and structural properties of semiconductor nanomaterials [110, 116]. RE metal doping is very beneficial for TiO₂ based semiconductor NSs because of visible light activity with improved photonic efficiencies [29]. These metals are very promising dopants for TiO₂ NSs because of the enhancement of their optical absorption properties and thermal stability of the anatase to rutile phase transformation [73].

Doping is a process of the addition of impurities into the crystal lattice of a host semiconductor material which results in the modification of its optical, electrical, and structural properties. Doping with RE metal ions creates additional energy levels into the band structure of TiO₂. These additional energy levels in between the conduction band (CB) and valence band (VB) are mainly used to trap the charge carriers to separate them from the bands and facilitate their diffusion towards the surface for the various processes to occur on the surface of the TiO₂ (**Figure 3B**) [2, 4]. These sub-energy band gap levels which are formed leads to the red shift in their absorption spectra and reduce the band gap energy of the materials promoting the visible light absorption. Interestingly, the reduction in band gap energy could be tuned by varying the dopants and their concentrations [2, 117]. Along with the concentration of the dopants, the ionic radius of the dopants is also an important factor that decides the position of the dopant within the crystal lattice of TiO₂ [22, 118, 119].

In the case of RE metal ion doping in TiO₂ based NSs, there are many possibilities for dopants to be incorporated within the crystal lattice or accumulated on the surface. These dopants may occupy the interstitial site of the TiO₂ lattice or substitutional doping may occur or it can form an oxide layer on the surface [29, 61]. Generally, substitutional or interstitial doping occurs if the ionic size of the dopant ions is equal or smaller to the ionic size of Ti⁴⁺ in TiO₂ respectively. On the other hand, when the ionic radius of the dopant is larger, the dopant ions form their oxide layers on the surface of TiO₂ NSs [29]. It mainly affects the growth and structural properties of the 1D TiO₂ NSs leading to several advantages to the doped semiconductor photocatalysts. Since, the RE metal ions are of a larger ionic radius as compared to that of the Ti⁴⁺, in the case of RE metal ion doping in TiO₂ NSs, an oxide layer formation is expected [29, 120]. However, each type of doping

feature involving substitutional, interstitial, and oxide layer formation on the surface has been reported in the case of RE metal doping in 1D TiO₂ NSs depending on the various experimental conditions as discussed in detail below. These doping effects are attributed to the presence of 4f states of RE metal ions in the bandgap of TiO₂ through charge transfer between 4f states and CB or VB of TiO₂ [68, 113, 120, 121]. Here, we provide a brief about the doping of various RE metals in 1D TiO₂ nanostructures and the involved mechanisms of their distribution.

3.1 Doping with RE metals in 1D TiO₂ NSs

As shown in figure 3A and discussed above, there are several RE metals listed in the periodic table. Some of the RE metals have been extensively used as dopants for doping various TiO₂ NSs and have shown promising results in improving optoelectronic, structural, surface, and photocatalytic properties. Doping of various RE metals in TiO₂ NSs is discussed herewith in details:

3.1.1 La doping in 1D TiO₂ NSs

La is the most widely used RE metal for doping TiO₂ NSs to improve their properties for a wide range of applications in the field of energy and environment. La³⁺ ions have an ionic radius of 1.15 Å that is larger than the ionic radius of Ti⁴⁺ (i.e. 0.68 Å). Because of its larger ionic radius, there is more possibility that La³⁺ will not enter into the lattice of TiO₂ [122-124]. Meksi et al. [122] studied La doping in TiO₂ NRs and NTs was given doping effect on the structural growth of 1D TiO₂ NSs. It was concluded that doping of La into TiO₂ lattice had no evidence and no effect on the morphology of 1D TiO₂ NSs but it prevented the phase transition of TiO₂ from anatase to rutile and crystal growth even at a higher post-annealing temperature [123]. Even though, there was no formation of any oxide layer as evidenced from x-ray diffraction (XRD) data. Furthermore, it was found that La was dispersed over the surface of the NSs which significantly enhanced the lifetime of photo-generated charge carriers through the maintaining of smaller anatase crystalline domains and creating oxygen vacancies limiting the volume recombination rate [122]. In most such cases when there is no doping evidence of La ions into TiO₂ lattice, it has been found that La forms a very thin oxide layer on the surface. Whereas, at the interface between the oxide layer and TiO₂, there is a substitution of La³⁺ ions by Ti⁴⁺ in the lattice of the oxide layer leading to the formation of chemical bonds *i.e.* Ti-O-La [61, 123, 124]. For example, Wu et al. [61] reported La

doping in TiO₂ NTs wherein La³⁺ formed nanoclusters of La₂O₃ over the surface of NTs attributed to the Ti-O-La bond formation and La substitution by Ti ions in La₂O₃ formed at the interface. The RE metal doping produces charge imbalance, oxygen defects and Ti³⁺ species (Figure 3B) leading to the bandgap reduction and enhanced visible-light photocatalytic activity. On the other hand, contrary to the results shown by Meksi et al. [122] and Wu et al. [61], a few results are demonstrating the introduction of La into the TiO₂ lattice during the formation process and influenced the TiO₂ lattice parameters and cell volume resulting in the structural defects [61, 125, 126]. However, this is the case only when a very little amount of doping is taken place and when doping is increased, there is a formation oxide layer on the surface at the higher doping concentration [125]. Sadhu et al. [126] studied the growth of La doped TiO₂ NRs and demonstrated that even though XRD did not exhibit any signature of oxide formation or doping La into TiO₂ lattice due to mismatch of ionic radius of La³⁺ and Ti⁴⁺, scanning transmission electron microscopy (STEM) showed the homogeneous distribution of La ions into TiO₂ NRs. However, the reason was not very clear. There was an insufficient change in the shape of absorption and photoluminescence spectra of doped TiO₂ NRs except for a little enhancement in the visible light activities and optoelectronic properties. It is expected that due to the size variation of their ionic radius (La³⁺ and Ti⁴⁺), there may be the possibility of doping of La³⁺ ions interstitially into TiO₂ lattice [127]. Similarly, Rajabi et al. [128] reported very recently on the La³⁺ doping in TiO₂ lattice as evidenced through the distortion in XRD peaks. The La³⁺ doping in TiO₂ NRs improved the nonlinear optical properties of NRs exhibiting a potential application of 1D TiO₂ NSs in nonlinear optical device applications.

3.1.2 Ce doping in 1D TiO₂ NSs

Ce is another widely used RE metal for doping TiO₂ NSs and emerges as a promising dopant for improving their optoelectronic properties for many applications. Ce has a unique electronic structure that makes it special for doping TiO₂ NSs *i.e.* different electronic structures of 4f states. Unlike other RE metal ions, Ce ions exist in two redox states Ce³⁺ and Ce⁴⁺ with electronic structures 4f¹5d⁰ and 4f⁰5d⁰, respectively. Similarly, the ionic radius of Ce³⁺ and Ce⁴⁺ ions is 1.03 Å and 0.93 Å, respectively [129, 130]. As similar to La³⁺ ion doping in TiO₂ lattice, doping of Ce ions into TiO₂ crystal lattice is also difficult due to larger ionic size as Ce³⁺ and Ce⁴⁺ ions as compared to Ti⁴⁺ in TiO₂ lattice [130-132]. Therefore, Ce ions also do not enter into the

TiO₂ lattice to form stable solid solutions ruling out the possibility of substitutional or interstitial doping. Generally, Ce ions spread over the surface of the TiO₂ NSs and tend to bond to the oxygen anion on the surface forming a bond like Ce-O-Ti at the interface between Ce and TiO₂ [132]. Another possibility of Ce ions is to form an oxide layer CeO₂/Ce₂O₃ over TiO₂ surface which facilitates the migration of Ti⁴⁺ ions into the lattice of the oxide layer and substitution of Ce ions take place by Ti⁴⁺ ions as size of Ti⁴⁺ ions is less than that of Ce ions. Most of the literature has reported the formation of oxide layer CeO₂/Ce₂O₃ on the surface of TiO₂ NSs that facilitate the diffusion of ions as discussed above [130, 132, 133]. This is the best-accepted mechanism provided in the literature for the Ce doping in TiO₂ NSs leading to the suppression of the crystal growth and phase transformation. However, there are only a few reports which demonstrate the interstitial doping in the TiO₂ lattice of Ce ions. For example, Sun et al. [129] and Li et al. [131] proposed that a little amount of the Ce³⁺ ions were possibly localized in the octahedral interstitial site of Ce doped-TiO₂ NTs based on energy-dispersive x-ray spectroscopic (EDS) and X-ray photoelectron spectroscopic (XPS) analyses.

3.1.3 Eu doping in 1D TiO₂ NSs

Eu is another important dopant for TiO₂ based 1D NSs for improving optical, structural, and photocatalytic properties. One of its special features is that it is a very suitable dopant for upconversion or luminescent materials and is widely used in lasers, light-emitting diodes, solar cells, etc. along with photocatalysis [134-136]. Unlike other RE metals, extensive research has been carried on in the literature exhibiting the doping of Eu³⁺ ions in the lattice of TiO₂ nanocrystals. It has been found that some of Eu³⁺ ions may replace or occupy the interstitial site in the TiO₂ lattice irrespective of the size difference (ionic radius of Eu³⁺ = 0.95 Å) with Ti⁴⁺ and causes distortion in the TiO₂ lattice [137-140]. For example, Li et al. [96, 137] studied the synthesis of Eu doped TiO₂ NTs, NBs for enhanced optical properties mainly the luminescent properties. It was observed that there was a little shift in the main characteristics peak of TiO₂ towards the lower angle side due to the substitution of Eu with Ti ions. Similarly, Eu doping also restricts the phase transformation and decreases the crystallite size by the formation of Eu-O-Ti bond. Experimental evidence through the luminescence spectra of Eu doped TiO₂ NSs were proposed that certified the presence of Eu ions into TiO₂ lattice [136, 141]. Bianco et al. [136] studied the mechanism of Eu doping in NFs and confirmed the uniform distribution of Eu³⁺ ions in lattice of TiO₂ NFs with the

detection of new phase $\text{Eu}_2\text{Ti}_2\text{O}_7$ by Fourier transform infrared spectroscopy (FTIR), EDX and XRD analyses. These Eu-TiO₂ NFs exhibited strong luminescence of Eu^{3+} ions due to the notable distortion within the crystal due to incorporation of Eu ions. More details on Eu doping in 1D TiO₂ NSs are given in the further sections on the mechanism and upconversion or luminescent-based applications.

3.1.4 Er doping in 1D TiO₂ NSs

Er has been mostly used for TiO₂ based optical materials [142-145] but recently Er doped TiO₂ NSs have been considered in many other directions mainly in photocatalytic activities [143, 146-149]. It has been reported that Er-doped TiO₂ NSs show typical absorption peaks in the visible region such as at 490 nm, 523 nm, and 654 nm, which is attributed to the transition of 4f electrons [146-148]. It has been reported that Er doping causes improvement in the structural and optical properties of 1D TiO₂ which is mainly effective for photocatalytic degradation of organic molecules [146]. In most of the studies, substitutional doping has been achieved, for example, as in the case of Er^{3+} -TiO₂ NFs, replacement of Ti^{4+} ions by Er^{3+} ions into TiO₂ lattice has been reported resulting in the distortion, the expansion of crystal lattice, and the charge imbalance [148]. Similar to other RE metal ions doping, Er-O-Ti bond formation at the interface due to oxide layer (Er_2O_3) formed on TiO₂ surface and direct doping without forming oxide layer have also been reported in the literature [144, 146]. In some of the studies, it was found that Er doping had no effect on the lattice structure or shape of the 1D TiO₂ NSs on increasing temperature but doping formed dense structure and showed enhanced optoelectronic properties [145, 149].

3.1.5 Gd doping in 1D TiO₂ NSs

Gd^{3+} has the stable half-filled electronic configuration among the lanthanide series elements which has significant importance in the stability of the Gd^{3+} doped TiO₂ NSs [113]. The ionic radii of Gd^{3+} are 0.94 Å and similar to other RE metal ions, it cannot enter the lattice of TiO₂ completely. Therefore, it also mainly forms a uniformly dispersed oxide layer on the surface of the TiO₂ NSs and some of Ti^{4+} may substitute this Gd^{3+} in its oxide layer through the interface between them. Due to its extra stability, it shows the highest photocatalytic activity and enhanced hydrophilicity among all the RE elements [113, 150]. Moreover, Gd^{3+} doping provided higher

crystallinity as reported in the literature [150-152]. Recently, Liu et al. [150] studied the Gd doping in TiO₂ NTs and demonstrated that Gd doping greatly influenced the particle size growth and phase transformation without affecting the morphology of the NTs. Gd doping exhibited higher crystallinity in TiO₂ NTs resulting in remarkably enhanced photocatalytic properties under the extended visible light. Furthermore, the incorporation of Gd into TiO₂ lattice greatly influenced the hydrophilic properties of the doped TiO₂ NSs [113, 152].

3.1.6 Other RE metal doping in 1D TiO₂ NSs

As discussed above, due to the variation in the ionic radius of the RE metals ions with Ti⁴⁺ (in TiO₂), most of them mainly forms oxide layers on the surface of TiO₂ NSs and a few RE metal ions also enter into the TiO₂ lattice and sit at the interstitial position or substitute Ti such as in the case of Tb, Sm, Pr, Tm, Dy, Yb, etc. [153-158]. Pal et al. [154] demonstrated the replacement of Ti⁴⁺ ions (in TiO₂) by Yb³⁺ by estimating the Ti concentration with increasing Yb³⁺ amount. A decrease in Ti concentration with increasing Yb³⁺ dopant concentration was evidence by EDS which was further confirmed by XRD data that showed a shift in the characteristic peak of TiO₂ towards the lower diffraction angle as a result of Ti substitution by Yb. This shift of the diffraction peak indicates the doping within the lattice of the TiO₂. Similar results were reported recently by Liao et al. [159] in the case of Yb doped TiO₂ NFs. Similar substitution doping was also reported in the case of Sm doped TiO₂ NTs [153] along with the traces of Sm₂O₃ on the surface of TiO₂ [160]. Dy doping in 1D TiO₂ such as NBs, NTs, or other NSs leads to the substitution of Ti along with the formation of the oxide layer and change of the final morphology with increased Dy concentration [161-163]. In some cases, Ti⁴⁺ replaces RE metal ions in the oxide layer at the interface leading to the formation of bonds between RE metal-O-Ti as discussed above in the case of La, Ce, etc. While in some cases it has been reported that RE metal ions are fully doped within the TiO₂ lattice without forming an oxide layer on the TiO₂ surface. For example, Ho doping in TiO₂ NWs [164], Nd doping in TiO₂ NFs [110], NRs [93] and other NSs [111, 165]. It has been proposed that Nd occupies the octahedral interstitial site of Nd-doped TiO₂ [111]. Tb doped TiO₂ NSs showed emission bands in the blue and green regions attributed to the presence of Ti³⁺ and oxygen defects as well as the emission from Tb³⁺ transitions. The emitting colour could easily be tuned in the blue region by varying the Tb³⁺ concentration [166]. The overall picture of the RE

doping mechanism in 1D TiO₂ NSs and improvement in various properties have been shown in Figure 3B.

The RE doping mainly creates lattice distortion, charge imbalance, oxygen vacancies, etc. All these doping effects lead to the inhibition of crystal growth, phase transformation, and charge recombination in TiO₂ NSs. Most of the RE doping does not affect the morphology of the final doped TiO₂ NSs as compared to the undoped one. Furthermore, RE metal ions doping provide doped TiO₂ NSs with decreased bandgap, higher crystallinity, and surface area leading to visible light activity. Also, it improves the structural, optical, and electrical properties promising for their multifunctional applications in various research fields including energy and environmental application as discussed in detail in further sections.

3.2 Co-doping with rare-earth metals in 1D TiO₂ NSs

As discussed above, RE metal ions provide abundant energy levels originating from their special electron/photon transitions between 4f and 5d orbitals. Doping with RE metal ions has a great impact on TiO₂ NSs as a result of the reduction in their absorption threshold and utilization of solar light making them visible light active materials [167, 168]. Although these modifications are very sensitive to the materials properties, structures and compositions, doping with RE metals leads to the enhancement of structural and optoelectronic properties [167, 168]. However, studies reveal that these dopants may also act as recombination centers for the photo-generated electrons and holes that promote their recombination by reducing the charge carrier separation [167, 169, 170]. These mono-dopants may also disturb the TiO₂ lattice and act as trapping centers for photo-generated electrons and holes in place of visible light absorbance source [167, 169].

To overcome these issues, co-doping of RE metal-doped TiO₂ NSs with another dopant is very effective and has also been investigated extensively [77, 167-171]. Co-doping could be carried out with another RE, transition, or noble metals or non-metals which exhibits enhanced photocatalytic properties of co-doped TiO₂ NSs as compared to the mono dopant TiO₂ NSs [167, 170, 172]. There is extensive research carried out to study the effect of doping and co-doping using other metals such as transition/noble metals and non-metals and readers are encouraged to go through the relevant literature [4, 173-176]. Additionally, RE doping improves the structural, optoelectronic, and conducting properties of the TiO₂ NSs along with the stability of the systems [168, 177-179]. In a review by Chen et al. [169], the synergistic effects of co-doping of TiO₂ NSs

are discussed which reveals that the co-doping is promising for the improvement in their optical absorption, transport properties, and surface trapping of the photo-generated electrons and holes. Interestingly, metal co-doping has been shown to have a great impact on the photoelectric properties of 1D TiO₂ NSs [77, 94, 168, 180, 181].

Very recently, Wang et al. [94] studied the effect of Yb³⁺, Er³⁺ co-doping in TiO₂ NRs for their improved transport properties. These doped TiO₂ NRs were used as an electron transport layer in the perovskite-based solar cell device and found to be very promising for the enhancement of photovoltaic properties of solar cell devices. It was also found that co-doped TiO₂ NRs enhanced the absorption of light from visible to NIR region and reduced the band gap along with 25% enhancement in the current density of the solar cell. It also enhanced the efficiency of the solar cell by 17% as compared to the undoped TiO₂ NRs based solar cell. All that attributed to the higher recombination resistance of the photo-generated electrons and holes and a lower transfer resistance than those of the undoped NRs based device. Shanying et al. [182] reported that co-doping of La with Co enhanced the electrical conductivity of TiO₂ NWs due to an increase in the carrier concentration which showed great potential for nanoelectronic devices. Similarly, co-doping has a great impact on the improvement of the various properties of the 1D TiO₂ NSs making it versatile for several applications and is discussed in section 5 in more details.

4. Synthesis of RE doped 1D TiO₂ NSs

There are several promising physical and chemical methods that have been using for the synthesis of various 1D TiO₂ NSs as well as RE doped 1D TiO₂ NSs. These methods are briefly discussed here along with the recent advancement carried out in fabrication strategies by the researchers:

4.1 Hydrothermal synthesis

There are several techniques for the synthesis of 1D TiO₂ NSs. These include hydrothermal, solvothermal, anodic oxidation, chemical vapor deposition, etc. [2, 62, 183-189]. Among, these techniques, hydrothermal synthesis route is one of the promising techniques which provide the possibility of synthesizing all kind of 1D TiO₂ NSs through varying the various experimental parameters [62, 185, 190]. Since the last decade, this technique has become one of

the advanced nanomaterials synthesis techniques for NSs of various dimensions for different applications [4, 144, 191-193]. It also helps to learn fundamentals for manipulating materials at nanoscale varying physical and chemical parameters. Especially, 1D TiO₂ NSs as discussed in **Figure 2B**, transition metals /RE metals/ non-metals doped 1D TiO₂ NSs, their nanocomposites, etc. could be simply prepared by hydrothermal method [4, 112, 135, 190, 194-196]. Kasuga et al. [184] developed a new way to synthesize 1D NSs specially NTs with high surface area using the hydrothermal method and demonstrated that their optoelectronic properties could be greatly enhanced by incorporating metallic, organic, or inorganic materials.

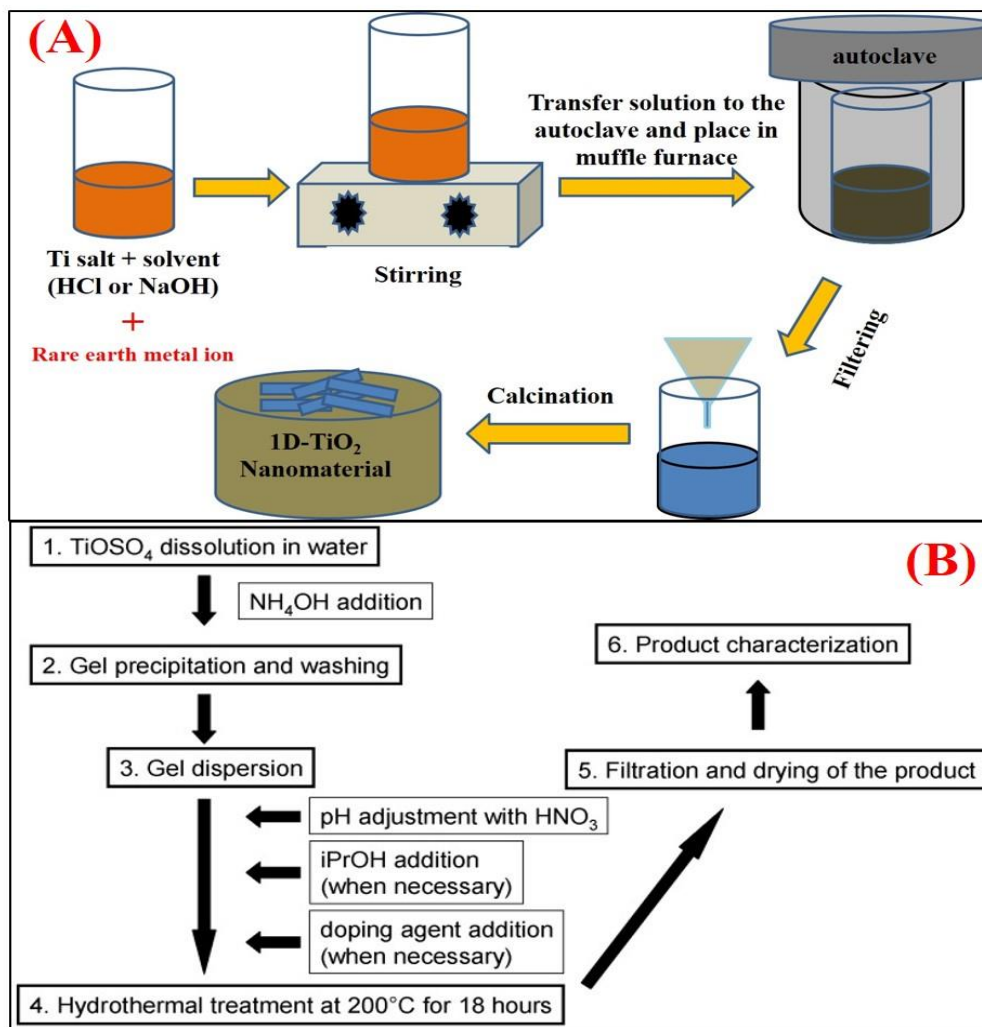


Figure 4. (A) Schematic illustration of the synthesis of 1D TiO₂ NSs using hydrothermal process. (B) Doping of RE metals in 1D TiO₂ NSs using sol-gel hydrothermal synthesis. **Permission may be required from [197].**

In the hydrothermal synthesis technique, 1D TiO₂ NSs are prepared using a stainless-steel autoclave reaction vessel. Simply, TiO₂ precursors or nanopowder either commercial or synthesized by any other methods such as sol-gel, are used for the preparation of 1D NSs. Various precursors such as titanium alkoxides, titanium isopropoxide, tetrabutyl titanate, titanium ethoxide, titanium halides (TiCl₄, TiF₄), titanium (IV) bis (ammonium lactate) dihydroxide, etc. are generally used in the hydrothermal method. These starting materials are first dissolved in either concentrated aqueous or alkaline solutions (or their aqueous solutions are prepared), followed by stirring, and then the final solution is poured into the autoclave. The autoclave is then kept in the furnace at elevated temperature for calcination and or pressure to obtain the final product (**Figure**

4A) [197-199]. To prepare 1D TiO₂ NSs, generally acidic or alkaline solvents are used for dissolving TiO₂ precursors. Particularly alkaline solvents are used in case of hydrothermal synthesis of NRs and NTs [56, 198, 200]. This method is very simple and cost-effective. This is also very important to note that various parameters play an important role in the production of the final product. Various experimental parameters such as temperature, pressure, solvent concentration, pH of the solutions, etc. have a great impact on the morphologies. Similarly, these parameters also affect various properties like thermal conductivity, viscosity, dielectric constant and heat capacity, etc. that could be tuned by changing these parameters [1, 198, 201-204]. For example, Yuan et al. [103] demonstrated that the morphologies of various TiO₂ NSs such as NFs, NTs, NWs could be controlled due to the different precursors, alkaline solutions and their concentrations along with changing the duration of the reaction and operating temperatures.

RE metal-doped 1D TiO₂ NSs could also be synthesized similarly using a hydrothermal technique. However, to synthesize RE doped 1D TiO₂ NSs, the following two strategies are applied:

- (i) direct doping of RE metal ions by mixing the appropriate amount of metal precursors in TiO₂ precursors/nanopowder before dissolving it to the suitable acidic or alkaline solvent followed by the thermal treatment as shown in **Figure 4A** (in red color) [205, 206];
- (ii) the sol-gel hydrothermal method in which, first using sol-gel method, TiO₂ gel is prepared followed by addition of the RE metal ion as its precursor as shown in **Figure 4B** [197]. Various RE doped 1D TiO₂ NSs have been prepared using the hydrothermal method for several applications and are discussed in **detail in section 5**.

4.2 Solvothermal synthesis

Solvothermal synthesis of 1D TiO₂ NSs is similar to that of the hydrothermal method as discussed above. The major difference is the solvents used in the synthesis process. It includes the use of non-aqueous solvents and autoclaves in an almost similar manner with control of various experimental parameters for producing 1D NSs of a variety of materials [207, 208]. For example, Das et al. [208] demonstrated the synthesis of various 1D TiO₂ NSs such as NRs, NTs, and NWs using different non-aqueous solvents and studied their effect on the morphologies and structural properties (**Figure 5**).

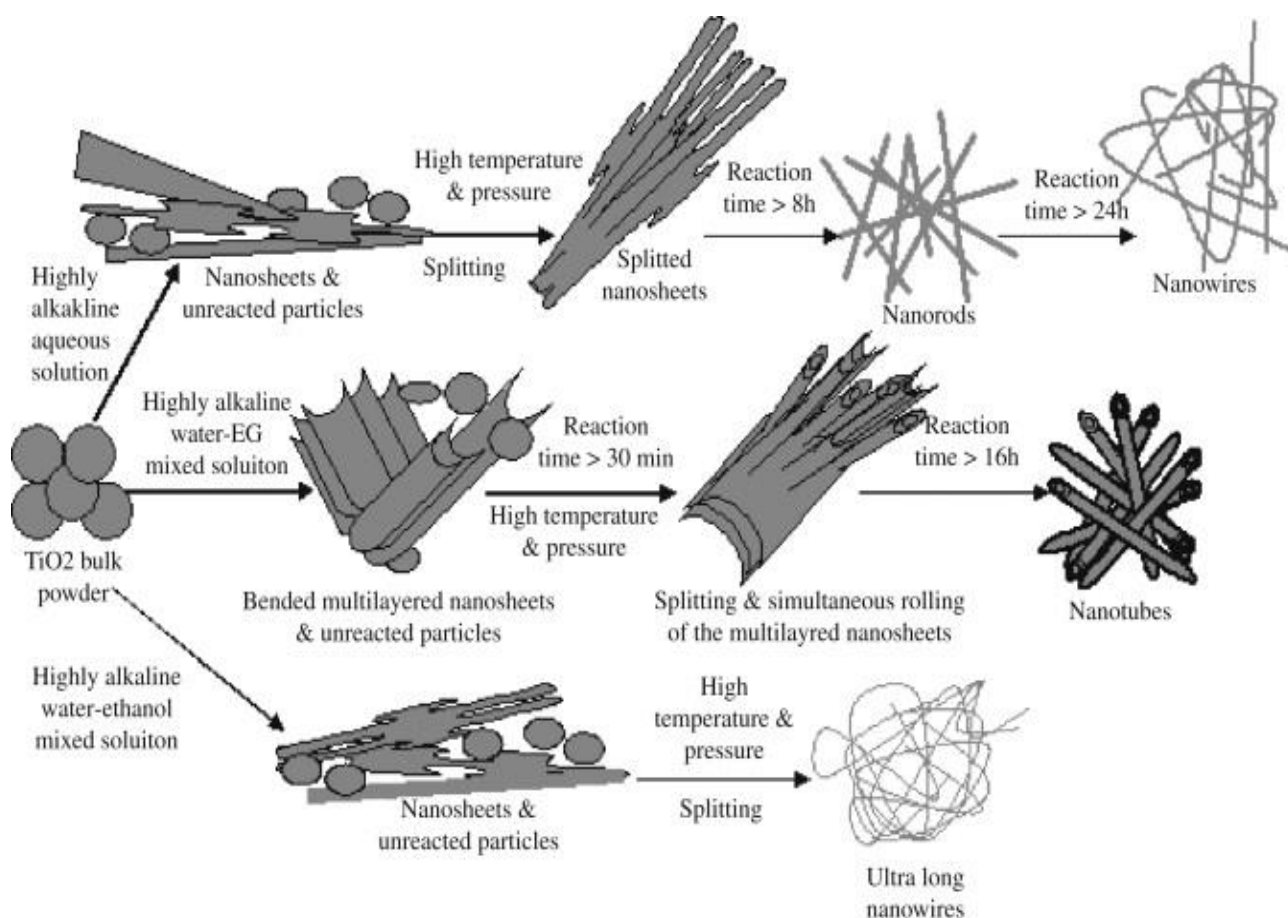
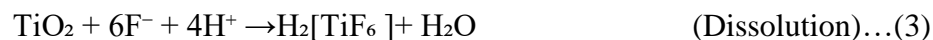


Figure 5. Schematic of synthesis of various 1D TiO₂ NSs using the solvothermal process under different organic solvents. **Permission is required from** [208].

In the solvothermal process, Ti salt is treated with a highly alkaline aqueous solution that gives layered sodium titanate nanosheets which are converted into 1D sodium titanates NSs in different organic solvents. The further procedure is the same as in the hydrothermal method followed by post-synthesis calcination at high temperature to obtain the high crystalline and retained morphology [4, 208-210]. Similarly, RE metal-doped 1D TiO₂ NSs have also been synthesized using a solvothermal process [121, 126, 210]. For example, Sadhu et al. [126] reported on the solvothermal synthesis of La-doped TiO₂ NRs with excellent optoelectronic properties. Using an organic solvent, the solvothermal process has been proved to be beneficial over the hydrothermal process because of better control of morphology and structural properties [4].

4.3 Anodic oxidation synthesis

Another important method of synthesizing 1D TiO₂ is the anodic oxidation method which is mainly applied for the preparation of vertically aligned undoped or doped 1D TiO₂ NTs [120, 183, 211-215]. In this method, as starting material, titanium (Ti) foil or alloy is used. The anodization of the Ti foil or alloy is generally carried out at constant potential within an electrochemical cell after a rigorous cleaning process [183, 216, 217]. The electrochemical cell includes a working electrode as Ti anode, Pt, or C as a counter electrode in an electrolyte solution which is a mixture of generally deionized water, ethylene glycol, and ammonium fluoride solutions. During the synthesis process, when high voltage is applied, either the Ti metal gets oxidized forming an oxide layer or dissolves in the electrolyte leading to the formation of TiO₂ NTs. At the cathode, there is a production of H₂ gas [216, 218].



Li et al. [218] also explained the similar mechanism of anodic TiO₂ NTs formation. It was mentioned that the oxide layer thus formed reacts with the fluorinated electrolyte leading to the etching and pores formation for the further development of the NTs as shown in **Figure 6A** [219].

This is further followed by rinsing by methanol, drying process, and calcination at higher temperature to produce well vertically aligned TiO₂ NTs [120, 183, 211, 213, 214, 216]. These TiO₂ NTs arrays and RE doped NTs have been potentially applied for various applications [61, 85, 107, 120, 220, 221]. There are various experimental parameters such as anodizing time, applied potential, pH, temperature, electrolyte concentrations, etc. which influence the final morphology and thus the structural properties of TiO₂ NTs [183, 216, 222]. For example, Jedi-Soltanabadi et al. [213] studied the influence of anodizing time on mainly morphological properties of TiO₂ NTs and found that morphology was purely dependent on the anodic time. Morphology with higher NTs length could be possible like the formation of NWs but increasing time would damage the morphology leading to the formation of grass-like structures [213, 215, 223].

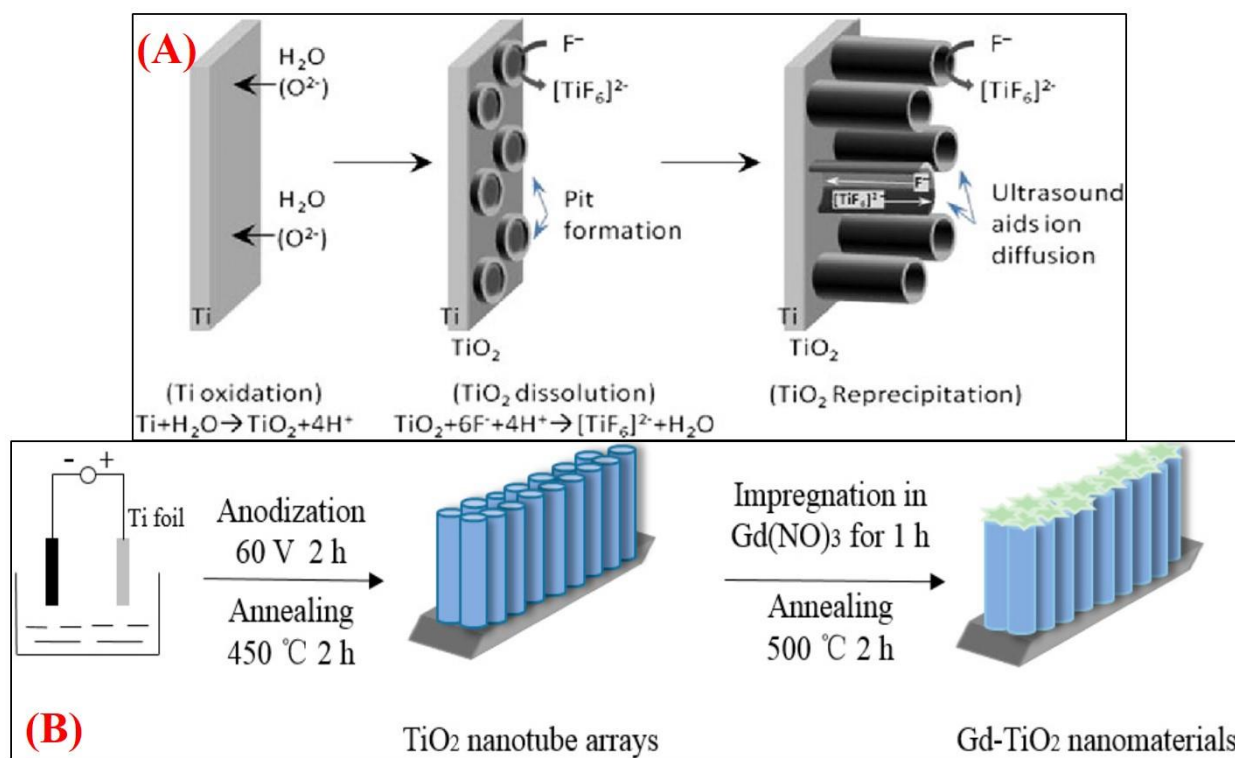


Figure 6. (A). Mechanism of anodic oxidation method for the preparation of TiO₂ NTs on a Ti foil. It involves the dissolution of Ti and re-precipitation of Ti as oxide layer leading to the formation of the nanotubular architecture in the presence of an electric field. **Permission is required from** [219]. (B) Anodic oxidation RE metal doping (Gd-doped TiO₂ NTs) of TiO₂ NTs array. **Permission is required from** [218].

RE metal-doped TiO₂ NTs using the anodic oxidation method can be obtained by either one-step or two-step anodization. In one-step anodization, either RE metal-doped Ti foil/substrate can be used as an anode or RE metal precursors can be added in the electrolyte for a similar process to be occurred as in NTs formation [120, 172, 224]. For example, Parnicka et al. [120] produced various RE metal-doped TiO₂ NTs using their alloy as anodic material. On the other hand, two-step anodization involves the first synthesis of anodic TiO₂ NTs followed by doping of RE metal ions after immersing NTs in corresponding precursor solutions of RE metal [218, 225] (**Figure 6B**).

4.4 Electrospinning synthesis

Electrospinning is an important and the only method for the synthesis of NFs structures out of all other 1D NSs [2, 226-229]. This method is known to create NF structures of a variety of materials such as semiconductors, polymeric, metals, nanocomposites materials, etc. for several applications ranging from environment, sensing, energy to biomedical applications [228, 230-233]. This is also a suitable method to produce doped NFs of a variety of materials including TiO₂ NFs using various dopants [2, 232, 234-236]. Using the electrospinning method, various RE metals doped and undoped TiO₂ NFs have been prepared for many applications. The main characteristics of TiO₂ NFs produced by using method include high aspect ratio, low density, high pore volume, etc.[229, 237]. Its handling is not so simple but this method has a very simple processing technique for NFs synthesis using electric force.

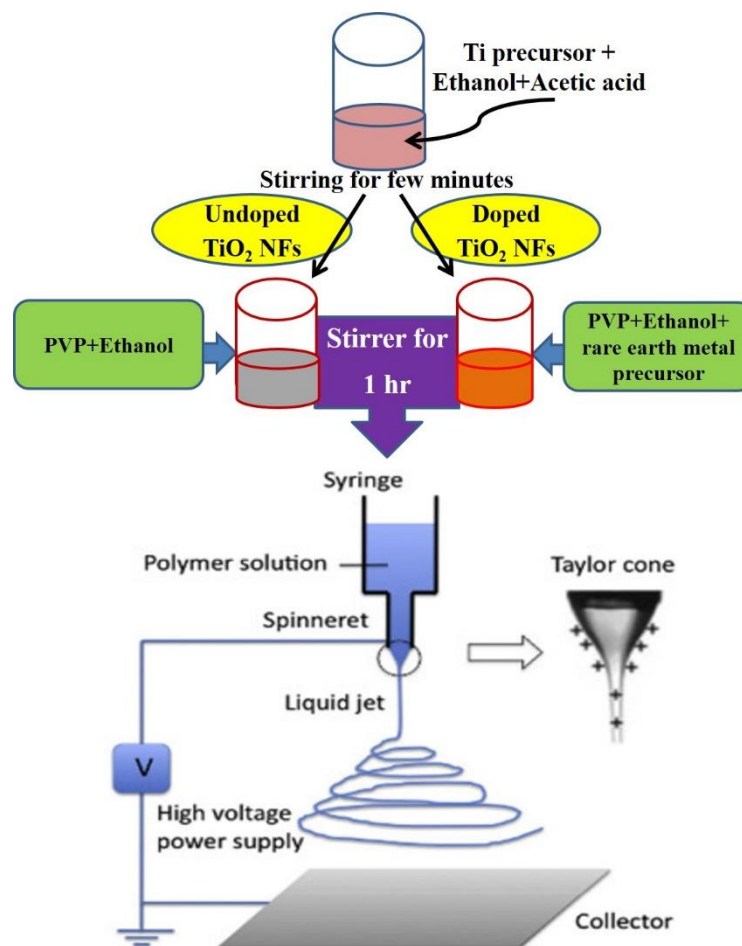


Figure 7: Schematic of functioning of electrospinning process for the fabrication of doped and undoped TiO₂ NFs. **Permission is required from** [233].

A typical electrospinning instrument components contain mainly, a syringe with a metal needle, high voltage power supply, and a conductive collector for collecting the NFs as shown in **Figure 7** [227, 229, 233]. Generally, a polymer such as Polyvinylpyrrolidone (PVP), is used in the TiO₂ NFs fabrication process in the electrospinning method because it provides better solubility to the TiO₂ precursor with alcoholic solvent for making a homogeneous mixture. Acetic acid is another important component that is used for stabilizing the mixture solution that also controls the hydrolysis reaction of TiO₂ precursor within the solution [2, 229]. As shown in **Figure 7**, the solution thus prepared, is then injected with the help of a syringe pump into the system and a high voltage is applied at the tip of the needle. As a result of the applied voltage, the polymer solution

at the tip of the needle gets polarized and distributes the induced charge over the surface. The drop as formed at the tip of the needle has a surface tension which overcomes by the electric force giving rise to a Taylor cone leading to the formation of tiny jets. The conducting collector serves as the receiver of the NFs thus produced from the Taylor cone (**Figure 7**). The NFs thus produced are calcined at higher temperature to remove the polymer and finally, NFs with the reduced diameter is obtained [186, 238-241]. Someswararao et al. [239] have simply demonstrated the fabrication procedure of TiO₂ NFs using TTIP as Ti precursor, methanol as the alcoholic solution with PVP polymer. Similarly, Li et al. [186] demonstrated the synthesis of TiO₂ NFs with the various diameter ranging between 20 to 200 nm by varying several parameters during the electrospinning process.

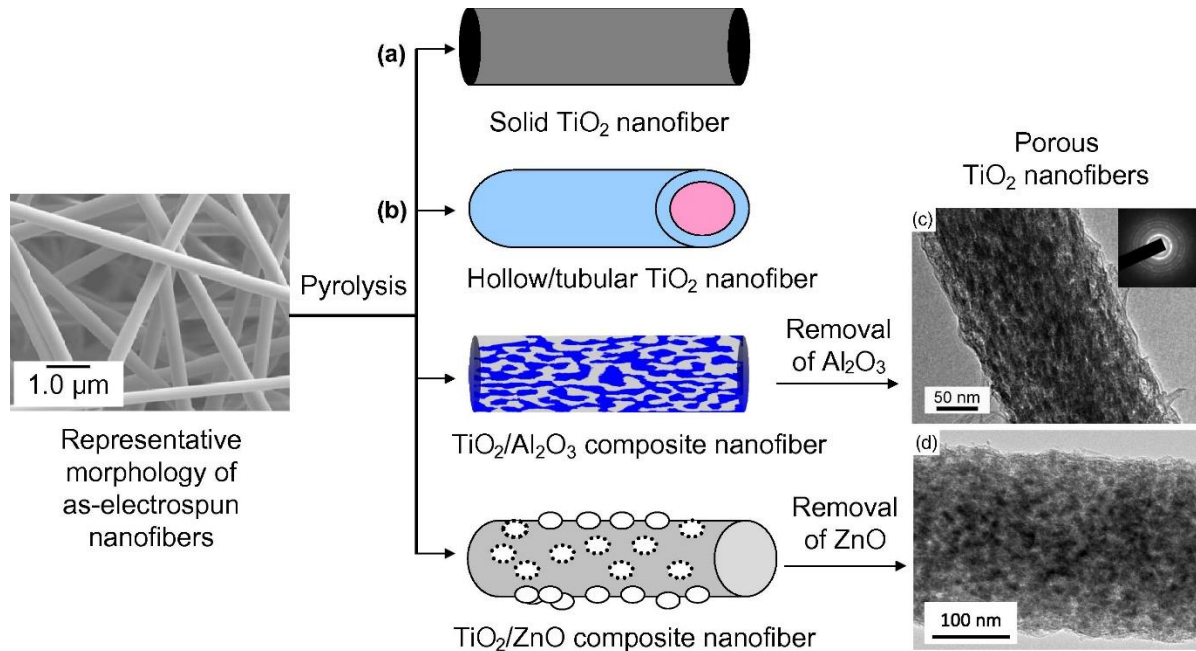


Figure 8: Schematic representation of fabricating TiO₂ NFs with different morphologies and surface areas using electrospinning method. **Permission is required from [238].**

However, as explained by Liu et al. [237], the electrospinning technique for fabricating NFs can be carried out in many different ways resulting in a change in morphologies of NFs. For example, He et al. [238] demonstrated that the co-axial spinneret electrospinning method could be used for fabricating NFs with different morphologies and surface areas (**Figure 8**). In some cases, NFs could be useful for fabricating other 1D TiO₂ NSs just by thermal treatment, for example, TiO₂ NTs from TiO₂ NFs [216]. The morphologies, as well as various properties of doped or undoped TiO₂ NFs, could be altered by varying several parameters which are polymer

concentration, applied electric voltage, the distance between the tip and the conducting collector, flow rate of the solution, etc. [2, 242].

Doping of TiO₂ NFs with RE metals is proved to an important aspect of improving their multifunctional properties [2, 110, 141, 234, 243]. Doping of TiO₂ NFs with RE metal ions is a similar process using an additional precursor of RE metals [2, 141, 243] as shown in **Figure 7**. For example, Singh et al. [2] exhibited the fabrication of Ta doped TiO₂ NFs for multifunctional applications using electrospinning technique as described above with the addition of Ta precursor tantalum ethoxide with TTIP and PVP. The synthesized Ta doped TiO₂ NFs showed enhanced photodegradation as well as sensing properties for dye molecules. The doping TiO₂ NFs with RE metals has been shown to enhance their optoelectronic, sensing and surface properties for various applications which have been discussed in the next section.

4.5 Template assisted method

Template assisted method is another promising and common method for the synthesis of 1D TiO₂ NSs [244]. As discussed above, like hydrothermal synthesis, the template-assisted method also combines the sol-gel with pre-prepared templates. In this method, 1D NSs are prepared with morphology using known shaped templates [245-248]. Either the template is dipped into the prepared TiO₂-sol or sol is poured into the pre-shaped templates [248]. This method is used to synthesis controlled morphologies of 1D NSs that depend upon the deposition temperature, concentrations or composition of a sol, template shape, and size, and also the duration of the process [248-252]. Generally, nanoporous materials (i.e. nanoporous alumina, silica, zeolites, zinc oxide, etc.) are used for preparing templates [250, 253-255]. After deposition and completion of the process, the used template is removed by some process such as chemical etching or combustion [244, 248, 250]. This process leads to the formation of desired NSs as a duplicate morphology of the template [248]. Atomic layer deposition is found to be very important for controlling the shape and size of the NSs during the use of the template-assisted method [256].

This method is classified as a negative and positive template-assisted method if the material is deposited or coated on the inner walls or outer wall of the template respectively [248, 257-260]. Doped 1D TiO₂ nanostructures are also formed by this method using the same procedure as in the case of undoped, where, dopant metal ion is added to the precursor solution before filling the pore into the template. The template-assisted method has some drawbacks due to which its use is

restricted such as it is a time-consuming process, require removal of the template after the formation of nanostructure which may damage the nanostructure [248, 261].

4.6 Chemical vapor deposition method

Chemical vapor deposition (CVD) is another interesting method for producing 1D NSs with good quality and uniformity for a variety of materials over a large surface area [189, 262]. Various modified and advanced CVD methods have been developed in the last few years [262-264]. Recent developments in this field show great potential for large-scale synthesis of 1D TiO₂ NSs arrays on substrates surface along with control over the shape, size, and various phases [262]. Simply, it is based on catalyzed growth of the solid 1D NSs i.e. through vapor-solid growth mechanism using a precursor of the metal oxide materials or metal itself [265]. Normally, a substrate is used where the volatile materials are deposited at a higher temperature depending on the type of material used [189, 266]. In the case of TiO₂, generally, Ti metal or any of its precursors is used. Using the CVD method, several 1D TiO₂ NSs such NRs [189, 264], NWs [262], NBs [267], etc. have been reported with uniformity. It has been found that CVD is a promising technique for producing 1D NSs with uniform morphology and large surface area deposition on the substrates. However, this method is known to be a little bit expensive and also involves harsh experimental conditions [262]. This technique still needs to explore more on doping 1D TiO₂ NSs as only a few reports are available [268-270].

5. Multifunctional applications of RE metal-doped 1D TiO₂ NSs

5.1 Photocatalytic degradation and ultrasensitive detection of organic pollutants

TiO₂ based NSs is one the most used semiconductor nanomaterials for photocatalytic degradation of dye molecules for wastewater treatments. However, the major challenge in photocatalysis is to develop a cost-effective way to enhance its spectral sensitivity up to the solar spectrum for its potential applications. Furthermore, it has been well achieved by the researchers in the last few years through various modifications as also discussed above. Doping TiO₂ based NSs with RE metals is one of the promising ways which have been extensively used to enhance their photocatalytic properties for the degradation of dye molecules.

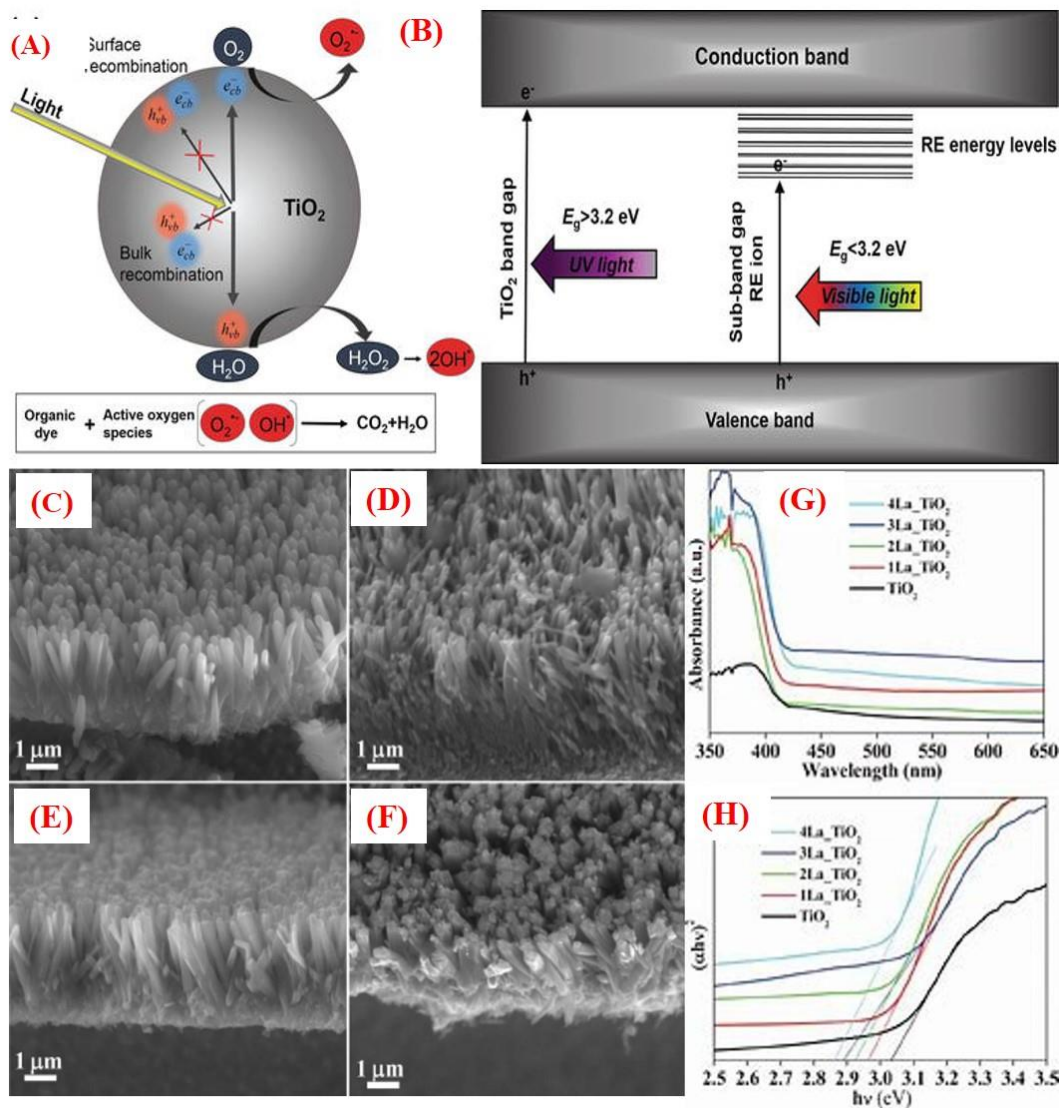


Figure 9. (A) Basic photocatalytic mechanism under UV or visible light irradiation, (B) modification of bandgap with sub-band-gap energy levels of RE ions. **Permission not required [271].** SEM micrographs of (C) 1 mol% (D) 2 mol% (D) 3 mol% and (F) 4 mol% La-doped TiO₂ NRs, (G) UV-visible diffuse reflectance spectroscopy (DRS) spectra, (H) dependence of the absorption coefficient as a function of energy plot for pure TiO₂ and La-doped TiO₂ NRs with various amounts of doping. **Permission is required from [126].**

As a photocatalyst, TiO₂ NSs under the influence of UV radiation, produces charge carriers, electrons, and holes in the CB and VB, respectively. These separated charge carriers move to the surface where they react with the atmospheric oxygen (O₂) or adsorbed water molecules

(H₂O) to produce various ROS such as OH[•], O₂^{•-}, etc. where OH[•] production is very crucial for the photocatalytic degradation of dyes as shown in **Figure 9A** [4, 271]. As discussed earlier, the photo-generated charge carriers recombine at a fast rate preventing the production of ROS and thus photocatalytic activity is decreased. This could be improved by doping TiO₂ NSs with RE metals which create charge imbalance and separation with the availability of more electrons and holes to participate in oxidation and reduction processes with O₂ and H₂O [4, 41, 272]. This process leads to the production of more ROS and increases the photocatalytic degradation of dyes adsorbed on the surface of TiO₂ NSs. This RE metal doping also leads to the increased absorption of the visible light radiation by altering the absorption threshold to lower energy *i.e.* higher wavelength [272]. Doping with RE metal ions engineers the TiO₂ band gap by introducing sub-energy levels below the CB [2, 97]. Due to the presence of the variable energy levels as a result of the incorporation of RE metal ions, electrons from VB need less energy to be transferred to the sub energy level as compared to the energy required for the transition from VB to CB of TiO₂ (**Figure 9B**). This transition could be carried out by visible radiation leading to the absorption of visible light radiation and can be tuned to even NIR absorption by further modifying the morphology of TiO₂ NSs in combination with other functional nanomaterials [4, 41, 97]. All these modifications due to RE metal ion doping in TiO₂ NSs enhance the photocatalytic optical properties and photocatalytic efficiencies [4, 272].

Out of several RE metals, La has been extensively used for improving the optical, and structural properties of 1D TiO₂ NSs for photocatalysis as well as other applications. For example, La-doped 1D TiO₂ NSs includes La-TiO₂ NRs [85, 122, 126], NTs [61, 122, 273], NFs [110, 141, 274] and NWs [135] for multifunctional applications including photocatalytic properties. For example, Sadhu et al. [126] demonstrated homogeneous doping of La (1-4 mol%) in TiO₂ NRs which improved the electrical conductivity and optoelectronic properties of TiO₂ NR electrodes resulting in the enhanced charge carrier density and solar cell efficiency. **Figures 9 (C-F)** shows the SEM images of various La-doped TiO₂ NRs. The optical properties showed that doped TiO₂ NRs exhibited a wide range of absorption below 420 nm. The absorption was found to be enhanced absorption with increasing La concentration and the bandgap was decreased up to 2.9 eV (**Figure 9 G-H**). In another study, Song et al., [85] studied the enhanced photocatalytic properties of La and other RE metals (Sm, Eu, and Er) doped TiO₂ NRs as compared to the pure NRs and commercial TiO₂ for the degradation of methyl orange (MO) dye molecules. These studies show

the enhanced optoelectronic properties resulted in the enhanced absorption towards the visible region and reduced bandgap due to RE doping in 1D TiO₂ NSs.

Cacciotti et al. [141] studied La, Eu, and Er-doped TiO₂ NFs and compared their thermal and luminescence properties with undoped TiO₂ NFs. It was demonstrated the doping with RE metal ions provided thermal stability to the phase transition from anatase to rutile up to 900–1000 °C attributed to the development of RE-Ti-O intermediate phase along with enhanced luminescent properties as compared to the undoped NFs. Similarly, Hassan et al. [110] demonstrated the enhanced thermal and photocatalytic behavior of La, Ce and Nd-doped TiO₂ NFs in the photodegradation of Rhodamine 6G (R6G) dye. Interestingly, Singh et al. [2] demonstrated the multifunctional applications of Ta doped TiO₂ NFs including photocatalytic degradation and ultrasensitive detection of methylene blue (MB). They showed that 5% Ta doping was the optimized doping concentration of Ta in TiO₂ NFs which exhibited better photocatalytic activity along with detection of MB at a lower concentration through surface-enhanced Raman scattering (SERS) technique. The increased concentration of Ta beyond 5% doping resulted in the formation of its oxide which affects optoelectronic properties providing lower photocatalytic efficiency. The excellent bifunctional properties of Ta doped TiO₂ NFs was attributed to the induced sub energy levels below the CB of TiO₂ NFs due to the Ti³⁺ defects which not only improved the charge separation but also promoted the charge transfer for the enhanced SERS signals of MB as shown in Figure 10 (A-D). Similar work has been proposed by Liu et al. [220] who demonstrated the remarkable SERS signal enhancement of MB dye molecules using TiO₂ nanofoam NTs array even without any doping. This remarkable SERS signal enhancement was due to the unique structure of 1D TiO₂ NTs which allowed multiple laser scatterings among the periodic voids. Recent review summaries such as bifunctional nanostructured materials investigating photocatalytic as well as SERS activities [275]. It demonstrates the recyclable behavior of such NSs which could be improved by various modifications such as doping, forming nanocomposites, core-shell NSs etc. [275].

Bandi et al. [135] synthesized Eu and Ce-doped TiO₂ NWs arrays and studied the morphological, optical, structural, and photocatalytic properties for the photocatalytic degradation of toluidine blue-O dye. The RE doped TiO₂ NWs showed better photocatalytic mineralization of dye molecules as compared to undoped NWs due to the enhanced photoluminescent properties resulting in better charge separation and increased surface area as shown in Figure 10 (E-I). It can

be seen from the photoluminescence spectra that Ce doped TiO₂ NWs show better charge separation as compared to Eu doped and undoped TiO₂ NWs resulting in enhanced photocatalytic degradation. Very recently, Nwe et al. [162] reported on heterogeneous NSs of Dy-doped TiO₂ NPs hybrid with Monoclinic TiO₂ NBs which showed excellent UV and fluorescence light photocatalytic activity for the photodegradation of MB molecules with a very small amount of Dy doping. The high-performance photocatalytic activities were attributed to the RE doping as well as 1D geometry of the TiO₂ NBs.

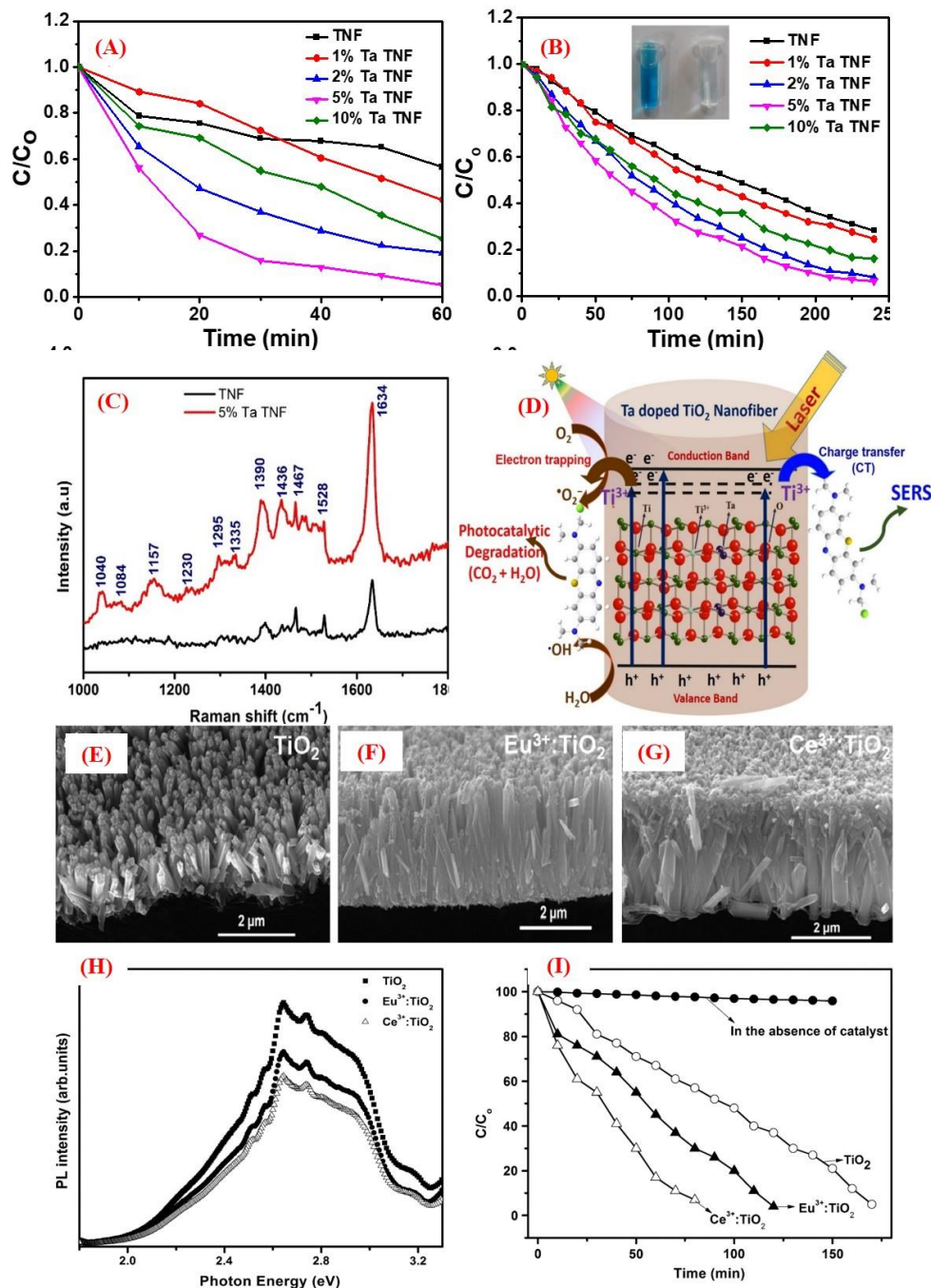


Figure 10. Photocatalytic activity of TiO₂ and Ta-doped TiO₂ NFs photocatalyst for degradation of MB dye under (A) UV light, (B) solar light. (C-D) SERS spectra of MB molecules and schematic of the mechanism of enhanced photocatalytic degradation and SERS performance of Ta-doped TiO₂ NFs. **Permission is required from [2].** SEM micrographs of (E) undoped TiO₂ NWs, (F) Eu doped TiO₂ NWs, (G) Ce doped TiO₂ NWs, (H) photoluminescent spectra of the undoped and Eu, Ce doped TiO₂ NWs, (I) photocatalytic degradation of toluidine blue-O dye as a function of time under UV irradiation. **Permission is required from [135].**

Wu et al. [61] reported that the photocatalytic efficiency of TiO₂ NTs was enhanced by La doping due to the Ti-O-La bond formation resulting in charge imbalance and other factors such as oxygen defects and presence of Ti³⁺ species etc. On the other hand, Zong et al. [273] demonstrated the effect of the La₂O₃ doping which not only maintained the morphology but also enhanced the surface area of the resulting La-doped TiO₂ NTs. It was found that the loading Pd NPs further enhanced the photocatalytic properties of La-doped TiO₂ NTs due to the electron trapping as a result of the Schottky barrier created at Pd and TiO₂ interface. These Pd doped and Pd loaded TiO₂ NTs/Pd-TiO₂ NTs were used for the photocatalytic degradation of propylene under visible light and found that Pd loaded La-TiO₂ NTs showed the best photocatalytic activity (Figure 11). Sun et al. [129] exhibited the excellent photodegradation behavior of Ce doped TiO₂ NTs towards MB under the visible light bombardment. It was shown that Ce doping extended the optical absorption towards the visible light up to the wavelengths of 600 nm resulting in the enhanced visible-light photocatalytic activity.

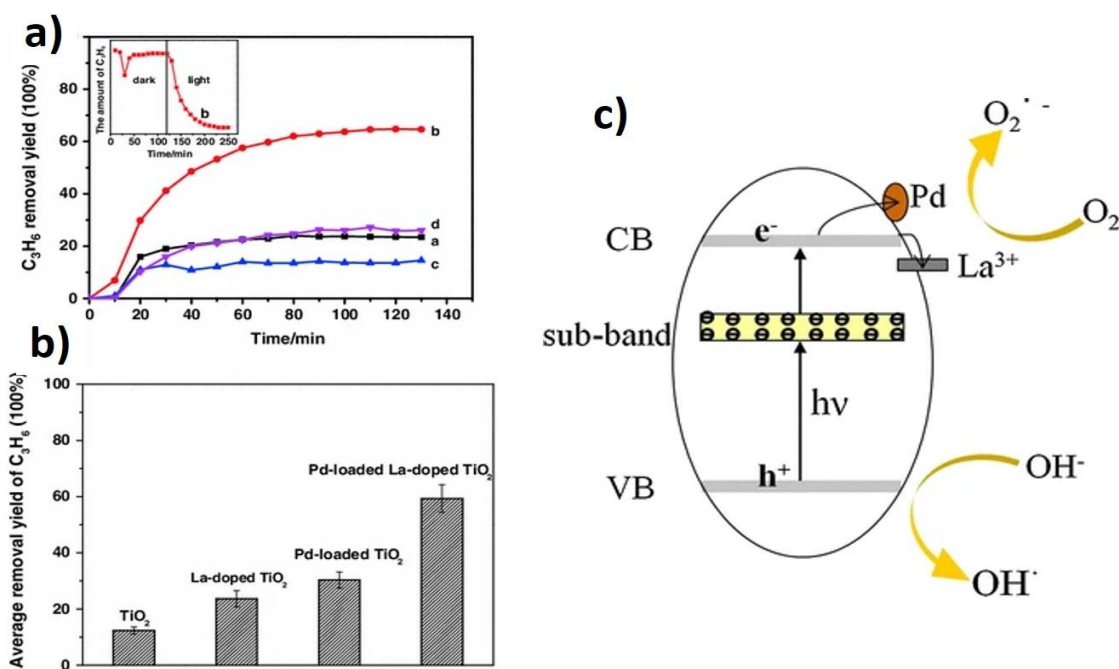


Figure 11. (a) Visible light photocatalytic activity of (a) La-doped TiO₂ NTs, (b) Pd-loaded La-doped TiO₂ NTs, (c) TiO₂ NTs, and (d) Pd-TiO₂ NTs, the inset figure shows the adsorption-desorption equilibrium and photocatalytic process of the sample, (b) the average removal yields of the C₃H₆ at the same condition (Figure 6), (c) photocatalytic reaction mechanism of Pd-loaded La-doped TiO₂ NTs. **Permission is required from [273].**

In light of the above discussion on RE doped TiO₂ NSs and their photocatalytic applications, it can be concluded that these materials have been widely studied for photocatalytic degradation of organic pollutants. It is also important to mention that improved photocatalytic properties with high-performance photocatalytic activities have been achieved. The doping of RE metal ions in 1D TiO₂ NSs results in enhanced absorption that extends up to the longer wavelength in the visible light radiation region. Along with this, various kind of structural, surface modifications is induced due to the doping which shows promising results in enhancing the charge separation, charge imbalance, generation of defects, etc. Moreover, tremendous progress has been observed in the design and development of RE doped TiO₂ NSs in the last few years, but still, more devoted efforts are required to enhance their efficiencies for practical industrial applications.

5.2 Solar cell applications

In solar cell industries, DSSCs, organic solar cells (OSCs), and perovskite solar cells (PSCs) are emerging and very promising research areas that can provide potential solar cell devices for future generations. As compared to the traditional silicon-based solar cells, these have more potentials to become better sources due to better photo-conversion efficiencies (PCE), cost-effective synthesis processes, low synthesis temperature, more flexibility, etc. [276-280]. In DSSCs, TiO₂ NSs play an important role in transferring photogenerated electrons from dye molecules to the electrode [281, 282] as shown in **Figure 12 (A-B)**. 1D TiO₂ NSs can provide a direct pathway for this transportation of electrons from dye molecules to the required electrode as they are more efficient in increasing charge collection efficiency [281, 283]. Further modifications of such 1D TiO₂ NSs could improve the efficiencies of DSSCs by improving the structural and optoelectronic properties [282, 284]. Recent literature shows that 1D TiO₂ NSs doped with RE metals possess promising optoelectronic properties for enhancing the PCE of solar cells [66, 282, 284-287].

Several studies have been reported for improved PCE of DSSCs due to the incorporation of 1D TiO₂ NSs within the device structure [221, 281, 288-292]. A few studies show that PCE of DSSCs could be enhanced using rare-earth-doped 1D TiO₂ NSs as compared to the undoped NSs based DSSCs [39, 93, 126, 293, 294]. For example, Sadhu et al. [126] showed that 4 mol% La-doped TiO₂ NR electrodes enhanced the PCE of DSSCs more than 20% as compared to the TiO₂

NRs (Figure 12 C). Similarly, Yao et al. [93] studied the effect of Nd-doped TiO₂ NRs on the performance of DSSC and observed that PCE was increased by 33% which was attributed to the enhanced transportation of photo-generated electrons and separation with holes as a result of Nd doping. Feng et al. [293] demonstrated the enhanced photovoltaic properties of DSSC using Ta doped TiO₂ NWs with very high open-circuit photovoltage.

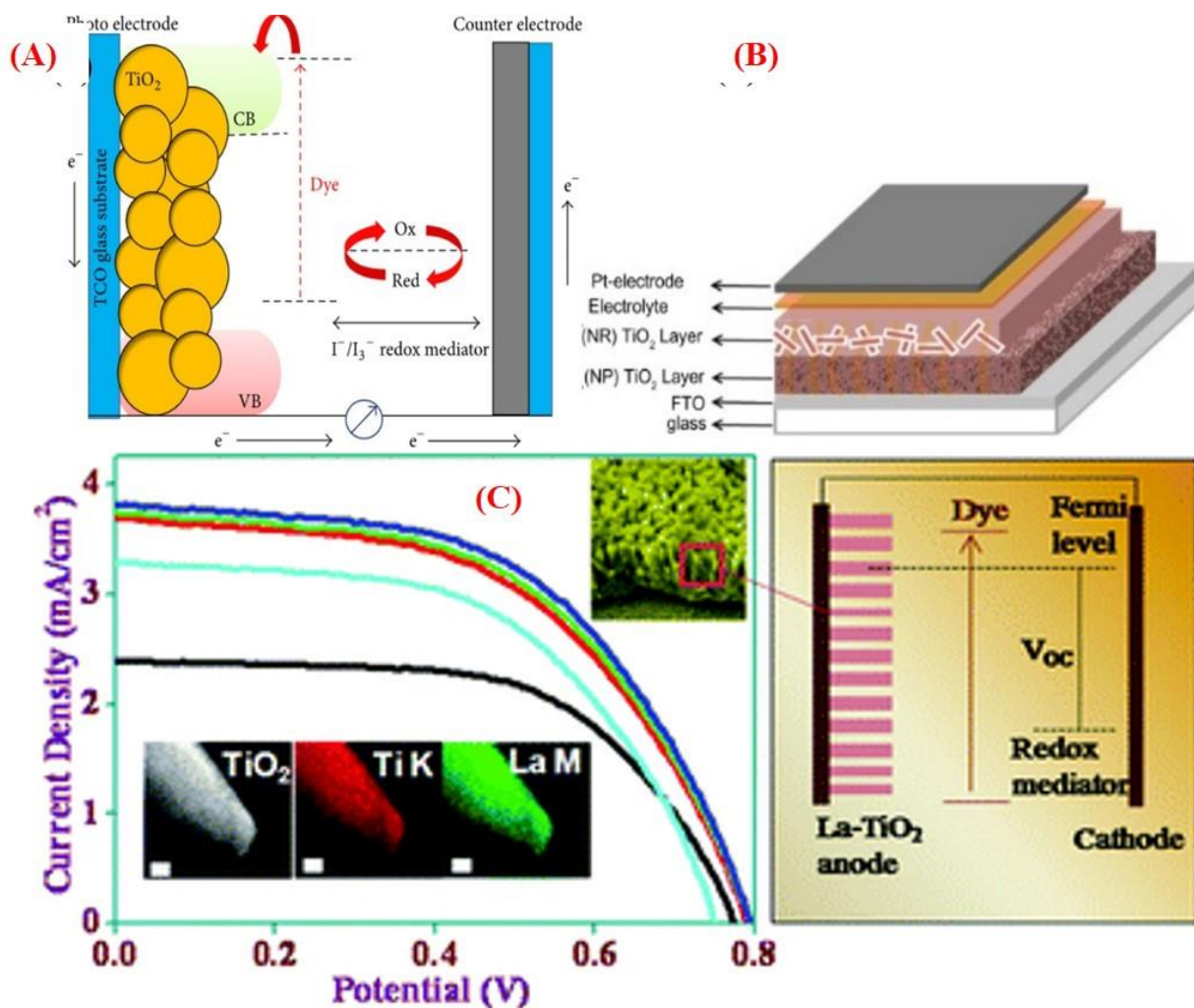


Figure 12. (A) Schematic diagram of DSSC and function of TiO₂ NSs. **Permission is not required** [295] (B) Schematic of DSSC device based on 1D TiO₂ NSs photoanode. **Permission is required** [281]. (C) La-doped TiO₂ NRs arrays electrode and optoelectronic properties for enhanced photoelectrochemical activity. **Permission is required from** [126].

Asemi et al. [39] studied the effect of Ce doping in 1D TiO₂ NSs (NRs and NTs), their optoelectronic, structural properties, and further overall impact on the performance of DSSCs. It was found that 3% Ce doped TiO₂ NSs showed the best electrical conductivity due to the induced

oxygen vacancies. Also, Ce doped TiO_2 NTs showed the better PCE of DSSC device due to relatively higher surface area as compared to Ce doped NRs. However, DSSCs devices with Ce doped TiO_2 NSs showed better PCE as compared to the undoped TiO_2 NSs attributed to the fact that larger amounts of dye molecules were adsorbed on the surface of the Ce doped TiO_2 NSs as compared to the undoped NSs (Figure 13). This study shows the importance of structural differences in various 1D TiO_2 NSs that can have an impact on the overall performance of the devices.

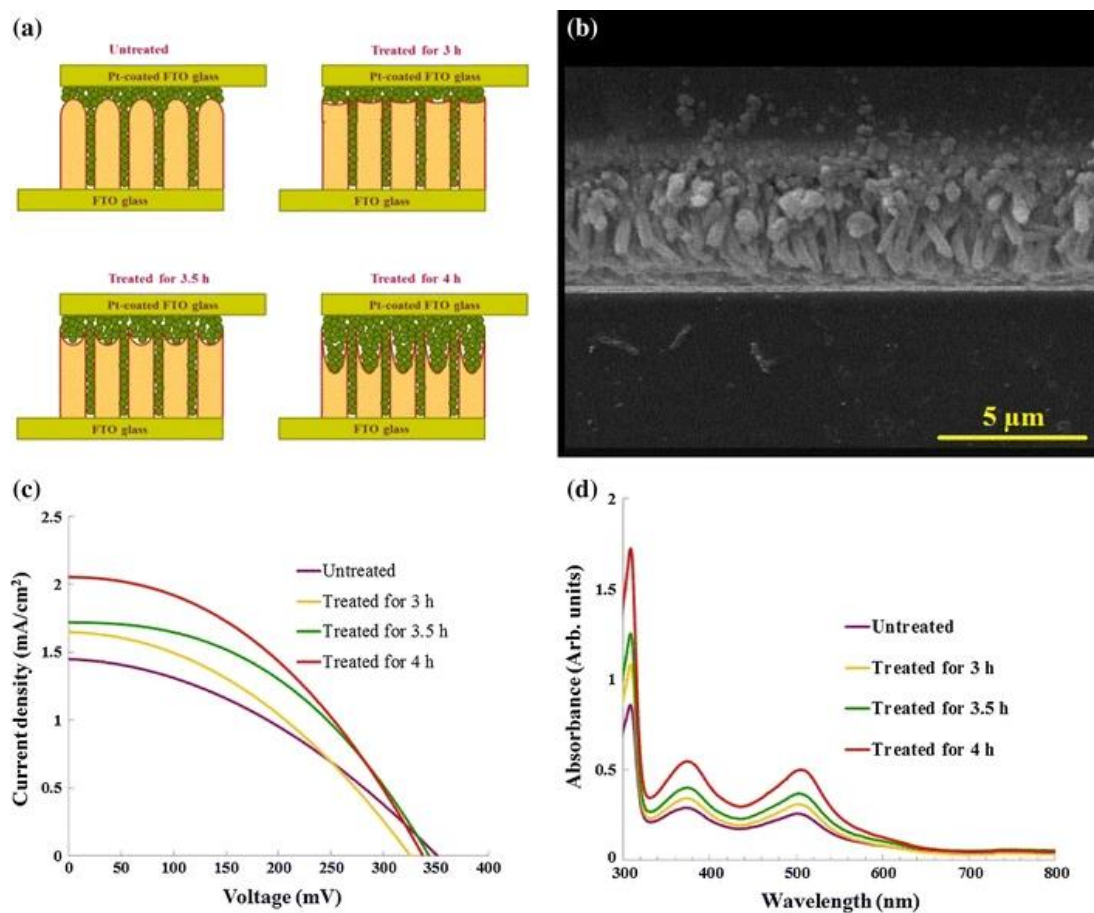


Figure 13. (a) Schematic images and (b) cross-sectional FE-SEM image of the constructed solid-state DSSCs based on 1D TiO_2 NSs (NRs and NTs), (c) current density–voltage characteristics of the solid-state DSSCs made from hydrothermally treated 3% Ce-doped TiO_2 NRs under simulated AM1.5G solar light (100 mW cm^{-2}), and (d) UV–vis absorption spectra of the desorbed N719 dye molecules from the photoanodes. **Permission is required from [39].**

In the last few years, PSCs have gained much attention because of their potential to be commercialized for real practical applications [55, 66, 149, 278, 296]. In a very short time, PCE

more than 22% has been recorded which shows a revolutionized progress in the solar cell industries. A PSC device consists of a light absorber material called perovskite material which produces charge carriers, an electron, and a hole transport material generally called electron transport materials (ETM) and hole transport materials (HTM) respectively along with electrodes (**Figure 14**)[168, 278]. The higher PCE as reported in recent literature is due to the unique optoelectronic properties of perovskite materials that could further be improved by engineering or modification of other components such as ETM or HTM [278]. As ETM, TiO_2 is the first choice in PSCs due to its better optoelectronic and transport properties. In PSCs, the TiO_2 layer promotes the collection and transport of the photo-generated electrons from the perovskite layer to the electrode [168, 278]. Other important factors for efficient PSCs is the band alignment of TiO_2 with perovskite material and electrical conductivity. If pure TiO_2 is applied as ETM, then it may lead to the accumulation of photo-generated electrons at the interface of ETM and perovskite layer resulting in the lower PCE of the PSCs [168]. Zhang et al. [168] mentioned that doping ETM with RE metal could be a promising way to avoid these issues and to improve the photovoltaic properties of PSCs. A planar PSC was designed using RE metal co-doped (Sm and Eu) TiO_2 layer as ETM and dopant concentrations were optimized to achieve the higher PCE as compared to the device with undoped TiO_2 (Figures 14 A-E). The co-doped TiO_2 electron transport layer showed improved transport properties such as greater electron extraction from the perovskite layer and lower interfacial charge recombination resulting in the enhanced photovoltaic properties and efficiency of the solar cell device [168]. Also, RE metal doping has been shown to tune the band alignment of TiO_2 with perovskite materials in PSC structure as a promising way for facilitating charge transport which further improves the performance of the device [297].

There are several reports on the enhancement of PCE and photovoltaic properties of PSCs using RE doped TiO_2 ETM [168, 181, 297-299]. For example, Gao et al. [297] demonstrated that the La-doped TiO_2 ETM layer could be useful for tuning its Fermi level which improved the efficiency of the device attributed to the induced oxygen vacancies. These modifications enhanced the open-circuit voltage, fill factor, and PCE (around 16% PCE) higher than PCE (12%) of the PSC device with undoped TiO_2 [297]. Similarly, PSCs using 1D TiO_2 NSs [300] and RE doped 1D TiO_2 NSs [77, 149, 180, 181] have extensively been reported with better photovoltaic properties and stability in recent years due to unique properties of 1D geometry of the NSs. For example, Zhang et al. [149] reported a 16.5% enhancement in PCE of perovskite-based solar cell

devices using RE doped TiO₂ NRs (Er-TiO₂ NRs) arrays as compared to undoped NRs based device. These doped NRs showed decreased bandgap and wide absorption up to near infra-red (NIR) radiation that upconverts that into the visible light. The designed PSC was made to use NIR absorption with a high-performance PCS device due to the upconversion properties of Er-doped TiO₂ NRs and improved optoelectronic properties (**Figure 14F**). Similarly, Chen et al. [77] and Wang et al. [180] reported 17% and around 21% enhancement in PCE of PSCs using Er/Mg and Er/Yb co-doped TiO₂ NRs arrays, respectively, as compared to that of the PSCs based on pure TiO₂ NRs arrays. Similarly, Wang et al [94] reported an inverted pyramid Er/Yb³⁺ co-doped TiO₂ NRs based PSC with NIR absorption exhibiting enhanced current density and PCE.

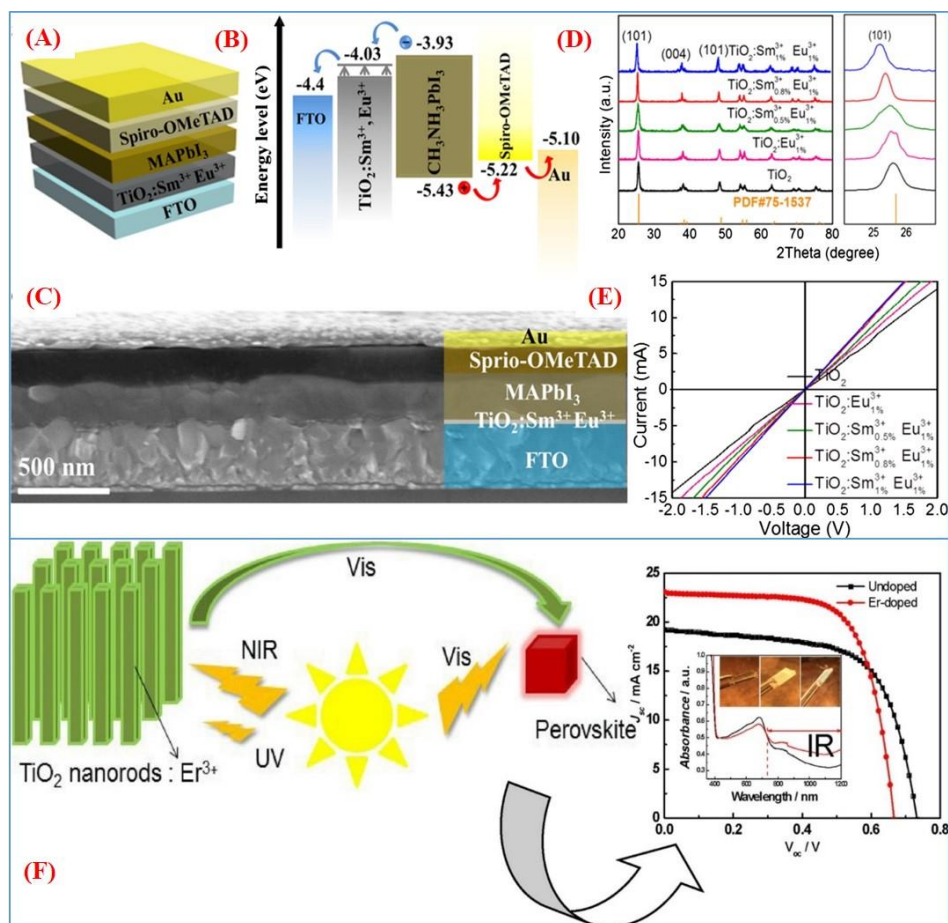


Figure 14. Schematic diagrams of (A) device architecture and (B) energy levels of each functional layer in the PSCs. (C) Cross-sectional SEM view of the device. (D) XRD patterns and (E) typical current-voltage curves (two probes system measurement) of different TiO₂ films prepared by PLD at applied voltage -2 to 2 V. **Permission is required from [168].** (F) PCS designed with Er-doped TiO₂ NRs arrays with high-performance photovoltaic properties. **Permission is required from [149]**

For the last few years, solar cell technology has many significant improvements especially PSCs where TiO_2 based various modified NSs have been used for enhancing the efficiency of the solar cells. Recent advances show that the doping 1D TiO_2 NSs introduced several modifications to improve optoelectronic properties such as reduction of NSs size, surface defects, and bandgap between CB and VB along with the enhancement of electron concentrations and electrical conductivity [284]. On the other hand, higher doping is introduced in the transformation of the morphologies and structural defects leading to the decay of such properties. However, it has been found that doping RE metal ions in TiO_2 NSs is a promising technique for producing novel transport materials to design efficient solar cells as shown by the number of published works in the literature. However, more developments are required to enhance their efficiencies and especially the stability of the perovskite materials for practical applications.

5.3 Photoelectrochemical water splitting applications

The photo-electrochemical (PEC) splitting of water to produce O_2 and hydrogen (H_2) using solar radiation is one of the promising ways to handle issues related to energy and the environment [301]. **Figure 15** shows a schematic of PEC device where splitting of H_2O with two electrode systems is shown [302]. In a PEC device, a suitable semiconductor electrode is immersed into an aqueous electrolyte which under the influence of sunlight provides excited charge carriers for the splitting of H_2O into H_2 and O_2 as shown in **Figure 15**. This is the process of how photon energy converts into electrochemical energy [302, 303].

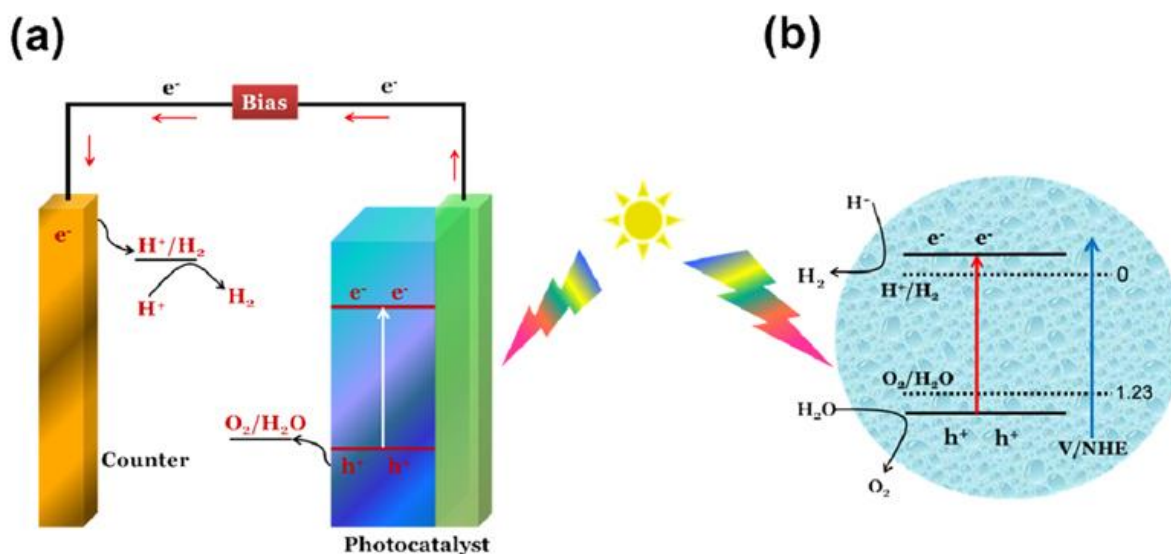


Figure15. The mechanism of (a) PEC cell and (b) photocatalytic water splitting [302] (**permission not required**)

Various semiconductor nanomaterials including TiO₂ NSs have been researched in photocatalytic water splitting but due to less effectiveness in charge transport and visible light absorption, it is still a challenging area to produce a suitable material with the required qualities [302-304]. Recent literature indicates that improvement of these properties by tailoring the shape, doping 1D TiO₂ NSs, heterojunction formation, etc. could be a promising technique in PEC splitting of H₂O as studied experimentally as well as theoretically [92, 225, 305-312]. For example, Cho et al. [308] demonstrated that hierarchically branched TiO₂ NRs were proven to be model NSs for high-performance PEC devices with photocurrent nearly twice as greater as compared to the device using unbranched NRs. It was attributed to the increased contact area of branched TiO₂ NRs, ability to trap the electrons and straight conductive pathway for charge transport, etc. Several studies have been reported with RE metal-doped 1D TiO₂ NSs for improving the efficiency of PEC cells for water splitting, for example, Nb-doped TiO₂ NTs, NRs, NFs [92, 313, 314], Gd doped TiO₂ NRs [89], Ta doped TiO₂ NRs [315, 316], NTs [69, 211], NWs [317], etc.

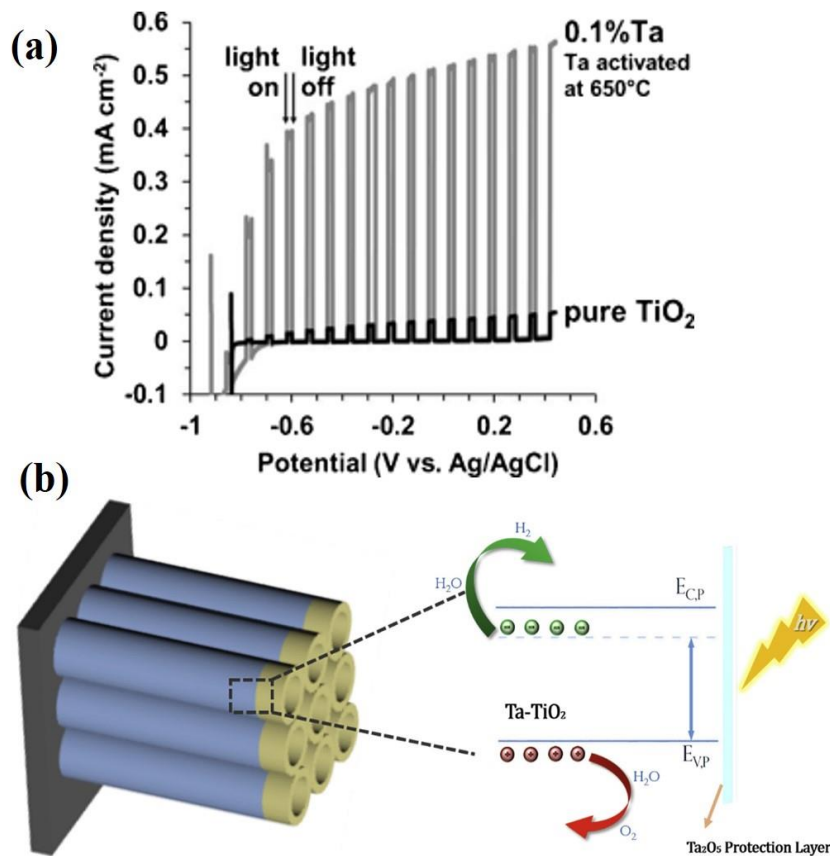


Figure 16. (a) Enhanced photocatalytic water splitting activity of Ta doped TiO₂ NTs under simulated sunlight conditions. **Permission is required from** [69] (b) proposed model for the Ta doped TiO₂ NTs PEC water splitting. **Permission is required from** [211].

Wang et al. [92] studied the effect of Nb doping in TiO₂ NRs (produced by hydrothermal technique) for investigating the charge transport behavior and its role in H₂O oxidation as a photoanode. It was found that 0.25% Nb-doped TiO₂ NRs based PEC cell exhibited photocurrent enhancement of 65% as compared to that made of undoped NRs. A few recent reviews are discussing the improved charge transport in doped 1D TiO₂ NSs based electrodes for PEC applications [306, 310]. Altomare et al. [69] showed that optimized Ta doped TiO₂ NTs showed better PEC H₂O splitting as compare to the pure TiO₂ NTs (Figure 16 (a)). Yan et al. [211] reported Ta doped TiO₂ NTs with enhanced photoconversion efficiency from 0.28% to 0.63% when compared to undoped NTs. TiO₂ NTs were prepared by anodic oxidation of Ti followed by magnetron sputtering of Ta and further annealing. It was proposed that when Ta doped TiO₂ NTs photoelectrodes were irradiated with the sunlight, Ta₂O₅ distributed on the surface of the NTs prevent the recombination of the charge carriers. Also, a decrease in bandgap and enhanced charge transfer properties finally enhanced the efficiency of the PEC cell (Figure 16 (b)).

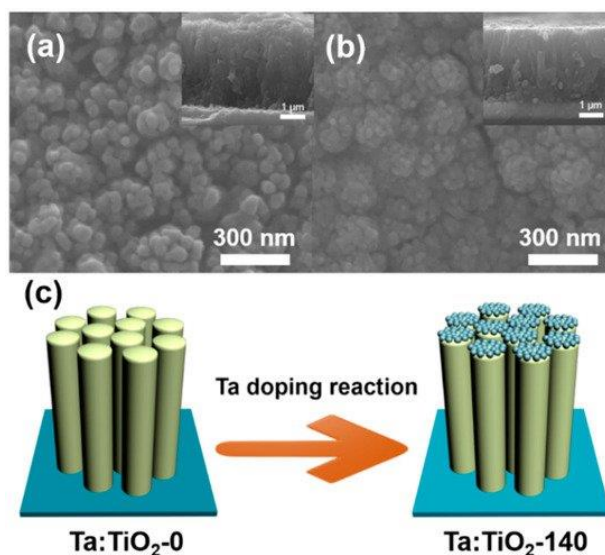


Figure 17. SEM micrographs of (a) Ta doped TiO₂ NRs and (b) Ta doped TiO₂ NRs deposited with nanoparticles on the top. The inserts in (a, b) are the corresponding cross images, (c) the schematic description of the morphology change after the Ta doping reaction [318]. **Permission is not required.**

Similarly, Gd doped TiO₂ NRs synthesized by the hydrothermal method were studied for PEC performance [89]. It was shown that Gd doping existed into TiO₂ lattice and deposited on the

surface in the form of Gd_2O_3 nanoparticles which played important role in preventing the recombination of photo-generated charge carriers and improving the charge transfer process. This assembly provided increased photocurrent and photoconversion efficiency of PEC cells as compared to bare TiO_2 NRs. Interestingly, He et al. [318] synthesized hierarchical Ta doped TiO_2 NRs arrays with deposited Ta nanoparticles on the top of the NRs as a suitable photoanode for the PEC water splitting. These NSs assemblies improved the charge separation and interfacial area between the electrolytes respectively for effective charge transport with enhanced photoconversion efficiency as compared to bare NRs (**Figure 17**). The same group [315] recently reported Ta doped porous TiO_2 NRs arrays with efficient PEC water oxidation using the modified hydrothermal technique on Ti foil. The PEC device formed with these nanoporous Ta doped TiO_2 NRs exhibited excellent photo conversion efficiency around 4 times greater than that of pure NRs and attributed to the porous structure of TiO_2 NRs. Hoang et al. [317] synthesized Ta and N co-doped TiO_2 NWs and implemented them as photoanode in PEC for photocatalytic oxidation of H_2O . It was observed that co-doped NWs showed better response because of photocatalytic activities as compared to N doped TiO_2 NWs.

In recent years, PEC technology has been very progressing and a variety of materials have been used showing greater efficiencies. Out of various nanomaterials, TiO_2 based NSs have shown promising aspects in this field with several modifications. Doping has been found as a simple technique for PEC to modify its properties in combination with various synthesis techniques to tailor the shape and size of the TiO_2 NSs which additionally improves the surface properties along with the optoelectronic properties. RE doped 1D TiO_2 NSs in combination with other functional nanomaterials should also be explored in PEC for better results.

5.4 Applications in photocatalytic reduction of CO_2

The photocatalytic reduction of CO_2 , to convert into useful fuel like products such as methane, alcohol, etc., is one of the important research fields because of energy and environmental applications [319-324]. This process is beneficial in two ways, on one hand, it helps in the mitigation of its emission, and on the other hand, it provides industry-based useful chemicals [323]. The production of new and potential photocatalyst materials for the photocatalytic reduction of CO_2 has been progressing very fast for the last few years. Although, several research papers have been appeared related to this topic, however, conversion of CO_2 into useful products using solar

energy is not so promising for real practical applications due to the lack of efficient photocatalyst materials. **Figure 18** exhibits the schematic of photocatalytic reduction of CO_2 using (a) only a semiconductor photocatalyst and (b) PEC cell consist of semiconductor photocatalyst-based electrodes under the influence of solar light [323]. As discussed earlier, due to inefficient charge transfer capability, wide bandgap, and high recombination rate of the photo-generated charge carriers, TiO_2 NSs have been modified to make promising photocatalysts for this purpose. Due to the enhanced photocatalytic properties with reduced bandgap and extended visible light activity, modified 1D TiO_2 NSs have been considered as promising materials for the photocatalytic reduction of CO_2 [322, 325-331].

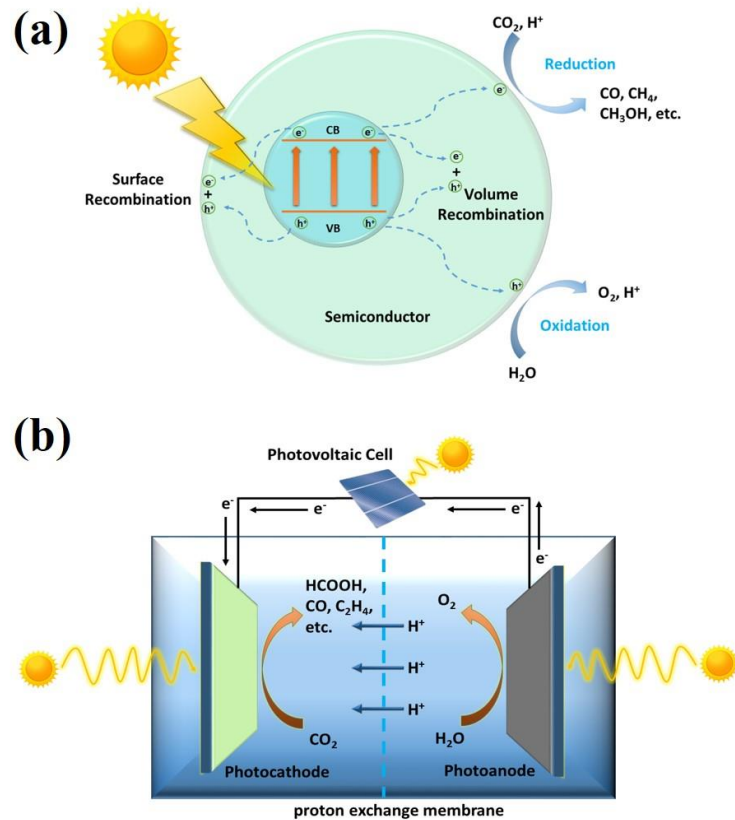


Figure 18. (a) The schematic of the photocatalytic reduction of CO₂. **(b)** photoelectrocatalytic reduction of CO₂. **Permission is required from [323].**

There are several studies using 1D TiO₂ NSs doped with transition metals to improve the optoelectronic and transport properties for the photocatalytic reduction of CO₂ [332-335]. Recently, Camarillo et al. [335] reported a remarkable enhancement in the photocatalytic reduction of CO₂ using Cu doped TiO₂ NFs. In this report, it has been mentioned that surface area, crystallites size, etc. does not make effect on photocatalytic reduction of CO₂. However, it has been suggested that the tubular morphology and greater length of the 1D TiO₂ NSs could be more promising to achieve higher reduction efficiency. There are only a few studies that have been carried out using RE doped TiO₂ NSs for photocatalytic CO₂ reduction which show improved photocatalytic CO₂ reduction efficiencies attributed to the incorporation of the RE metal ion doping in TiO₂ NSs. Luo et al. [336] performed an experimental and theoretical study on Cu and Ce co-doped TiO₂ NSs for CO₂ photoreduction. It was explained that along with Cu, Ce doping further enhanced the photocatalytic efficiency with the yield of methanol up to 188 μmol g⁻¹. Based on the theoretical investigation, it was demonstrated that Ce incorporation influenced the photocatalytic reaction better than that of Cu doping by activating the CO₂ and H₂O molecules on the surface of the photocatalyst. Similar results were obtained by only Ce doped TiO₂ by Xiong et al. [88]. Similarly, there are some reports on enhanced photocatalytic reduction of CO₂ using Sm, Ce, Nb, La-doped different TiO₂ NSs [87, 333, 337, 338]. Recently, CeO₂-TiO₂ nanocomposites-based 1D [339] and 2D [340] NSs were investigated for the CO₂ conversion. TiO₂-CeO₂ NRs prepared by the hydrothermal method and the effect of doping was investigated for the conversion of CO₂ and methanol to dimethyl carbonate [339]. It was reported that catalytic sites on the surface of NRs could be tailored through doping for promoting the catalytic effect. These CeO₂-TiO₂ nanocomposites NRs showed excellent activity with a methanol conversion of 5.38% and dimethyl carbonate selectivity of 83.1%. Liu et al. [341] researched on hydrogenated TiO₂ NRs/NWs from the surface chemistry point of view and found that some of the surface facets showed enhanced charge separation and excellent CO₂ photocatalytic reduction.

There are only a few studies focusing on the doping effect in 1D TiO₂ NSs using RE metals ions from the photocatalytic reduction of CO₂ point of view. However, this field is progressing and a great deal of research is being carried out in this direction. These materials could be explored

in this field due to their potential to upgrade the research output and better understanding of their mechanism.

5.5 Lithium-ion batteries applications

The lithium-ion battery (LIB) has proven to be a very reliably used system to store electrical energy for various applications, including mobiles, electric vehicles (EVs), stationary, etc. A commercial LIB consists of a negative electrode (e.g. carbon/graphite) and a positive electrode (e.g. LiCoO_2 , LiFePO_4), which are kept apart by a separator that is soaked with an electrolyte, typically a LiPF_6 salt in a mixture of organic solvents, as displayed in **Figure 19** [342].

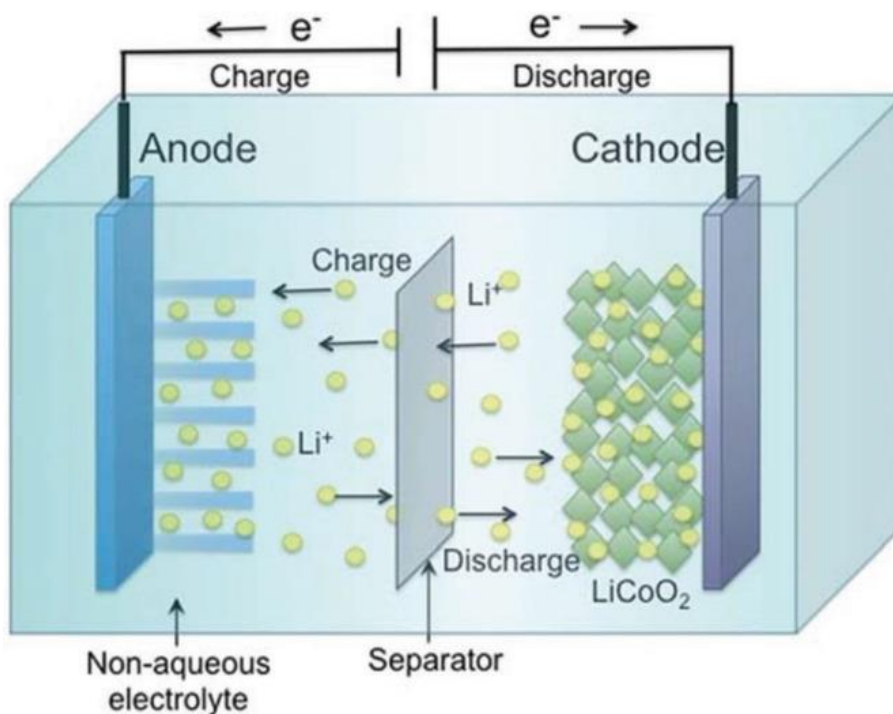
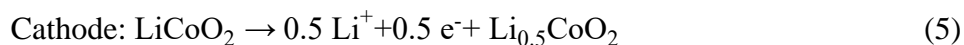


Figure 19. Schematic illustration of the lithium-ion battery. Reproduced with permission [342] Copyright © The Royal Society of Chemistry 2015.

During the charge progress, lithium ions are extracted from the lattice of the positive electrode material, migrate to the graphite anode through the electrolyte, and react with the graphite to generate LiC_6 , during the discharge progress, lithium ions are extracted from the negative electrode and embedded in the cathode material through the electrolyte, as showed in **Equation 5 and 6**. [343].





However, in terms of anodes, the commonly used graphite anode is the bottleneck to achieving high energy densities due to its lower theoretical capacity (372 mAh g^{-1}). Among various alternatives, transition metal oxides have attracted great attention from researchers [344-349]. For example, TiO_2 -based anodes are becoming one of the most attractive candidates for building safe and durable LIBs due to the high energy density, high Li^+ insertion/extraction voltage ($\sim 1.6 \text{ V}$ versus Li^+/Li) compared with other anodes (e.g. $\sim 0.1 \text{ V}$ for graphite, chemical stability, and inexpensive cost [346]). However, TiO_2 has its inherent drawbacks when employed for LIB anode applications, such as low ionic diffusivity and electronic conductivity [350]. A variety of TiO_2 NSs have been thoroughly investigated as anodes in LIBs. Indeed, developing anode materials for lithium-ion batteries with higher performance and competitive price is still the main hurdle to reduce weight and improve the performance of LIBs [351].

Nanoscale materials for battery electrodes have been found to increase lithium-ion diffusion, in particular, 1D NSs such as NRs, continuous NFs or NWs whose main advantage is high surface area and specific particle morphologies often tailored for that purpose [352-354]. In this regard, researchers have made many efforts including doping, coating, and other technologies to improve the conductivity of TiO_2 [355-363]. Among them, metallic/nonmetallic elements doped 1D TiO_2 will not only enhance the intrinsic electrical conductivity of TiO_2 but also can make electrons transit from Ti^{3+} sites with low valence states to Ti^{4+} sites with high valence states to improve the lithium-ions diffusion [364].

Transition metals have drawn great attention in the field of the doping process [365, 366]. For example, Wang et al. [367] firstly synthesized the Nb-doped (6.5%) TiO_2 anode material for LIBs via a polymer-assisted sol-gel process. This device achieved a specific capacity of 160 mAh g^{-1} after 100 cycles due to the fast Li-ion diffusion of Nb-doped TiO_2 . Bi et al. [368] used a hydrothermal approach with annealing under the ammonia atmosphere to prepare a Cr and N-codoped 1D TiO_2 electrode for LIBs. The battery showed an excellent specific capacity of 159.6 mAh g^{-1} at a current density of 1675 mA g^{-1} with a doping level of 5.68 at.% for Cr and N codoped 1D TiO_2 . Zhang et al. [369] utilized a facile ion-exchange approach to preparing a novel Ni-doped TiO_2 electrode for LIBs. Zhang and co-workers [370] fabricated Mn-doped TiO_2 nanosheet electrodes for application in LIBs. Thi et al. [371] reported a Mo-doped anatase-type TiO_2 anode electrode via a solvothermal approach to improving the LIB electrochemical

performance. Moreover, Zhou et al. [372] utilized thermal-oxidation stabilization, hydrothermal reaction, and carbonization method to prepare a MoS₂-doped 1D TiO₂ NFs electrode for application in lithium-ion batteries. Furthermore, the N-doping method is also usually used to improve the conductivity of TiO₂ [358, 373-377].

Although the doping of these elements can improve the electronic conductivity and the capacity of the TiO₂ electrode material to a certain extent, the large capacity change in the initial cycle and the capacity attenuation after multiple cycles are still unaddressed problems. Therefore, some researchers used RE elements, including Sm, Gd, La, and so on, to enhance the cyclic stability of lithium-ion batteries by using 1D TiO₂ as an anode electrode. For example, Li et al. [378] utilized a solvothermal synthesis method to manufacture a Gd-doped single-crystalline Li₄Ti₅O₁₂/TiO₂ (rutile phase) electrode in lithium-ion batteries. The device delivered excellent cyclic stability with 96.1% capacity retention at a current density of 200 mA g⁻¹ after 200 cycles. Moreover, even at 5 A g⁻¹, the device also obtained a high specific capacity of 145.8 mAh g⁻¹ after 500 cycles. These results illustrated that the intrinsic conductivity and the structural stabilization of the anode electrode were enhanced due to the addition of Gd³⁺. Furthermore, Abhilash et al. [379] firstly analyze the electrochemical performance of the TiO₂ anode electrode with the addition of Sm³⁺ ions via a sol-gel approach. As displayed in Figure 2a, Sm doped TiO₂ electrode was characterized by the XRD technique. The peaks at 54.02° and 55.02° were attributed to the formation of the Ti-O-Sm bond, which demonstrated that the Sm was successfully doped into TiO₂. Moreover, The Sm doped TiO₂ electrode (Sm_{0.1}Ti_{0.9}O₂) could provide more free volume for the intercalation of the ions through the lattice at the lower concentration of Sm ions. The corresponding lattice fringes with nanocrystalline domains in the Sm_{0.1}Ti_{0.9}O₂ materials clearly illustrate the formation of uniform nanoparticles with a smaller particle size than the parent TiO₂ sample, as presented in Figure 20 b-d. To study the electrochemical performance of Sm doped TiO₂, the long cycle performance and CV measurement were conducted, as shown in Figure 20e. The Sm_{0.1}Ti_{0.9}O₂ electrode delivered a discharge specific capacity of 194.09 mAh g⁻¹ and displayed the lower irreversible capacity loss (0.71%) in comparison with bare TiO₂. Even after 50 cycles, the device with the Sm_{0.1}Ti_{0.9}O₂ electrode exhibited approximately 100% capacity retention, demonstrating excellent cyclic stability of the Sm doped TiO₂ electrode. To further identify the electrochemical cyclic performance of TiO₂ without or with Sm ion-doped, the CV test was measured at a scan rate of 0.1 mV s⁻¹ after 5 cycles (Figure 20e, Inset figure). Compared with the

pristine TiO_2 electrode, the $\text{Sm}_{0.1}\text{Ti}_{0.9}\text{O}_2$ electrode exhibited a larger area and higher current, illustrating the better electrochemical performance of the device.

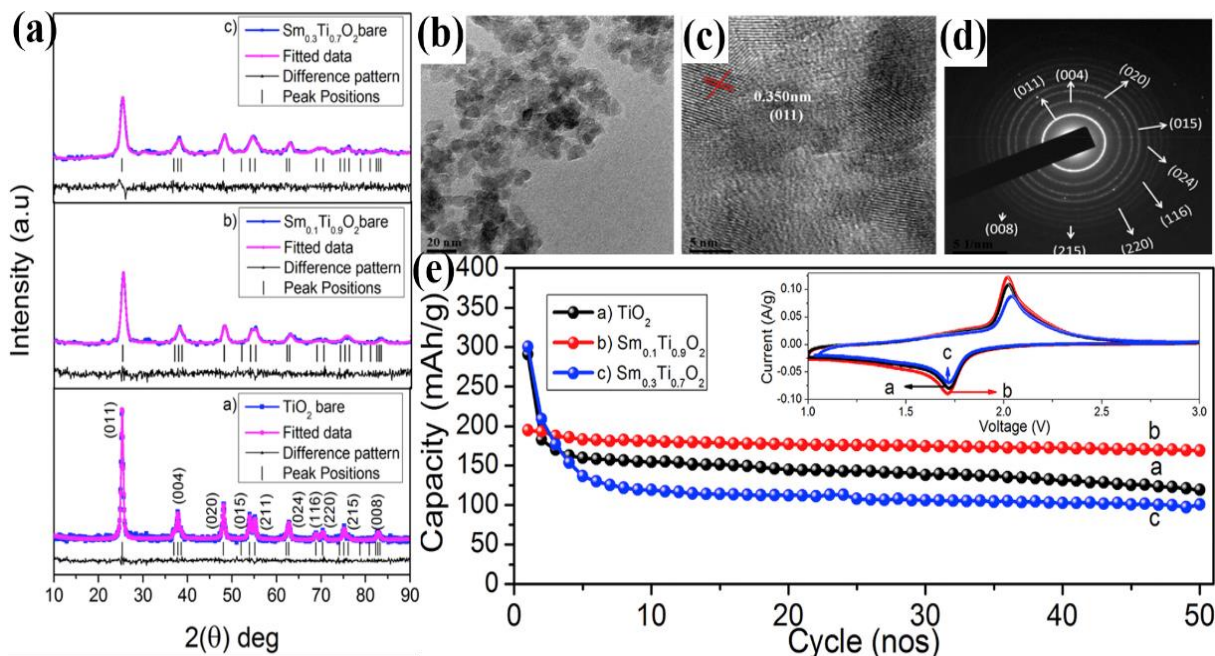


Figure 20. (a) XRD spectra of TiO_2 with or without Sm doped, (b-d) TEM images of $\text{Sm}_{0.1}\text{Ti}_{0.9}\text{O}_2$ electrode, (e) electrochemical performance of the TiO_2 electrode with different Sm content. The inset figure is the CV curves with different doping Sm content. Reproduced with permission [379]. Copyright © 2017 Elsevier B.V. All rights reserved.

Zhang et al. [380] reported a $\text{TiO}_{2-\delta}\text{-La}$ electrode, which was prepared by heating the ethanol solution of $\text{La}(\text{NO}_3)_3 \cdot 6\text{H}_2\text{O}$. Figure 21a exhibited the preparation progress of the $\text{TiO}_{2-\delta}\text{-La}$ electrode. Figure 21b displayed the electron spin resonance (ESR) result of bare TiO_2 and $\text{TiO}_{2-\delta}\text{-La}$ electrode. The ESR signal of $g = 2.003$ was attributed to single-electron-trapped oxygen vacancy (named as SETOV, V_o) and the reaction mechanism was shown in Equations 3 and 4. The signal of oxygen vacancy demonstrated the presence of Ti^{3+} ions. However, there was no signal of Ti^{3+} in bare TiO_2 . Therefore, the Ti^{3+} species can be stabilized by the addition of La and could enhance the electrochemical performance of TiO_2 . As displayed in Figure 21 c-d, the $\text{TiO}_{2-\delta}\text{-La}$ electrode delivered a higher rate performance than pristine TiO_2 and the device with $\text{TiO}_{2-\delta}\text{-La}$ electrode exhibited high discharge capacities of 152 mAh g^{-1} and 142 mAh g^{-1} at 10 C and 20 C, respectively. Moreover, the $\text{TiO}_{2-\delta}\text{-La}$ electrode exhibited excellent cyclic stability with 87% capacity retention at a current density of 10 C after 1,000 cycles compared with bare TiO_2 (81%). The initial capacity of the TiO_2 electrode enhanced from 80 mAh g^{-1} to 150 mAh g^{-1} with the

introduction of La. The excellent electrochemical performance of La-doped TiO₂ could be attributed to the following reasons: (1) the doping La ions enhance the stability of Ti³⁺ in TiO₂ nanotube; (2) Ti³⁺ may effectively improve the electronic conductivity of TiO₂; (3) TiO₂ NTs with hollow structure could promote the kinetics of the lithium intercalation/deintercalation.

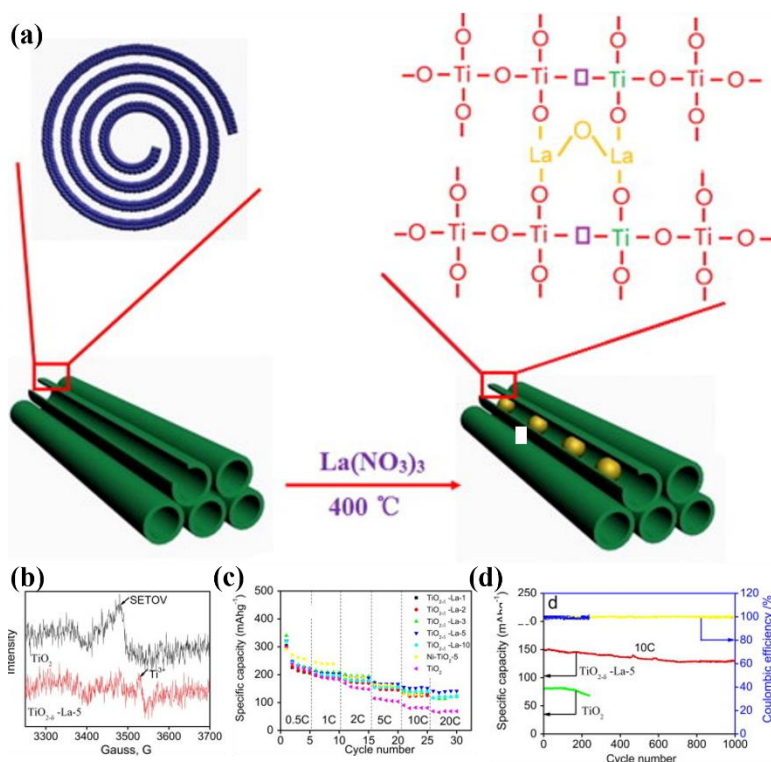


Figure 21. (a) The preparation progress of the TiO_{2-δ}-La electrode, (b) ESR spectra of bare TiO₂ and TiO_{2-δ}-La, (c, d) electrochemical performance of bare TiO₂ and TiO_{2-δ}-La electrode. Reproduced with permission [380]. Copyright © 2014 Elsevier B.V. All rights reserved.

The doped TiO₂ NSs elaborated by various synthesis techniques presented a higher rate capability in electrochemical cycling experiments than undoped NSs attributed to the reduction of Li⁺ diffusion path lengths and enhanced intimate interparticle contact, in combination with improved intraparticle conductivity. The doping had shown a significant effect on the electronic structure and provoked a substantial decrease in particle size, increase in electronic properties [234] leading to enhanced electrochemical performances in the case of Li-ion batteries. This is one the hot research field and lots of progress are being carried out using different strategies for the betterment of society.

5.6 Applications in supercapacitors

Supercapacitors, which are often called electrical double-layer capacitors (EDLCs) or pseudocapacitors, have attracted extensive research interests worldwide because of their potential applications as energy storage devices in many fields. Supercapacitors have considerably higher specific powers and longer cycle lifetimes compared to most rechargeable batteries, including Li-ion batteries. Long service life, strong environmental adaptability, high charge, and discharge efficiency, and high energy density are the four significant characteristics of supercapacitors. Recently, a highly integrated energy system with multi-functional performance has attracted worldwide attention from researchers. With this perspective, electrochromic (EC) supercapacitors are one of the most important systems for portable electronic devices and the use of renewable energy [381, 382].

1D TiO₂ NSs have attracted great attention from researchers in the field of EC devices due to their excellent electrochemical activity, high energy density, and environmentally friendly nature. [383, 384] For example, Lv et al. [385] utilized a single-source precursor Ti₈O₇(OEt)₂₁Er to prepare a novel Er-doped TiO₂ electrode for EC supercapacitor, and the structure of precursor was presented in Figure 22 a. Using this kind of precursor could dope Er ions homogeneously into the TiO₂ matrix and improve the electric conductivity and enhance the structural stability during the charge/discharge progress. Figure 22 b-d displayed the color change of EC supercapacitor at different states. Before cycling, the assembled EC supercapacitor showed yellow color. However, due to the high adsorption of the device, which reduced the transmittance of incident light in the visible range during the charge progress. So, the EC supercapacitor exhibited a dark gray color when the potential got up to 1.3 V (Figure 22 c). At the discharge state, the color of the EC supercapacitor was changed to bleached when the potential less than 0.3 V (Figure 22 d). To study the electrochemical performance of the EC supercapacitor, galvanostatic charge/discharge profiles were measured at different current densities, as shown in Figure 22 e. The charge/discharge curves exhibited the pseudocapacitance behavior due to the redox reaction of Er-doped 1D TiO₂. The device exhibited a capacity of 0.020 F cm⁻² at a current density of 0.5 mA cm⁻² and 0.016 F cm⁻² at a current density of 1.0 mA cm⁻². These results illustrate that it is feasible and effective to amalgamate EC supercapacitor with nanostructured Er-doped TiO₂, and it is worthy of further research in practical applications.

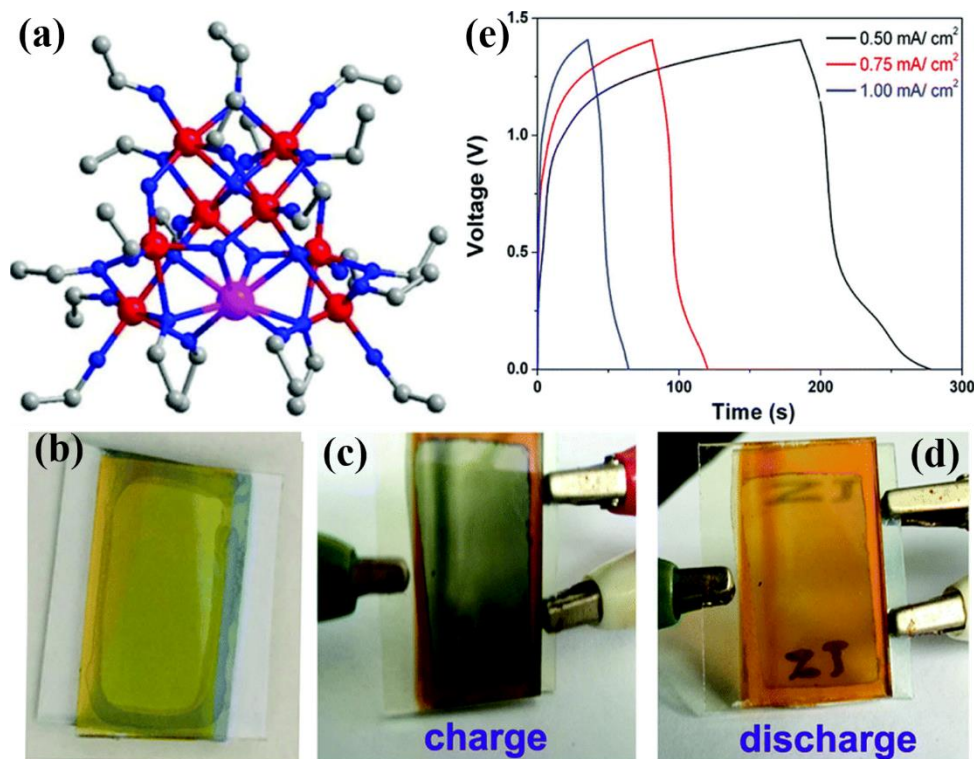


Figure 22. (a) The structure of heterometallic polyoxotitanate cage $[\text{Ti}_8\text{O}_7(\text{OEt})_{21}\text{Er}]$. EC supercapacitor at different states: (b) before cycling; (c, d) at charge and discharge states, respectively. Reproduced with permission [385]. Copyright © the Partner Organisations 2016.

5.7 Upconversion properties for photocatalytic applications

RE metal doping in TiO_2 has shown great potential to improve various properties including photocatalytic properties as discussed above. Particularly, La-doped upconversion nanophosphors are promising in this regard due to their upconversion properties. Upconversion luminescence is a nonlinear optical process that allows to conversion of photons with low energy (visible or NIR) into high energy (UV light). The ladder-like energy levels of trivalent lanthanide ions embedded in suitable host material emits UV or visible photons through sequential absorption of multiple visible or NIR photons. The process of transformation of light photons from visible/NIR to UV/visible could be used to excite wide bandgap semiconductors, for example, TiO_2 . Most explored lanthanide ions to activate TiO_2 photocatalysts through NIR to UV or visible to UV upconversion process are Er^{3+} , Ho^{3+} , Nd^{3+} and Tm^{3+} ions. The upconversion mechanism takes place primarily through ground-state absorption (GSA) or excited state absorption (ESA) [386]. The anti stokes shift occurs by subsequent absorption of two or more photons to reach the excited

state and subsequently emitting higher energy photon. The upconversion property of lanthanide-doped TiO₂ can be directly related to their photocatalytic activity [73].

Er³⁺ doping in TiO₂ NSs

The upconversion property of Er³⁺ doped TiO₂ photocatalyst has been widely explored. Upon irradiation of visible/NIR light photons, the presence of Er³⁺ ion promotes the upconversion and convert light photons from visible/NIR to UV which can be further effectively utilized to activate TiO₂ photocatalyst. Obregón et. al., [387] have observed frail UV photoluminescence emissions centered at 390 nm and 415 nm on the illumination of Er³⁺ doped TiO₂ photocatalyst using 980 nm laser. The sequential absorption of three photons (⁴I_{15/2} → ⁴I_{11/2}, ⁴I_{11/2} → ⁴F_{7/2}, and ⁴S_{3/2} → ²G_{7/2}) results in further multiphoton relaxation by decaying to lower ²G_{11/2} and ²H_{9/2} states. The emission produced by ²G_{11/2} → ⁴I_{15/2} transition in UV region at approximately 390-400 nm as shown in Figure 23. Thus, the availability of photons with appropriate energy results in the improved photocatalytic activity of Er³⁺-TiO₂ photocatalyst. Mao et. al.,[388] observed intense green and red emission peaks centered at 490 nm and 670 nm, respectively, after excitation of Er³⁺ doped TiO₂ by a laser of 980 nm. In another study, Salhi et. al.,[389] has studied the upconversion properties of RE metal ions doped TiO₂ samples and observed emission peaks at 550, 525 nm (green region), and 655 nm (red region).

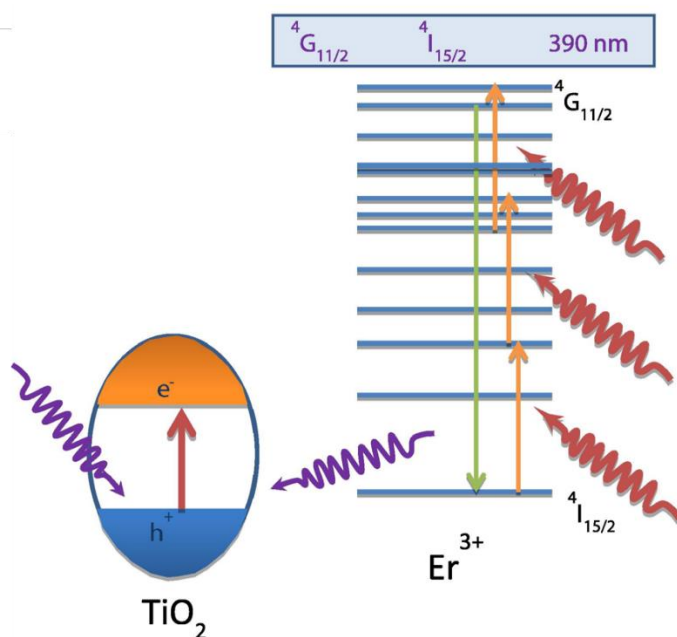


Figure 23. Energy level diagrams representing upconversion mechanism in Er^{3+} ions under 980 nm (NIR light) excitation. Reprinted and modified with permission from ref. [387] Copyright @ 2013 Elsevier publication.

Furthermore, Zhou et. al., [77] have fabricated Er and Mg co-doped 1D TiO_2 NRs arrays with a length of 900 nm using facile hydrothermal synthesis route. It was inferred that Mg doping onto TiO_2 narrows down the conduction band of TiO_2 and thereby redshift its absorption. Furthermore, doped Er^{3+} ions enable absorption of NIR light photon through ESA process and convert them into visible light. The converted photons were captured via TiO_2 to generate a charge carrier to initiate photocatalytic reactions. Similarly, Er^{3+} - Yb^{3+} - Li^+ tri-doped TiO_2 was used for effective conversion and utilization of NIR light photons for photocatalytic applications [390]. It was observed that loading of Li^+ ions enhances the upconversion luminescence as compared to Er^{3+} - Yb^{3+} doped TiO_2 . The introduction of Li^+ ions improves the crystallinity of samples and distortion of local symmetry around Er^{3+} ions. Furthermore, a detailed mechanism of upconversion was investigated via Guo et. al., for TiO_2 NWs arrays/ Er^{3+} - Yb^{3+} ions - TiO_2 nanoparticles system synthesized via a hydrothermal and spin coating process [391]. The presence of activator Yb^{3+} ions in composite shows strong absorptions around 980 nm NIR light. An optimized amount of the activator (Yb^{3+}) and sensitizers (Er^{3+}) were doped in TiO_2 photocatalyst. Similarly, Huang et. al., [392] have also optimized the dopant (Yb^{3+} and Er^{3+}) concentration in narrow band gap oxide $\text{Bi}_{20}\text{TiO}_{32}$ to design a highly fluorescent upconversion photocatalyst. The emitted green light photons (540 nm) are effectively utilized by $\text{Bi}_{20}\text{TiO}_{32}$ due to their suitable bandgap (~ 2.23 eV). Wei et. al., [90] have synthesized a well-organized CdSe-sensitized TiO_2 NRs array grown over FTO substrate coated with TiO_2 : Yb^{3+} / Er^{3+} thin film. TiO_2 nanotube array offers high surface area while Yb^{3+} / Er^{3+} doped TiO_2 thin film acted as a medium for converting NIR photons to visible photons via the upconversion process. It can be concluded that the full solar spectrum (UV, visible, and NIR) can be effectively utilized for photocatalytic applications by rationally designing a well-organized photocatalytic system.

Tm³⁺ doping in TiO₂ NSs

Doping of Tm^{3+} ions in anatase TiO_2 shows absorption in visible region centered at 469 nm, 696 nm and 795 nm which corresponds to the transitions $^3\text{H}_6(\text{Tm}^{3+}) \rightarrow ^1\text{G}_4(\text{Tm}^{3+})$, $^3\text{H}_6(\text{Tm}^{3+}) \rightarrow ^3\text{F}_3(\text{Tm}^{3+})$ and $^3\text{H}_6(\text{Tm}^{3+}) \rightarrow ^3\text{H}_4(\text{Tm}^{3+})$, respectively [393]. The increase in the absorption

intensity of the peaks was observed with an increase in the concentration of dopant ions. The presence of the ladder-like energy levels in Tm^{3+} ion results in the photonic absorption process and subsequently the photoluminescence emission properties. Santos et. al., [394] showed multiple absorptions centered at 466, 685, and 785 nm, belongs to Tm^{3+} ion transitions. Also, there are many reports in the literature where Yb^{3+} ions were used as an activator along with Tm^{3+} ions (sensitizer) doped in TiO_2 as shown in **Figure 24** [395-398]. The excitation of samples with 980 nm laser results in weak emissions in UV regions which are effectively utilized by TiO_2 .

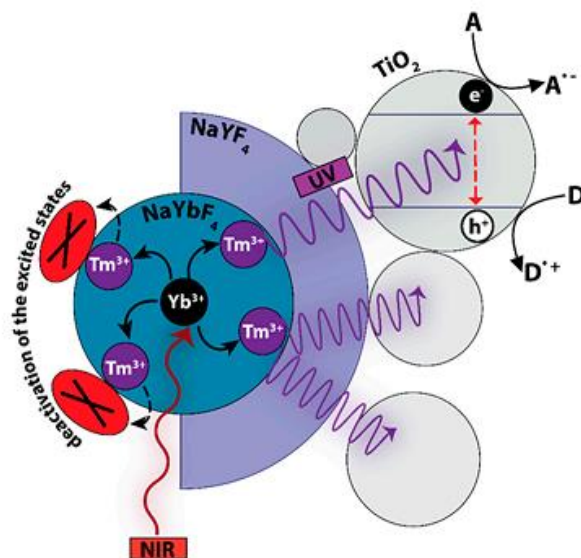


Figure 24. Proposed mechanism for the conversion of NIR photons to UV to activate TiO_2 photocatalyst. Reprinted with permission from ref. [397] Copyright @ 2020 MDPI publication. **Permission is not required.**

Ho³⁺ doping in TiO₂ NSs

Trivalent Ho^{3+} ions are found to be ideal activators due to their adequate ladder-like energy levels to show visible-light-driven photocatalysis. Energy transfer and photon upconversion occur through the energy transfer upconversion (ETU) mechanism on excitation of activator using 642 nm laser where multiple photon absorption and emission in UV region occur as shown in **Figure 25a**. However, it was observed that the presence of adventitious carbon over the surface of photocatalyst quench the luminescence of lanthanides which results in lower photocatalytic activity [399]. Xe et. al., [400] have reported the excellent photocatalytic activity of TiO_2 doped with upconversion Ho^{3+} ions. The activator Ho^{3+} ions show the strongest excitation under the visible region (450 nm) and the emitted light photons (290 nm) are effectively utilized by TiO_2

which results in separation of charge carriers. The same research group has also reported excitation of Ho^{3+} ions at 450 nm and 532 nm and the emitted UV light was utilized to activate TiO_2 .

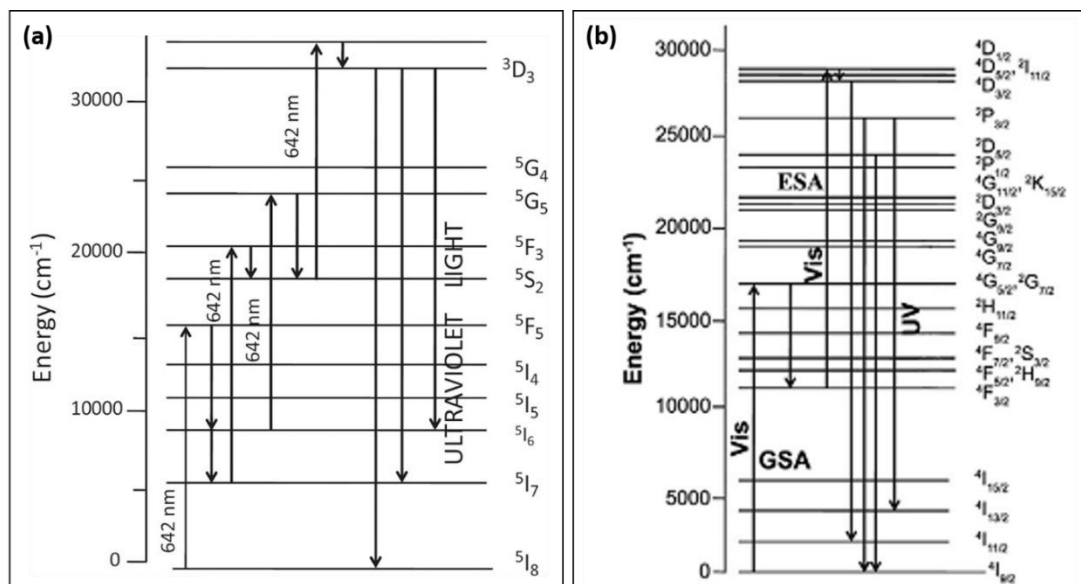


Figure 25. Simplified energy-levels diagrams of and excitation path for the upconversion emission (a) Ho^{3+} under 642 nm excitation and (b) Nd^{3+} under 578 nm excitation. Reprinted and modified with permission from ref. [399, 401] @ Elsevier publication.

Nd^{3+} doping in TiO_2 NSs

Nadolna et. al., [401] has reported enhanced photocatalytic activity by doping Nd^{3+} ions onto TiO_2 photocatalyst under visible light irradiation. The amount of doping of RE metal ions affects the catalytic activity of photocatalyst. The energy level diagram for upconversion excitation of Nd^{3+} ions through GSA and ESA are shown in Figure 4b. The emitted light photons in UV regions were further utilized by TiO_2 photocatalyst. Similarly, Rai et. al., [402] observed the upconversion properties of Nd^{3+} doped TiO_2 photocatalyst under 578 nm xenon lamp excitation and emissions at 380 nm ($4D_{3/2}$ - $4I_{11/2}$), 399 nm ($2P_{3/2}$ - $4I_{11/2}$), 420 nm ($2D_{5/2}$ - $4I_{9/2}$) and 452 nm ($2P_{3/2}$ - $4I_{13/2}$).

The upconversion properties of RE metal ions doped TiO_2 photocatalyst has been extensively studied for photocatalytic applications. The aforementioned literature reports clearly suggests that even very low loading of RE element can drastically improve the upconversion property and thereby the photocatalytic properties of the samples. Thus, this is a cost-effective approach for effectively utilizing the visible and NIR regions of solar spectrum, in addition to UV region. From the previous literature it can be inferred that the Er^{3+} , Ho^{3+} , Tm^{3+} and Nd^{3+} has been

widely explored as activators due to their ladder like arrangement while in few studies Yb^{3+} was used as sensitizer. In addition to above mentioned lanthanides, other lanthanide elements such as Tb^{3+} , Gd^{3+} , Pr^{3+} , Pr^{3+} , Sm^{3+} and Dy^{3+} have also been doped in TiO_2 to improve its photocatalytic activity [97, 403].

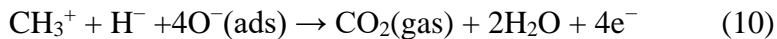
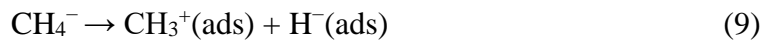
5.8 Environmental gas sensing applications

A gas sensor is a device which detects the presence or concentration of gases in the atmosphere. A specific gas can be detected by measuring the change in resistance of a material connected to two metal electrodes. The sensor produces a corresponding potential difference between the electrodes by changing the resistance of the material inside the sensor that depends on the concentration of the gas present that is measured as output voltage. The output voltage value provides significant information about the type and concentration of the gas [404-407]. Monitoring and detection of toxic and combustible gases in residential areas and different workplaces are of the uttermost importance which can prevent occurrences of fatal incidents such as fire, explosions, and poisoning [406]. For instance, high concentration of O_2 in underground mines and also the mixture of air and fuel in automobile engines poses a threat as it promotes combustion and therefore it needs to be monitored continuously. High concentration (>25 ppm) of poisonous ammonia (NH_3) in products such as fertilizers, pesticides and bleach is dangerous and if inhaled it can cause respiratory problems and may lead to fatal death [408]. Enhanced sensitivity and selectivity for specific type of gases, fast response and recovery at low temperature and concentration [406] are fundamental characteristics of modern age gas sensing devices. The major toxic and often odourless gases are hydrogen, nitrogen dioxide (NO_2), sulphur dioxide (SO_2), methane (CH_4), radon (Rn), NH_3 and carbon monoxide (CO) among others in addition to volatile organic compounds (VOC). In addition, due to the explosive characteristics of H_2 , it is very appealing to fabricate a sensor that can work at room temperature as this could reduce the risk of any calamity [407]. Meanwhile, working at room temperature also means low power consumption, simplified fabrication, and hence reduced operating cost.

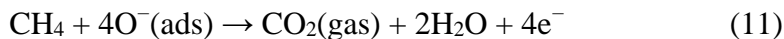
Oxide semiconductors are one kind of material investigated for the reliable detection of toxic and explosive gases. A highly resistive shell layer is established on the semiconducting surface by the adsorption of oxygen with a negative charge (O^- or O^{2-}). The oxidative or reductive interaction between the charged surface oxygen and target gases causes a change in the electrical

conductivity in proportion to the gas concentration. The gas sensitivity increases rapidly when the dimensions of oxide sensing materials become comparable or smaller than the typical thickness of the electron depletion layer near the surface (several nm). Therefore, various 1D TiO₂ NSs as discussed in **sections 2-4**, with a high surface area to volume ratio have been widely examined to achieve ultra-high gas sensitivity. There are two generally accepted and well established sensing mechanisms for metal oxide (TiO₂) based gas sensors; (i) oxygen-vacancy mechanism and (ii) ionosorption mechanism [407]. The former is based on the surface reduction/oxidation of the TiO₂ and the simultaneous change of surface oxygen vacancies under reducing and oxidizing gas exposure.

Tshabalala et al. [409] found an improved sensitivity of TiO₂ NTs that was attributed to a larger surface area provided by the hollow NTs that resulted to an improvement in gas adsorption and the increase in the relatively high concentration of oxygen vacancies. The gas sensing mechanism (resistance) is dependent on the electrical properties of TiO₂. Surface boundaries between the grains are affected by the adsorption and desorption of gaseous molecules and directly influence the resistance of the material, which play a vital role in the sensing mechanisms. Oxygen molecules in air (atmosphere) adsorbed on the TiO₂ surface or grain boundary, extract electrons from the conduction band and trap the electrons in the form of oxygen ions at the surface, thus leading to an increase in a depletion layer and the sensor resistance (Figure 26(a)). However, in the presence of a reducing gas CH₄; the gas molecules react with the TiO₂ surface and replace the oxygen ions with electrons deposited into the material (Eqs. 9–11). The depletion layer decreases, while the resistance decreases (Figure 26 (b)) [406].



Or



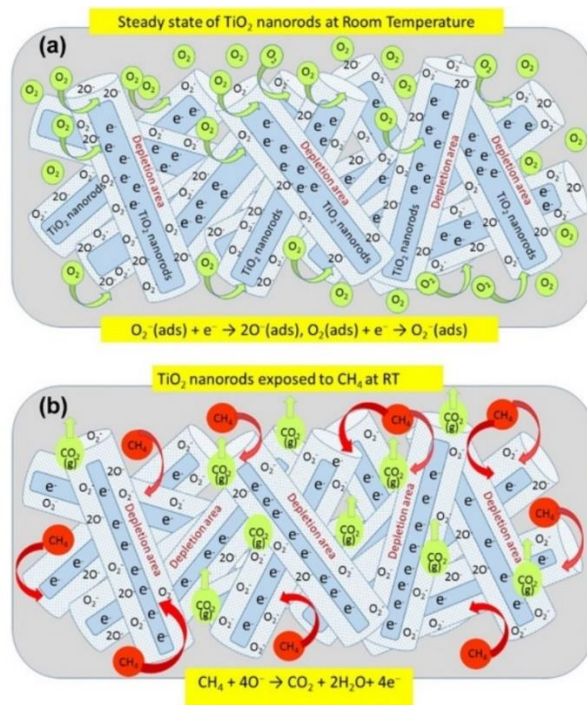


Figure 26. Schematic diagram demonstrating the sensing mechanism of (a) TiO₂ exposed in air and (b) exposed to CH₄ gas at room temperature. **Permission is required from [406].**

Similarly, various 1D TiO₂ NSs based gas sensors have been developed with excellent sensing performances [410-414]. For examples, Mor et al. [410] developed a room-temperature recyclable TiO₂ NTs hydrogen sensor with self-cleaning ability from the environmental contaminations. Zhou et al. [415] studied that effect of different crystalline phases of TiO₂ NWs for sensing ethanol gas and found that rutile phase was dominated for high performance sensing properties. Sennik et al. [414] studied the H₂ and VOC sensing properties of TiO₂ NRs. Wang et al.[416] developed TiO₂ NRs based O₂ sensor at room temperature. A recent review by Kaur et al. [404] on gas sensing properties and applications of 1D TiO₂ NSs reported that there had been a great development in fabrication of such NSs for enhanced sensing performance and summarized the effect of various parameters on the sensing mechanisms/properties of these NSs for different gas analytes. In the last a few years, many new strategies have been developed for the further enhancement in sensing properties of these 1D TiO₂ NSs. Excellent sensing performances have been reported by modifying 1D TiO₂ NSs through various doping strategies and heterostructure/composite formations [86, 412, 414, 417, 418]. The enhanced sensing properties could be achieved by improving their chemical, physical, optical, electrical properties. Recently, Tong et al. [417] studied the Co doping and its effect on the H₂S gas sensing properties of TiO₂

NTs and found that doped NTs showed better sensing response with greater selectivity, stability and repeatability. Theoretical simulation showed that band gap was decreased upto 1.1418 eV that improved the sensing properties of the doped TiO₂ NTs. Ren et al. [419] demonstrated that TiO₂ NWs with decorated AuPd alloy nanoparticles (optimized concentration) showed better sensitivity as compared to Au or Pd deposited NWs.

There are extensive research on improvement of sensing properties of TiO₂ based NSs due to RE doping. For example, Krishnan et al. [420] studied the sensing performance of RE Y doped TiO₂ NSs using various gases CH₄O, NH₃, C₃H₈O, C₂H₆O and C₃H₆O with the function of temperature and gas concentration. The morphological changes were observed due to the doping of different concentrations of Y. Optical studies showed tunable band gap based on the Y concentrations (3.20–3.78 eV). Higher gas sensing performance of doped TiO₂ was reported for NH₃ at 150 °C with 300 ppm gas concentration. Following the order of the gas sensitivity was reported with excellent sensing performance as compared to undoped TiO₂:NH₃ > C₂H₆O > C₃H₆O > CH₄O > C₃H₈O. Similarly, higher sensing properties were reported by several authors by Y doped TiO₂ NSs for VOC [421] and CO [422]. Song et al. [86] performed a comparative study on sensing properties of various RE-doped TiO₂ nanoparticles such as Nd, Ho, and Y-doped TiO₂. The Ho doped TiO₂ exhibited better sensing properties towards methanol with high selectivity in the concentration range of 0–10 ppm. Jing et al. [423] studied La/Y co-doped TiO₂ NSs and reported that co-doping enhanced the gas sensitivity towards 2-chlorophenol which was attributed to the optimum ratio of co-doped elements and rutile/anatase phases of TiO₂. Several other studies on sensing properties of RE doped TiO₂ NSs also showed the enhanced sensing properties due to the incorporation of RE metals [86, 424]. Due to the high luminescence properties of RE, RE doped TiO₂ NSs have also been used as luminescence-based gas sensors [424, 425]. For example, Eltermann et al. [424] proposed Sm³⁺ doped TiO₂ as an optical oxygen sensor material. The mechanism of enhanced oxygen gas sensitivity was explained as resonant excitation energy transfer from Sm³⁺ to the acceptor defects, the latter being switched on and off the resonance by electron exchange with surface-adsorbed oxygen. Oxygen vacancy-related defects were proposed as most likely candidates of energy acceptors. They proposed that these RE doped TiO₂ nanomaterials could be used for luminescence lifetime based oxygen sensing devices.

The above discussion reveals that 1D TiO₂ NSs have been extensively studied for gas sensing applications and excellent sensitivities have been reported. In addition to the various kind

of modifications of TiO₂ NSs, it is also clear that doping with RE enhances their sensitivity with long-term stability, selectivity, and repeatability. There are not many studies on RE doped 1D TiO₂ NSs for gas sensing applications, however, incorporation of RE ions into 1D TiO₂ NSs could be very promising for the improvement of gas sensitivity due to the synergistic effect of 1D geometry and RE dopants induced improvement of optoelectronic properties. Detailed and systematic studies must be carried out in the case of RE doped 1D TiO₂ NSs to understand the role of RE in the enhancement of sensitivity to 1D TiO₂ NSs and real applications.

5.9 Other important energy and environmental applications

RE doped 1D TiO₂ NSs are have been widely applied in various fields of energy and environment as discussed in details above. There are several research fields where various metal oxide nanomaterials have been extensively used that can also be explored with doped 1D TiO₂ NSs due to the fascinating optical and electrical properties. For example, light-emitting diodes (LEDs), one of the important research fields in the illumination industry and for society, their tunable optical properties have shown to have great potential to make artificial light sources. Typical LEDs depend on the blue or UV diodes for light generation, therefore, it needs a conversion layer for the downshifting of this radiation at wavelengths suitable for illumination applications. In this regard, RE doped nanomaterials have been intensively studied for color conversion [426-429]. Li et al. [427] studied Eu³⁺ doped TiO₂ luminescent nanocrystals and reported Efficient nonradiative energy transfer from the TiO₂ host to Eu³⁺ ions that accounted for bright red emissions either by exciting the TiO₂ host with UV light shorter than 405 nm or by directly exciting Eu³⁺ at a wavelength beyond the absorption edge (405 nm) of TiO₂. Xu et al. [428] demonstrated that Eu³⁺ doped TiO₂ down conversion phosphor that could be excited by X-ray and UV light showed intense visible luminescence. Red light-emitting Eu³⁺ doped TiO₂ nanophosphors were synthesized for white LED applications [430, 431]. Chang et al. [432] produced Eu³⁺ doped TiO₂ NRs using hydrothermal assisted sol-gel method and studied luminescence decay properties with the existence of multiple sites of Eu³⁺ ions in TiO₂ lattice. Recently, Su et al. [433] produced Eu-doped luminescent TiO₂ NTs with strong photoluminescence properties with a possible application as a biosensor [434, 435]. The LEDs research could be explored using RE doped 1D TiO₂ NSs for more exciting results. Similarly, TiO₂ based photocatalyst NSs have been used for boosting fuel cell performance [436, 437] that can be

further improved using RE doped 1D TiO₂ NSs. Extensive research has been carried out in the last decade for bacterial disinfection using various doped 1D and other TiO₂ NSs [438-441] which is also one of the important issues in the health and environment.

The above-discussed research fields are very important from an energy and environmental issues point of view, where limited work has been conducted using RE doped 1D TiO₂ NSs. Looking at the excellent and enhanced optoelectronic properties of these doped NSs, it would be an interesting subject for the scientific community to explore RE-doped 1D TiO₂ NSs for multifunctional applications. **Table 1** provides a list of some of the important results of RE doped 1D TiO₂ NSs in many fields of energy and environment.

5.10. Electrochemical sensing and biosensing applications

Another important application of TiO₂ nanostructured materials is in the development of electrochemical sensors and biosensors. Once these metallic compounds present interesting characteristics already mentioned in this detailed review, the use in electroanalytical chemistry opens new options for the detection of analytes in clinical, environmental, and food samples, for example. Indeed, some works have been published showing the great field that is the use of TiO₂ in electroanalysis. Electrochemical sensors allow fast and low-cost responses by using different platforms. In this context, Sethi and colleagues have proposed two electrochemical sensors based on ruthenium and TiO₂ nanoparticles, one for the determination of flufenamic acid and mefenamic acid (<https://doi.org/10.1016/j.aca.2018.11.041>) and another with carbon nanotubes for the same application (<https://doi.org/10.1016/j.aca.2018.11.041>). Some other approaches were used by the same group using different synthesis and application (<https://doi.org/10.1016/j.snb.2017.03.102> , <https://doi.org/10.1016/j.colsurfb.2019.02.022> , <https://doi.org/10.1016/j.jelechem.2016.08.024> , <https://doi.org/10.1016/j.microc.2019.104124> . Oliveira et. al. have developed a thin film based on nitrogen-doped titanium dioxide nanoparticles, which was applied for the determination of estradiol hormone in tap water and synthetic urine samples, <https://doi.org/10.1002/elan.201700392> .

Interesting work has been published by Kumar et. al., in which they used the compound bimetallic made of MoS₂/TiO₂ for electrochemical determination and photocatalytic degradation of paracetamol drug. Beyond the simple nanocomposite presented two applications, it was tested

against human skin keratinocytes cells to verify the cytotoxicity of the catalyst.
<https://doi.org/10.1016/j.sbsr.2019.100288>

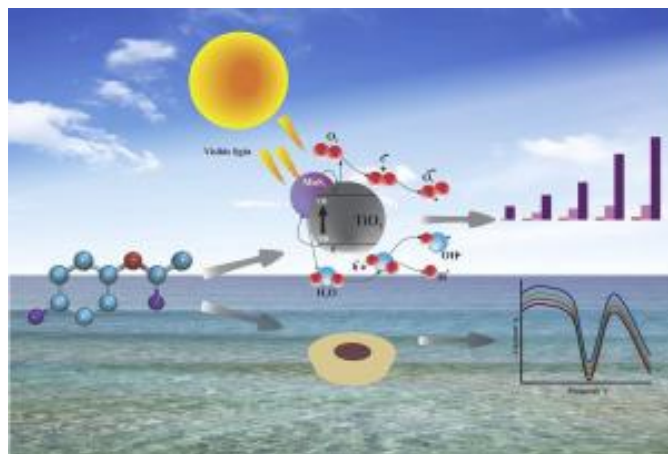


Figure 27. Electrochemical sensor and photocatalyst of paracetamol drug made of MoS₂ and TiO₂ proposed by Kumar et al. <https://doi.org/10.1016/j.sbsr.2019.100288> **Permission is not required.**

Photoelectrochemistry is also used to improve the selectivity of sensors and is a great alternative for the determination of molecules of biological interest. In this regard, Yan et. al. have proposed a photoelectrochemical sensor for dopamine using graphene quantum dots and TiO₂ nanoparticles. Figure 28 shows the schematic response of the proposed sensor.
<https://doi.org/10.1016/j.aca.2014.10.021>

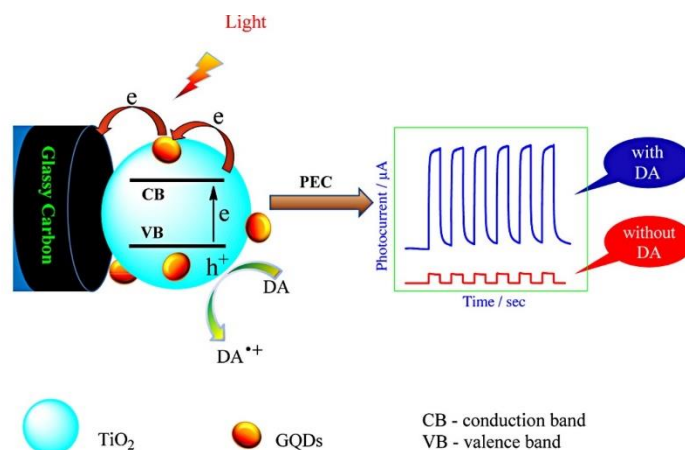


Figure 28. Photoelectrochemical sensor proposed by Yan et al. which is based on graphene quantum dots and TiO₂ nanoparticles applied for dopamine determination. **Reproduced with permission** <https://doi.org/10.1016/j.aca.2014.10.021> . Copyright © 2014 Elsevier B.V. All rights reserved.

An interesting review was published by Bay and Zhou (<https://www.sciencedirect.com/science/article/abs/pii/S2451963417300353>), which one exclusive topic highlights the progress of TiO₂ in biosensing. Although less explored commercially, electrochemical biosensors are an interesting alternative for analysis. They consist of the biological material (DNA, antibody/antigen, enzyme, cell) and a transducer, which converts reactions in a measurable signal (<https://doi.org/10.1016/j.talanta.2019.120644>). Sethi and colleagues have explored the use of TiO₂ hybrids for healthcare, including biosensing. (<https://doi.org/10.1016/j.colsurfb.2019.03.013>).

Enzyme biosensors have been extensively explored and to understand the process of immobilization of biomolecules on the nanostructures, as a proof-of-concept. In this instance, glucose oxidase and polyphenol oxidases can be highlighted. For example, Amir AL-Mokaram et. al. proposed a biosensor by using polypyrrole, chitosan, TiO₂, and the glucose oxidase enzyme for glucose detection, and the schematic cell and the amperometric results are presented in Figure 29 <https://doi.org/10.3390/nano7060129>. Other examples can be observed in the literature for the same purpose with different architectures. <https://doi.org/10.1039/C5DT00678C> <https://doi.org/10.1016/j.talanta.2014.08.019>

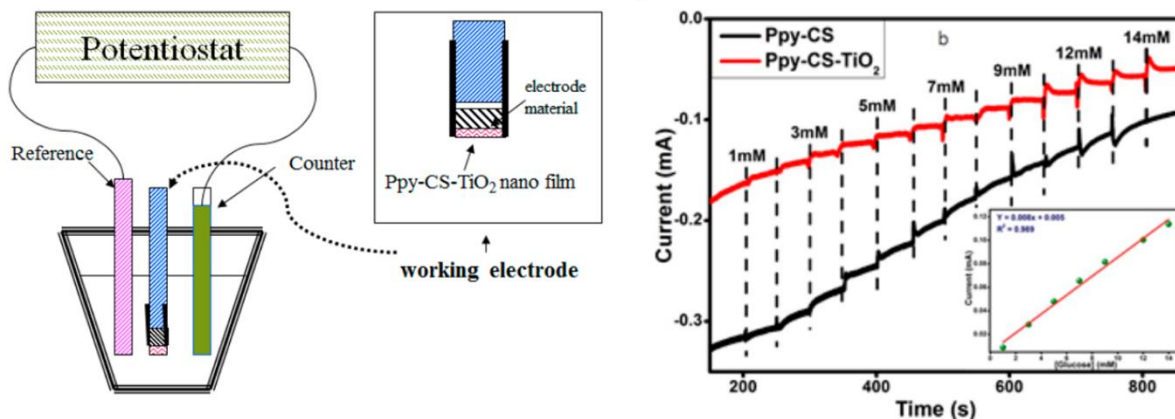


Figure 29. The electrochemical cell of polypyrrole, chitosan, and TiO₂ film preparation. (b) Amperometric responses to the successive addition of glucose concentration at +0.13 V (vs. Ag/AgCl) proposed by Amir AL-Mokaram et. al. (<https://doi.org/10.3390/nano7060129>) The inset presents the calibration curve for the proposed biosensor. **Permission is not required.**

In past years hundred of papers about electrochemical immunosensors have been published for clinical purposes. They are strategies that can be used in medicine soon. This type of sensor consists of the interaction of antibodies and antigens, promoting electrochemical signals using potentiometry, voltammetry, and/or impedance that can be monitored by portable equipment. (<https://doi.org/10.1166/jnn.2014.9234>) In this context, TiO₂ is very useful, once it presents biocompatibility, in other words, it allows biological tissues immobilizations with success. A fascinating immunosensor was prepared by Wang et. al. <https://doi.org/10.1016/j.carbon.2019.02.008>. They proposed a new composite material based on carbon nitride, copper, and TiO₂, which was applied for the determination of carcinoembryonic antigen, which can be observed in Figure 29.

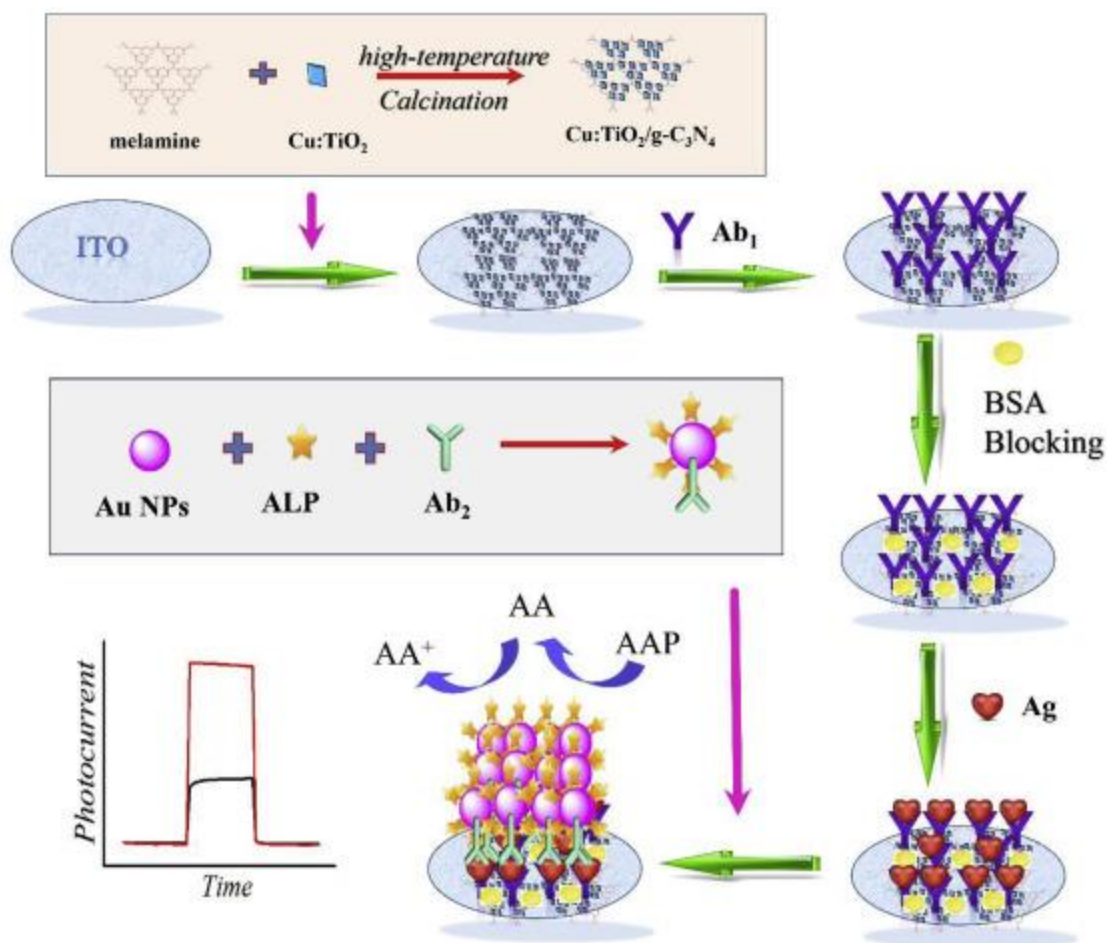


Figure 30. Scheme of preparation and application of the immunosensor using TiO_2 proposed by Wang et. al. **Reproduced with permission** <https://doi.org/10.1016/j.carbon.2019.02.008> Copyright © 2019 Elsevier B.V. All rights reserved.

In the next years, the use of TiO_2 in paper-based electrochemical sensors and 3D-printing are fields that can be explored by the researchers to obtain new conductive and selective materials for analytical chemistry. Further detailed study along with the development of simple synthesis methods is necessary to execute their potential in multifunctional applications.

6. Critical issues, future aspects, and summary

Due to the modernization in industries or academia, the development of low-cost, portable, and high-performance devices for solar panels, energy storage, environmental monitoring or healthcare, etc. is the basic need for the progress of society. To meet this

requirement, highly active, low-cost materials with the possibility to tune their functionality and that can also be used for multipurpose should be implemented. Metal oxide semiconductors-based nanomaterials are novel materials with tunable structural, optical, and electronic properties for multifunctional applications in a variety of fields including energy and environment. TiO₂ based nanomaterials are such active materials which are being used in all domain of science due to their fascinating properties and capability of tuning of their properties using modern technologies. Particularly, 1D TiO₂ NSs have shown better opportunities to modify their properties through doping strategies as discussed in this article which provides remarkable physical and chemical properties with enhanced functionality for high-performance device applications. The 1D geometry provides a synergistic effect in maximizing the efficiency/performance of the device exhibiting quick response, higher stability as a result of higher surface-to-volume ratio, well-defined crystal orientations, controlled unidirectional electrical properties, and recyclability.

Due to the technological advancement for the preparation of materials at the nanoscale, these materials are the emerging nanomaterials with tremendous new possibilities to improve their functionality that can be exploited for the fabrication of excellent and high-performance nanodevices [411]. Advancement in science also improves the fundamental understanding of the chemical/physical processes that occur at the surface/interface and structural tunability of these nanostructured materials which explore chemical stability for long-term implementation of these materials. The thermal and chemical stability of the nanostructured materials are one of the major issues for consistent and higher performance as well as long-term applications in the devices used for either energy or environmental or medical applications. For example, materials working against corrosion in the electrolytes and charge transfer processes from the surface of semiconductor materials through the electrolyte solution must have high chemical stability [302]. Even though there is a great development in this direction using TiO₂ and other metal oxide-based 1D NSs for improving its surface and interfacial properties, however, more advanced researches are required for getting better results. These RE doped TiO₂ NSs have been used extensively in some of the research fields such as sensing, CO₂ reduction, LEDs, and fuel cells and these researches should be explored to use 1D TiO₂ NSs for their high-performance output. It is suggested that NSs fabricated by RE doping and co-doping should be widely studied and utilized for real applications [423]. Future research should also be focused on the large-scale production methods and their proper implications [412]. Also, emphasis should be given to the production of tunable,

cost-effective multifunctional nanomaterials for interdisciplinary applications. The development of nanocomposites based RE doped 1D TiO₂ NSs with other functional nanomaterials or polymers can improve their handling, thermal stability, and functionality [119, 442, 443]. It could help in making more functional from the practical point of view due to multicomponent this review, recent progress in developing novel RE doped 1D TiO₂ NSS and their multifunctional applications in the fields of energy and environment has been discussing in details with emphasis on their fundamental mechanisms. Various synthesis methods of undoped and RE doped 1D TiO₂ NSs, mechanism of doping/co-doping, effect on microstructural, optical, and electrical properties, have been discussed in detail. Firstly, the introduction of the various dimensional TiO₂ NSs and their importance have been discussed along with recent progress in the field of 1D TiO₂ NSs. It is then followed by various characteristics, properties, and functionality of 1D TiO₂ NSs. Thereafter, RE doping and co-doping have been discussed with emphasis on the various mechanisms involved in altering the surface or interface properties of 1D TiO₂ NSs. Various RE elements from the periodic table have been discussed because of their doping mechanisms and effect on the various physical and chemical properties of 1D TiO₂ NSs. Various synthesis methods for the preparation of 1D TiO₂ NSs and doped 1D TiO₂ NSs have been discussed in detail along with recent progress of synthesis strategies in the last few years. Thereafter, various energy and environmental applications of RE doped 1D TiO₂ NSs have been discussed with emphasis on the basic working principle of the devices in the fields and the role of RE doped 1D TiO₂ NSs in the enhancement of their efficiencies/activities. Finally, future requirements and various challenges faced by the researchers particularly in these energy and environmental fields have been discussed with emphasis on the improvement of functionality and multidisciplinary applications. We hope that this effort will serve the scientific community to improve the basic understanding and potential application in other important fields also.

Conflicts of interest

There are no conflicts of interest to declare

Acknowledgements

The author (JP) thank the Fonds de Recherche du Québec-Nature et Technologies (FRQNT), Quebec, Canada for Merit Scholarship-2017 (Ranked#1) and department of science and

technology (DST), India for the prestigious INSPIRE Faculty award [INSPIRE/04/2015/002452(IFA15-MS-57)] along with research grant. JP also acknowledges University of the Free State and National Research Foundation, South Africa for “Promising Young researcher ‘Y1 rating’ award”, including incentive funding.

References

- [1] Zhou W, Liu H, Boughton RI, Du G, Lin J, Wang J, et al. One-dimensional single-crystalline Ti–O based nanostructures: properties, synthesis, modifications and applications. *Journal of Materials Chemistry*. 2010;20:5993-6008.
- [2] Singh N, Prakash J, Misra M, Sharma A, Gupta RK. Dual Functional Ta-Doped Electrospun TiO₂ Nanofibers with Enhanced Photocatalysis and SERS Detection for Organic Compounds. *ACS Applied Materials & Interfaces*. 2017;9:28495-507.
- [3] Jai P, Tripathi A, Rigato V, Pivin JC, Jalaj T, Keun Hwa C, et al. Synthesis of Au nanoparticles at the surface and embedded in carbonaceous matrix by 150 keV Ar ion irradiation. *Journal of Physics D: Applied Physics*. 2011;44:125302.
- [4] Prakash J, Sun S, Swart HC, Gupta RK. Noble metals-TiO₂ nanocomposites: From fundamental mechanisms to photocatalysis, surface enhanced Raman scattering and antibacterial applications. *Applied Materials Today*. 2018;11:82-135.
- [5] Kumar P, Mathpal MC, Prakash J, Hamad S, Rao SV, Viljoen BC, et al. Study of Tunable Plasmonic, Photoluminescence, and Nonlinear Optical Behavior of Ag Nanoclusters Embedded in a Glass Matrix for Multifunctional Applications. *physica status solidi (a)*. 2019;216:1800768.
- [6] Ashraf R, Sofi HS, Akram T, Rather HA, Abdal-hay A, Shabir N, et al. Fabrication of multifunctional cellulose/TiO₂/Ag composite nanofibers scaffold with antibacterial and bioactivity properties for future tissue engineering applications. *Journal of Biomedical Materials Research Part A*. 2020;108:947-62.
- [7] Cai J, Shen F, Shi Z, Lai Y, Sun J. Nanostructured TiO₂ for light-driven CO₂ conversion into solar fuels. *APL Materials*. 2020;8:040914.
- [8] Prakash J, Kumar V, Kroon RE, Asokan K, Rigato V, Chae KH, et al. Optical and surface enhanced Raman scattering properties of Au nanoparticles embedded in and located on a carbonaceous matrix. *Physical Chemistry Chemical Physics*. 2016;18:2468-80.
- [9] Masjedi-Arani M, Salavati-Niasari M. A simple sonochemical approach for synthesis and characterization of Zn₂SiO₄ nanostructures. *Ultrasonics Sonochemistry*. 2016;29:226-35.
- [10] Salavati-Niasari M, Fereshteh Z, Davar F. Synthesis of oleylamine capped copper nanocrystals via thermal reduction of a new precursor. *Polyhedron*. 2009;28:126-30.
- [11] Prakash J, Tripathi A, Gautam S, Chae KH, Song J, Rigato V, et al. Phenomenological understanding of dewetting and embedding of noble metal nanoparticles in thin films induced by ion irradiation. *Materials Chemistry and Physics*. 2014;147:920-4.

- [12] Balasubramaniam B, Singh N, Kar P, Tyagi A, Prakash J, Gupta RK. Engineering of transition metal dichalcogenide-based 2D nanomaterials through doping for environmental applications. *Molecular Systems Design & Engineering*. 2019;4:804-27.
- [13] Tavakoli F, Salavati-Niasari M, badiel A, Mohandes F. Green synthesis and characterization of graphene nanosheets. *Materials Research Bulletin*. 2015;63:51-7.
- [14] Kumar P, Mathpal MC, Tripathi AK, Prakash J, Agarwal A, Ahmad MM, et al. Plasmonic resonance of Ag nanoclusters diffused in soda-lime glasses. *Physical Chemistry Chemical Physics*. 2015;17:8596-603.
- [15] Medhi R, Marquez MD, Lee TR. Visible-Light-Active Doped Metal Oxide Nanoparticles: Review of their Synthesis, Properties, and Applications. *ACS Applied Nano Materials*. 2020;3:6156-85.
- [16] Mortazavi-Derazkola S, Salavati-Niasari M, Amiri O, Abbasi A. Fabrication and characterization of Fe₃O₄@SiO₂@TiO₂@Ho nanostructures as a novel and highly efficient photocatalyst for degradation of organic pollution. *Journal of Energy Chemistry*. 2017;26:17-23.
- [17] Zinatloo-Ajabshir S, Salavati-Niasari M, Zinatloo-Ajabshir Z. Nd₂Zr₂O₇-Nd₂O₃ nanocomposites: New facile synthesis, characterization and investigation of photocatalytic behaviour. *Materials Letters*. 2016;180:27-30.
- [18] Singh JP, Chen CL, Dong CL, Prakash J, Kabiraj D, Kanjilal D, et al. Role of surface and subsurface defects in MgO thin film: XANES and magnetic investigations. *Superlattices and Microstructures*. 2015;77:313-24.
- [19] Mallick P, Rath C, Prakash J, Mishra DK, Choudhary RJ, Phase DM, et al. Swift heavy ion irradiation induced modification of the microstructure of NiO thin films. *Nuclear Instruments and Methods in Physics Research Section B: Beam Interactions with Materials and Atoms*. 2010;268:1613-7.
- [20] Amiri M, Salavati-Niasari M, Akbari A. Magnetic nanocarriers: Evolution of spinel ferrites for medical applications. *Advances in Colloid and Interface Science*. 2019;265:29-44.
- [21] Prakash J, Pivin JC, Swart HC. Noble metal nanoparticles embedding into polymeric materials: From fundamentals to applications. *Advances in Colloid and Interface Science*. 2015;226:187-202.
- [22] Pathak TK, Kumar V, Prakash J, Purohit LP, Swart HC, Kroon RE. Fabrication and characterization of nitrogen doped p-ZnO on n-Si heterojunctions. *Sensors and Actuators A: Physical*. 2016;247:475-81.
- [23] Ghanbari D, Salavati-Niasari M. Synthesis of urchin-like CdS-Fe₃O₄ nanocomposite and its application in flame retardancy of magnetic cellulose acetate. *Journal of Industrial and Engineering Chemistry*. 2015;24:284-92.
- [24] Komba N, Zhang G, Wei Q, Yang X, Prakash J, Chenitz R, et al. Iron (II) phthalocyanine/N-doped graphene: A highly efficient non-precious metal catalyst for oxygen reduction. *International Journal of Hydrogen Energy*. 2019;44:18103-14.
- [25] Yang X, Zhang G, Prakash J, Chen Z, Gauthier M, Sun S. Chemical vapour deposition of graphene: layer control, the transfer process, characterisation, and related applications. *International Reviews in Physical Chemistry*. 2019;38:149-99.
- [26] Patel SP, Chawla AK, Chandra R, Prakash J, Kulriya PK, Pivin JC, et al. Structural phase transformation in ZnS nanocrystalline thin films by swift heavy ion irradiation. *Solid State Communications*. 2010;150:1158-61.
- [27] Matheswaran P, Abhirami KM, Gokul B, Sathyamoorthy R, Prakash J, Asokan K, et al. 130MeV Au ion irradiation induced dewetting on In₂Te₃ thin film. *Applied Surface Science*. 2012;258:8558-63.
- [28] Licht S, Liu X, Licht G, Wang X, Swesi A, Chan Y. Amplified CO₂ reduction of greenhouse gas emissions with C₂CNT carbon nanotube composites. *Materials Today Sustainability*. 2019;6:100023.
- [29] Hernández-Alonso MD. Metal Doping of Semiconductors for Improving Photoactivity. In: Coronado JM, Fresno F, Hernández-Alonso MD, Portela R, editors. *Design of Advanced Photocatalytic Materials for Energy and Environmental Applications*. London: Springer London; 2013. p. 269-86.
- [30] Liang L, Kang X, Sang Y, Liu H. One-Dimensional Ferroelectric Nanostructures: Synthesis, Properties, and Applications. *Advanced Science*. 2016;3:1500358.

- [31] Udom I, Ram MK, Stefanakos EK, Hepp AF, Goswami DY. One dimensional-ZnO nanostructures: Synthesis, properties and environmental applications. *Materials Science in Semiconductor Processing*. 2013;16:2070-83.
- [32] Chen S, Li W, Li X, Yang W. One-dimensional SiC nanostructures: Designed growth, properties, and applications. *Progress in Materials Science*. 2019;104:138-214.
- [33] Cheng BC, Xiao YH, Wu GS, Zhang LD. Controlled Growth and Properties of One-Dimensional ZnO Nanostructures with Ce as Activator/Dopant. *Advanced Functional Materials*. 2004;14:913-9.
- [34] Xia Y, Yang P, Sun Y, Wu Y, Mayers B, Gates B, et al. One-Dimensional Nanostructures: Synthesis, Characterization, and Applications. *ChemInform*. 2003;34.
- [35] Zhao Z, Tian J, Sang Y, Cabot A, Liu H. Structure, Synthesis, and Applications of TiO₂ Nanobelts. *Advanced Materials*. 2015;27:2557-82.
- [36] Pavlenko M, Siuzdak K, Coy E, Załęski K, Jancelewicz M, Iatsunskyi I. Enhanced solar-driven water splitting of 1D core-shell Si/TiO₂/ZnO nanopillars. *International Journal of Hydrogen Energy*. 2020;45:26426-33.
- [37] Rodchanasuripron W, Seadan M, Suttiruengwong S. Properties of non-woven polylactic acid fibers prepared by the rotational jet spinning method. *Materials Today Sustainability*. 2020;10:100046.
- [38] Kusior A, Klich-Kafel J, Trenczek-Zajac A, Swierczek K, Radecka M, Zakrzewska K. TiO₂-SnO₂ nanomaterials for gas sensing and photocatalysis. *Journal of the European Ceramic Society*. 2013;33:2285-90.
- [39] Asemi M, Ghanaatshoar M. Hydrothermal growth of one-dimensional Ce-doped TiO₂ nanostructures for solid-state DSSCs comprising Mg-doped CuCrO₂. *Journal of Materials Science*. 2017;52:489-503.
- [40] Kwok Y. Methodologies for Achieving 1D ZnO Nanostructures Potential for Solar Cells. 2019.
- [41] Jai P, Promod K, Harris RA, Chantel S, Neethling JH, Vuuren AJv, et al. Synthesis, characterization and multifunctional properties of plasmonic Ag-TiO₂ nanocomposites. *Nanotechnology*. 2016;27:355707.
- [42] Do HH, Nguyen DLT, Nguyen XC, Le T-H, Nguyen TP, Trinh QT, et al. Recent progress in TiO₂-based photocatalysts for hydrogen evolution reaction: A review. *Arabian Journal of Chemistry*. 2020;13:3653-71.
- [43] Bakbolat B, Daulbayev C, Sultanov F, Beissenov R, Umirzakov A, Mereke A, et al. Recent Developments of TiO₂-Based Photocatalysis in the Hydrogen Evolution and Photodegradation: A Review. *Nanomaterials*. 2020;10:1790.
- [44] He X, Wang A, Wu P, Tang S, Zhang Y, Li L, et al. Photocatalytic degradation of microcystin-LR by modified TiO₂ photocatalysis: A review. *Science of The Total Environment*. 2020;743:140694.
- [45] Hasanzadeh Kafshgari M, Goldmann WH. Insights into Theranostic Properties of Titanium Dioxide for Nanomedicine. *Nano-Micro Letters*. 2020;12:22.
- [46] Li R, Li T, Zhou Q. Impact of Titanium Dioxide (TiO₂) Modification on Its Application to Pollution Treatment—A Review. *Catalysts*. 2020;10:804.
- [47] Rath H, Dash P, Som T, Prakash J, Tripathi A, Avasthi DK, et al. Surface evolution of titanium oxide thin film with swift heavy ion irradiation. *Radiation Effects and Defects in Solids*. 2011;166:571-7.
- [48] Mudhoo A, Paliya S, Goswami P, Singh M, Lofrano G, Carotenuto M, et al. Fabrication, functionalization and performance of doped photocatalysts for dye degradation and mineralization: a review. *Environmental Chemistry Letters*. 2020;18:1825-903.
- [49] Mikrut P, Kobielski M, Indyka P, Macyk W. Photocatalytic activity of TiO₂ polymorph B revisited: physical, redox, spectroscopic, and photochemical properties of TiO₂(B)/anatase series of titanium dioxide materials. *Materials Today Sustainability*. 2020;10:100052.
- [50] Alagarasi A, Rajalakshmi PU, Shanthy K, Selvam P. Solar-light driven photocatalytic activity of mesoporous nanocrystalline TiO₂, SnO₂, and TiO₂-SnO₂ composites. *Materials Today Sustainability*. 2019;5:100016.

- [51] Li Y, Tsang SCE. Recent progress and strategies for enhancing photocatalytic water splitting. *Materials Today Sustainability*. 2020;9:100032.
- [52] Kikuchi Y, Sunada K, Iyoda T, Hashimoto K, Fujishima A. Photocatalytic bactericidal effect of TiO₂ thin films: dynamic view of the active oxygen species responsible for the effect. *Journal of Photochemistry and Photobiology A: Chemistry*. 1997;106:51-6.
- [53] Mills A, Le Hunte S. An overview of semiconductor photocatalysis. *Journal of Photochemistry and Photobiology A: Chemistry*. 1997;108:1-35.
- [54] Fu G, Vary PS, Lin C-T. Anatase TiO₂ Nanocomposites for Antimicrobial Coatings. *The Journal of Physical Chemistry B*. 2005;109:8889-98.
- [55] Fan R, Wang L, Chen Y, Zheng G, Li L, Li Z, et al. Tailored Au@TiO₂ nanostructures for the plasmonic effect in planar perovskite solar cells. *Journal of Materials Chemistry A*. 2017;5:12034-42.
- [56] Ge M, Cao C, Huang J, Li S, Chen Z, Zhang K-Q, et al. A review of one-dimensional TiO₂ nanostructured materials for environmental and energy applications. *Journal of Materials Chemistry A*. 2016;4:6772-801.
- [57] Bashiri R, Samsudin MFR, Mohamed NM, Suhaimi NA, Ling LY, Sufian S, et al. Influence of growth time on photoelectrical characteristics and photocatalytic hydrogen production of decorated Fe₂O₃ on TiO₂ nanorod in photoelectrochemical cell. *Applied Surface Science*. 2020;510:145482.
- [58] He Z, Han Y, Liu S, Cui W, Qiao Y, He T, et al. Toward the Intrinsic Superiority of Aligned One-Dimensional TiO₂ Nanostructures: the Role of Defect States in Electron Transport Process. *ChemElectroChem*. 2020;7:4390-7.
- [59] Moshoeu DE, Sanni SO, Oseghe EO, Msagati TAM, Mamba BB, Ofomaja AE. Morphological Influence of TiO₂ Nanostructures on Charge Transfer and Tetracycline Degradation Under LED Light. *ChemistrySelect*. 2020;5:1037-40.
- [60] Burda C, Chen X, Narayanan R, El-Sayed MA. Chemistry and Properties of Nanocrystals of Different Shapes. *Chemical Reviews*. 2005;105:1025-102.
- [61] Wu H-H, Deng L-X, Wang S-R, Zhu B-L, Huang W-P, Wu S-H, et al. The Preparation and Characterization of La Doped TiO₂ Nanotubes and Their Photocatalytic Activity. *Journal of Dispersion Science and Technology*. 2010;31:1311-6.
- [62] Rosales M, Zoltan T, Yadarola C, Mosquera E, Gracia F, García A. The influence of the morphology of 1D TiO₂ nanostructures on photogeneration of reactive oxygen species and enhanced photocatalytic activity. *Journal of Molecular Liquids*. 2019;281:59-69.
- [63] Shao F, Sun J, Gao L, Yang S, Luo J. Growth of Various TiO₂ Nanostructures for Dye-Sensitized Solar Cells. *The Journal of Physical Chemistry C*. 2011;115:1819-23.
- [64] Zhang X, Wang Y, Liu B, Sang Y, Liu H. Heterostructures construction on TiO₂ nanobelts: A powerful tool for building high-performance photocatalysts. *Applied Catalysis B: Environmental*. 2017;202:620-41.
- [65] Li Y, Yang X-Y, Feng Y, Yuan Z-Y, Su B-L. One-Dimensional Metal Oxide Nanotubes, Nanowires, Nanoribbons, and Nanorods: Synthesis, Characterizations, Properties and Applications. *Critical Reviews in Solid State and Materials Sciences*. 2012;37:1-74.
- [66] Rajeswari R, Islavath N, Raghavender M, Giribabu L. Recent Progress and Emerging Applications of Rare Earth Doped Phosphor Materials for Dye-Sensitized and Perovskite Solar Cells: A Review. *The Chemical Record*. 2020;20:65-88.
- [67] Ismael M. A review and recent advances in solar-to-hydrogen energy conversion based on photocatalytic water splitting over doped-TiO₂ nanoparticles. *Solar Energy*. 2020;211:522-46.
- [68] Amritha A, Sundararajan M, Rejith RG, Mohammed-Aslam MA. La-Ce doped TiO₂ nanocrystals: a review on synthesis, characterization and photocatalytic activity. *SN Applied Sciences*. 2019;1:1441.
- [69] Altomare M, Lee K, Killian MS, Selli E, Schmuki P. Ta-Doped TiO₂ Nanotubes for Enhanced Solar-Light Photoelectrochemical Water Splitting. *Chemistry – A European Journal*. 2013;19:5841-4.
- [70] Ji L, Zhang Y, Miao S, Gong M, Liu X. In situ synthesis of carbon doped TiO₂ nanotubes with an enhanced photocatalytic performance under UV and visible light. *Carbon*. 2017;125:544-50.

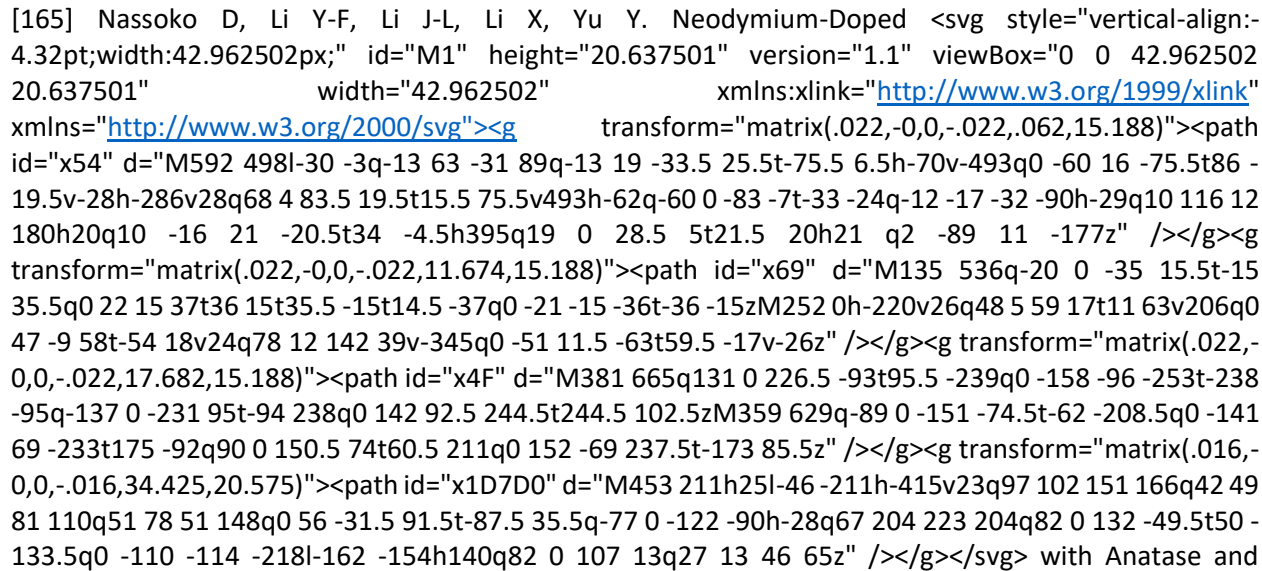
- [71] Bjelajac A, Petrović R, Popović M, Rakočević Z, Socol G, Mihailescu IN, et al. Doping of TiO₂ nanotubes with nitrogen by annealing in ammonia for visible light activation: Influence of pre- and post-annealing in air. *Thin Solid Films*. 2019;692:137598.
- [72] Wang X, Sun M, Murugananthan M, Zhang Y, Zhang L. Electrochemically self-doped WO₃/TiO₂ nanotubes for photocatalytic degradation of volatile organic compounds. *Applied Catalysis B: Environmental*. 2020;260:118205.
- [73] Mazierski P, Mikolajczyk A, Bajorowicz B, Malankowska A, Zaleska-Medynska A, Nadolna J. The role of lanthanides in TiO₂-based photocatalysis: A review. *Applied Catalysis B: Environmental*. 2018;233:301-17.
- [74] Fung C-M, Tang J-Y, Tan L-L, Mohamed AR, Chai S-P. Recent progress in two-dimensional nanomaterials for photocatalytic carbon dioxide transformation into solar fuels. *Materials Today Sustainability*. 2020;9:100037.
- [75] Kumar P, Chandra Mathpal M, Prakash J, Jagannath G, Roos WD, Swart HC. Plasmonic and nonlinear optical behavior of nanostructures in glass matrix for photonics application. *Materials Research Bulletin*. 2020;125:110799.
- [76] Bakiyaraj G, Gunasekaran B, Prakash J, Kalidasan M, Asokan K, Dhanasekaran R, et al. Improvement of opto-electro-structural properties of nanocrystalline CdS thin films induced by Au⁹⁺ ion irradiation. *Thin Solid Films*. 2017;626:117-25.
- [77] Chen H, Zhu W, Zhang Z, Cai W, Zhou X. Er and Mg co-doped TiO₂ nanorod arrays and improvement of photovoltaic property in perovskite solar cell. *Journal of Alloys and Compounds*. 2019;771:649-57.
- [78] Li W, Xie L, Zhou L, Ochoa-Lozano J, Li C, Chai X. A systemic study on Gd, Fe and N co-doped TiO₂ nanomaterials for enhanced photocatalytic activity under visible light irradiation. *Ceramics International*. 2020;46:24744-52.
- [79] Shayegan Z, Haghghat F, Lee C-S. Carbon-doped TiO₂ film to enhance visible and UV light photocatalytic degradation of indoor environment volatile organic compounds. *Journal of Environmental Chemical Engineering*. 2020;8:104162.
- [80] Shin SG, Kim IT, Choi HW. A study of perovskite solar cell with a Fe³⁺/Ga³⁺ doped TiO₂ layer. *Japanese Journal of Applied Physics*. 2020;59:SGGF05.
- [81] Kumaravel V, Rhatigan S, Mathew S, Michel MC, Bartlett J, Nolan M, et al. Mo doped TiO₂: impact on oxygen vacancies, anatase phase stability and photocatalytic activity. *Journal of Physics: Materials*. 2020;3:025008.
- [82] Crișan M, Ianculescu A-C, Crișan D, Drăgan N, Todan L, Nițoi I, et al. Chapter 10 - Fe-doped TiO₂ nanomaterials for water depollution. In: Amrane A, Rajendran S, Nguyen TA, Assadi AA, Sharoba AM, editors. *Nanotechnology in the Beverage Industry*: Elsevier; 2020. p. 265-313.
- [83] Shayegan Z, Haghghat F, Lee C-S. Surface fluorinated Ce-doped TiO₂ nanostructure photocatalyst: A trap and remove strategy to enhance the VOC removal from indoor air environment. *Chemical Engineering Journal*. 2020;401:125932.
- [84] Keskin OY, Dalmis R, Birlik I, Ak Azem NF. Comparison of the effect of non-metal and rare-earth element doping on structural and optical properties of CuO/TiO₂ one-dimensional photonic crystals. *Journal of Alloys and Compounds*. 2020;817:153262.
- [85] Song L, Zhao X, Cao L, Moon J-W, Gu B, Wang W. Synthesis of rare earth doped TiO₂ nanorods as photocatalysts for lignin degradation. *Nanoscale*. 2015;7:16695-703.
- [86] Song H, Chen W, Wang X, Ji B. Detection of Methanol by a Sensor Based on Rare-earth Doped TiO₂ Nanoparticles. *Journal of Wuhan University of Technology-Mater Sci Ed*. 2018;33:1070-5.
- [87] Peng H, Guo R, Lin H. Photocatalytic reduction of CO₂ over Sm-doped TiO₂ nanoparticles. *Journal of Rare Earths*. 2019.

- [88] Xiong Z, Zhao Y, Zhang J, Zheng C. Efficient photocatalytic reduction of CO₂ into liquid products over cerium doped titania nanoparticles synthesized by a sol–gel auto-ignited method. *Fuel Processing Technology*. 2015;135:6-13.
- [89] Ahmad A, Yerlikaya G, Zia ur R, Paksoy H, Kardaş G. Enhanced photoelectrochemical water splitting using gadolinium doped titanium dioxide nanorod array photoanodes. *International Journal of Hydrogen Energy*. 2020;45:2709-19.
- [90] Fu K, Huang J, Yao N, Xu X, Wei M. Enhanced photocatalytic activity of TiO₂ nanorod arrays decorated with CdSe using an upconversion TiO₂: Yb³⁺, Er³⁺ thin film. *Industrial & Engineering Chemistry Research*. 2015;54:659-65.
- [91] Akman E, Akin S, Ozturk T, Gulveren B, Sonmezoglu S. Europium and terbium lanthanide ions co-doping in TiO₂ photoanode to synchronously improve light-harvesting and open-circuit voltage for high-efficiency dye-sensitized solar cells. *Solar Energy*. 2020;202:227-37.
- [92] Wang H-Y, Yang H, Zhang L, Chen J, Liu B. Niobium Doping Enhances Charge Transport in TiO₂ Nanorods. *ChemNanoMat*. 2016;2:660-4.
- [93] Yao Q, Liu J, Peng Q, Wang X, Li Y. Nd-Doped TiO₂ Nanorods: Preparation and Application in Dye-Sensitized Solar Cells. *Chemistry – An Asian Journal*. 2006;1:737-41.
- [94] Wang L, Chen K, Tong H, Wang K, Tao L, Zhang Y, et al. Inverted pyramid Er³⁺ and Yb³⁺ Co-doped TiO₂ nanorod arrays based perovskite solar cell: Infrared response and improved current density. *Ceramics International*. 2020;46:12073-9.
- [95] Kumar V, Tiwari SP, Ntwaeaborwa OM, Swart HC. 10 - Luminescence properties of rare-earth doped oxide materials. In: Dhoble SJ, Pawade VB, Swart HC, Chopra V, editors. *Spectroscopy of Lanthanide Doped Oxide Materials*: Woodhead Publishing; 2020. p. 345-64.
- [96] Li H, Zheng K, Sheng Y, Song Y, Zhang H, Huang J, et al. Facile synthesis and luminescence properties of TiO₂:Eu³⁺ nanobelts. *Optics & Laser Technology*. 2013;49:33-7.
- [97] Mazierski P, Lisowski W, Grzyb T, Winiarski MJ, Klimczuk T, Mikołajczyk A, et al. Enhanced photocatalytic properties of lanthanide-TiO₂ nanotubes: An experimental and theoretical study. *Applied Catalysis B: Environmental*. 2017;205:376-85.
- [98] Haggerty JES, Schelhas LT, Kitchaev DA, Mangum JS, Garten LM, Sun W, et al. High-fraction brookite films from amorphous precursors. *Scientific Reports*. 2017;7:15232.
- [99] Nakata K, Fujishima A. TiO₂ photocatalysis: Design and applications. *Journal of Photochemistry and Photobiology C: Photochemistry Reviews*. 2012;13:169-89.
- [100] Wang B, Xue D, Shi Y, Xue F. Titania 1D nanostructured materials: Synthesis, properties and applications. *Nanorods, Nanotubes and Nanomaterials Research Progress*. 2008:163-202.
- [101] Patzke GR, Krumeich F, Nesper R. Oxidic Nanotubes and Nanorods—Anisotropic Modules for a Future Nanotechnology. *Angewandte Chemie International Edition*. 2002;41:2446-61.
- [102] Camposeco R, Castillo S, Navarrete J, Gomez R. Synthesis, characterization and photocatalytic activity of TiO₂ nanostructures: Nanotubes, nanofibers, nanowires and nanoparticles. *Catalysis Today*. 2016;266:90-101.
- [103] Yuan Z-Y, Su B-L. Titanium oxide nanotubes, nanofibers and nanowires. *Colloids and Surfaces A: Physicochemical and Engineering Aspects*. 2004;241:173-83.
- [104] Xing M, Li X, Zhang J. Synergistic effect on the visible light activity of Ti³⁺ doped TiO₂ nanorods/boron doped graphene composite. *Scientific Reports*. 2014;4:5493.
- [105] Rutar M, Rozman N, Pregelj M, Bittencourt C, Cerc Korošec R, Sever Škapin A, et al. Transformation of hydrogen titanate nanoribbons to TiO₂ nanoribbons and the influence of the transformation strategies on the photocatalytic performance. *Beilstein J Nanotechnol*. 2015;6:831-44.
- [106] Jitputti J, Suzuki Y, Yoshikawa S. Synthesis of TiO₂ nanowires and their photocatalytic activity for hydrogen evolution. *Catalysis Communications*. 2008;9:1265-71.

- [107] Shokuhfar T, Sinha-Ray S, Sukotjo C, Yarin AL. Intercalation of anti-inflammatory drug molecules within TiO₂ nanotubes. *RSC Advances*. 2013;3:17380-6.
- [108] Wang Y, Du G, Liu H, Liu D, Qin S, Wang N, et al. Nanostructured Sheets of TiO₂ Nanobelts for Gas Sensing and Antibacterial Applications. *Advanced Functional Materials*. 2008;18:1131-7.
- [109] Zeng W, Liu T-m, Liu D-j, Lv C-l. Hydrothermal synthesis and volatile organic compounds sensing properties of La-TiO₂ nanobelts. *Physica E: Low-dimensional Systems and Nanostructures*. 2011;44:37-42.
- [110] Hassan MS, Amna T, Yang OB, Kim H-C, Khil M-S. TiO₂ nanofibers doped with rare earth elements and their photocatalytic activity. *Ceramics International*. 2012;38:5925-30.
- [111] Shah SI, Li W, Huang C-P, Jung O, Ni C. Study of Nd³⁺, Pd²⁺, Pt⁴⁺, and Fe³⁺ dopant effect on photoreactivity of TiO₂ nanoparticles. *Proceedings of the National Academy of Sciences*. 2002;99:6482-6.
- [112] Wu Z, Dong F, Zhao W, Wang H, Liu Y, Guan B. The fabrication and characterization of novel carbon doped TiO₂ nanotubes, nanowires and nanorods with high visible light photocatalytic activity. *Nanotechnology*. 2009;20:235701.
- [113] Xu A-W, Gao Y, Liu H-Q. The Preparation, Characterization, and their Photocatalytic Activities of Rare-Earth-Doped TiO₂ Nanoparticles. *Journal of Catalysis*. 2002;207:151-7.
- [114] Kumar V, Prakash J, Singh JP, Chae KH, Swart C, Ntwaeaborwa OM, et al. Role of silver doping on the defects related photoluminescence and antibacterial behaviour of zinc oxide nanoparticles. *Colloids and Surfaces B: Biointerfaces*. 2017;159:191-9.
- [115] Prakash J, Harris RA, Swart HC. Embedded plasmonic nanostructures: synthesis, fundamental aspects and their surface enhanced Raman scattering applications. *International Reviews in Physical Chemistry*. 2016;35:353-98.
- [116] Huang F, Yan A, Zhao H. Influences of Doping on Photocatalytic Properties of TiO₂ Photocatalyst. 2016.
- [117] Kumar P, Chandra Mathpal M, Prakash J, Viljoen BC, Roos WD, Swart HC. Band gap tailoring of cauliflower-shaped CuO nanostructures by Zn doping for antibacterial applications. *Journal of Alloys and Compounds*. 2020;832:154968.
- [118] Lin Y-P, Ksari Y, Prakash J, Giovanelli L, Valmalette J-C, Themlin J-M. Nitrogen-doping processes of graphene by a versatile plasma-based method. *Carbon*. 2014;73:216-24.
- [119] Prakash J, Kumar V, Erasmus LJB, Duvenhage MM, Sathiyam G, Bellucci S, et al. Phosphor Polymer Nanocomposite: ZnO:Tb³⁺ Embedded Polystyrene Nanocomposite Thin Films for Solid-State Lighting Applications. *ACS Applied Nano Materials*. 2018;1:977-88.
- [120] Parnicka P, Mazierski P, Lisowski W, Klimczuk T, Nadolna J, Zaleska-Medynska A. A new simple approach to prepare rare-earth metals-modified TiO₂ nanotube arrays photoactive under visible light: Surface properties and mechanism investigation. *Results in Physics*. 2019;12:412-23.
- [121] Silva AMT, Silva CG, Dražić G, Faria JL. Ce-doped TiO₂ for photocatalytic degradation of chlorophenol. *Catalysis Today*. 2009;144:13-8.
- [122] Meksi M, Berhault G, Guillard C, Kochkar H. Design of TiO₂ nanorods and nanotubes doped with lanthanum and comparative kinetic study in the photodegradation of formic acid. *Catalysis Communications*. 2015;61:107-11.
- [123] Li FB, Li XZ, Hou MF. Photocatalytic degradation of 2-mercaptobenzothiazole in aqueous La³⁺-TiO₂ suspension for odor control. *Applied Catalysis B: Environmental*. 2004;48:185-94.
- [124] Li FB, Li XZ, Ao CH, Lee SC, Hou MF. Enhanced photocatalytic degradation of VOCs using Ln³⁺-TiO₂ catalysts for indoor air purification. *Chemosphere*. 2005;59:787-800.
- [125] Wu X, Ding X, Qin W, He W, Jiang Z. Enhanced photo-catalytic activity of TiO₂ films with doped La prepared by micro-plasma oxidation method. *Journal of Hazardous Materials*. 2006;137:192-7.

- [126] Sadhu S, Poddar P. Growth of oriented single crystalline La-doped TiO₂ nanorod arrays electrode and investigation of optoelectronic properties for enhanced photoelectrochemical activity. *RSC Advances*. 2013;3:10363-9.
- [127] Anandan S, Ikuma Y, Murugesan V. Highly Active Rare-Earth-Metal La-Doped Photocatalysts: Fabrication, Characterization, and Their Photocatalytic Activity. *International Journal of Photoenergy*. 2012;2012:921412.
- [128] Rajabi M, Abrinaei F. High nonlinear optical response of Lanthanum-doped TiO₂ nanorod arrays under pulsed laser irradiation at 532 nm. *Optics & Laser Technology*. 2019;109:131-8.
- [129] Sun P, Liu L, Cui S-C, Liu J-G. Synthesis, Characterization of Ce-doped TiO₂ Nanotubes with High Visible Light Photocatalytic Activity. *Catalysis Letters*. 2014;144:2107-13.
- [130] Xue W, Zhang G, Xu X, Yang X, Liu C, Xu Y. Preparation of titania nanotubes doped with cerium and their photocatalytic activity for glyphosate. *Chemical Engineering Journal*. 2011;167:397-402.
- [131] Li FB, Li XZ, Hou MF, Cheah KW, Choy WCH. Enhanced photocatalytic activity of Ce³⁺-TiO₂ for 2-mercaptobenzothiazole degradation in aqueous suspension for odour control. *Applied Catalysis A: General*. 2005;285:181-9.
- [132] Xu Y-h, Zeng Z-x. The preparation, characterization, and photocatalytic activities of Ce-TiO₂/SiO₂. *Journal of Molecular Catalysis A: Chemical*. 2008;279:77-81.
- [133] El-Bahy ZM, Ismail AA, Mohamed RM. Enhancement of titania by doping rare earth for photodegradation of organic dye (Direct Blue). *Journal of Hazardous Materials*. 2009;166:138-43.
- [134] Qi X, Song Y, Sheng Y, Zhang H, Zhao H, Shi Z, et al. Controllable synthesis and luminescence properties of TiO₂:Eu³⁺ nanorods, nanoparticles and submicrospheres by hydrothermal method. *Optical Materials*. 2014;38:193-7.
- [135] Bandi VR, Raghavan CM, Grandhe Bk, Kim SS, Jang K, Shin D-S, et al. Synthesis, structural and optical properties of pure and rare-earth ion doped TiO₂ nanowire arrays by a facile hydrothermal technique. *Thin Solid Films*. 2013;547:207-11.
- [136] Bianco A, Cacciotti I, Fragalà M, Lamastra F, Speghini A, Piccinelli F, et al. Eu-Doped Titania Nanofibers: Processing, Thermal Behaviour and Luminescent Properties. *Journal of nanoscience and nanotechnology*. 2010;10:5183-90.
- [137] Li H, Sheng Y, Zhang H, Xue J, Zheng K, Huo Q, et al. Synthesis and luminescent properties of TiO₂:Eu³⁺ nanotubes. *Powder Technology*. 2011;212:372-7.
- [138] Mezzi A, Kaciulis S, Cacciotti I, Bianco A, Gusmano G, Lamastra FR, et al. Structure and composition of electrospun titania nanofibres doped with Eu. *Surface and Interface Analysis*. 2010;42:572-5.
- [139] Zhang Y, Zhang H, Xu Y, Wang Y. Europium doped nanocrystalline titanium dioxide: preparation, phase transformation and photocatalytic properties. *Journal of Materials Chemistry*. 2003;13:2261-5.
- [140] Zhao H, Zheng K, Sheng Y, Li H, Zhang H, Qi X, et al. Template synthesis and luminescence properties of TiO₂:Eu³⁺ nanotubes. *Journal of Solid State Chemistry*. 2014;210:138-43.
- [141] Cacciotti I, Bianco A, Pezzotti G, Gusmano G. Synthesis, thermal behaviour and luminescence properties of rare earth-doped titania nanofibers. *Chemical Engineering Journal*. 2011;166:751-64.
- [142] Bahtat A, Bouazaoui M, Bahtat M, Garapon C, Jacquier B, Mugnier J. Up-conversion fluorescence spectroscopy in Er³⁺: TiO₂ planar waveguides prepared by a sol-gel process. *Journal of Non-Crystalline Solids*. 1996;202:16-22.
- [143] Liang C-H, Hou M-F, Zhou S-G, Li F-B, Liu C-S, Liu T-X, et al. The effect of erbium on the adsorption and photodegradation of orange I in aqueous Er³⁺-TiO₂ suspension. *Journal of Hazardous Materials*. 2006;138:471-8.
- [144] Jeon S, Braun PV. Hydrothermal Synthesis of Er-Doped Luminescent TiO₂ Nanoparticles. *Chemistry of Materials*. 2003;15:1256-63.
- [145] Jia CW, Zhao JG, Duan HG, Xie EQ. Visible photoluminescence from Er³⁺-doped TiO₂ nanofibres by electrospinning. *Materials Letters*. 2007;61:4389-92.

- [146] Lee DY, Lee M-H, Cho N-I. Preparation and photocatalytic degradation of erbium doped titanium dioxide nanorods. *Current Applied Physics*. 2012;12:1229-33.
- [147] Lin H, Huang Y, Li S, Luan C, Huang W, Wang X, et al. Preparation of erbium ion-doped TiO₂ films and the study of their photocatalytic activity under simulated solar light. *Journal of Semiconductors*. 2017;38:113004.
- [148] Lee D, Park J-Y, Kim B-Y, Cho N-I. Effect of Collector Speed and Flow Rate on Morphology of Er Doped TiO₂ Nanofibers. *Journal of nanoscience and nanotechnology*. 2012;12:1599-603.
- [149] Zhang H, Zhang Q, Lv Y, Yang C, Chen H, Zhou X. Upconversion Er-doped TiO₂ nanorod arrays for perovskite solar cells and the performance improvement. *Materials Research Bulletin*. 2018;106:346-52.
- [150] Liu H, Liu G, Zhou Q, Xie G, Hou Z, Zhang M, et al. Preparation and photocatalytic activity of Gd³⁺-doped trititanate nanotubes. *Microporous and Mesoporous Materials*. 2011;142:439-43.
- [151] Xu J, Ao Y, Fu D, Yuan C. Synthesis of Gd-doped TiO₂ nanoparticles under mild condition and their photocatalytic activity. *Colloids and Surfaces A: Physicochemical and Engineering Aspects*. 2009;334:107-11.
- [152] LChobba MB, Messaoud M, Weththimuni ML, Bouaziz J, Lichhelli M, Leo FD, Urzi C. preparation and characterization of photocatalytic Gd-doped TiO₂ nanoparticles for waste water treatment. *Environmental Science pollution research International*. 2019;26:32734-32745.
- [153] Park DJ, Sekino T, Tsukuda S, Hayashi A, Kusunose T, Tanaka S-I. Photoluminescence of samarium-doped TiO₂ nanotubes. *Journal of Solid State Chemistry*. 2011;184:2695-700.
- [154] Pal M, Pal U, Silva Gonzalez R, Sanchez Mora E, Santiago P. Synthesis and Photocatalytic Activity of Yb Doped TiO₂ Nanoparticles under Visible Light. *Journal of Nano Research*. 2009;5:193-200.
- [155] Al-Maliki FJ, Al-Lamey NH. Synthesis of Tb-doped titanium dioxide nanostructures by sol-gel method for environmental photocatalysis applications. *Journal of Sol-Gel Science and Technology*. 2017;81:276-83.
- [156] Li M, Zhang X, Liu Y, Yang Y. Pr³⁺ doped biphasic TiO₂ (rutile-brookite) nanorod arrays grown on activated carbon fibers: Hydrothermal synthesis and photocatalytic properties. *Applied Surface Science*. 2018;440:1172-80.
- [157] Wang Z, Song Y, Cai X, Zhang J, Tang T, Wen S. Rapid preparation of terbium-doped titanium dioxide nanoparticles and their enhanced photocatalytic performance. *Royal Society Open Science*. 2019;6:191077.
- [158] Forissier S, Roussel H, Chaudouet P, Pereira A, Deschanvres J-L, Moine B. Thulium and Ytterbium-Doped Titanium Oxide Thin Films Deposited by Ultrasonic Spray Pyrolysis. *Journal of Thermal Spray Technology*. 2012;21:1263-8.
- [159] Liao F, Chu L-F, Guo C-X, Guo Y-J, Ke Q-F, Guo Y-P. Ytterbium Doped TiO₂ Nanofibers on Activated Carbon Fibers Enhances Adsorption and Photocatalytic Activities for Toluene Removal. *ChemistrySelect*. 2019;4:9222-31.
- [160] Tang J, Chen X, Liu Y, Gong W, Peng Z, Cai T, et al. Samarium-doped mesoporous TiO₂ nanoparticles with improved photocatalytic performance for elimination of gaseous organic pollutants. *Solid State Sciences*. 2013;15:129-36.
- [161] Wang ZB, Su LY, Guan YJ, Bai SL. Study on the Preparation of Dy-Doped TiO₂ Nanotube Arrays and its Visible Light Responsive Photocatalytic Properties. *Applied Mechanics and Materials*. 2012;130-134:1254-7.
- [162] Nwe TS, Sikong L, Kokoo R, Khangkhamano M. Photocatalytic activity enhancement of Dy-doped TiO₂ nanoparticles hybrid with TiO₂ (B) nanobelts under UV and fluorescence irradiation. *Current Applied Physics*. 2020;20:249-54.
- [163] Zikriya M, Nadaf YF, Bharathy PV, Renuka CG. Luminescent characterization of rare earth Dy³⁺ ion doped TiO₂ prepared by simple chemical co-precipitation method. *Journal of Rare Earths*. 2019;37:24-31.

- [164] Zhou W, He Y. Ho/TiO₂ nanowires heterogeneous catalyst with enhanced photocatalytic properties by hydrothermal synthesis method. *Chemical Engineering Journal*. 2012;179:412-6.
- [165] Nassoko D, Li Y-F, Li J-L, Li X, Yu Y. Neodymium-Doped  `<svg style="vertical-align:-4.32pt;width:42.962502px;" id="M1" height="20.637501" version="1.1" viewBox="0 0 42.962502 20.637501" width="42.962502" xmlns:xlink="http://www.w3.org/1999/xlink" xmlns="http://www.w3.org/2000/svg"><g transform="matrix(.022,-0,0,-.022,.062,15.188)"><path id="x54" d="M592 498l-30 -3q-13 63 -31 89q-13 19 -33.5 25.5t-75.5 6.5h-70v-493q0 -60 16 -75.5t86 -19.5v-28h-286v28q68 4 83.5 19.5t15.5 75.5v493h-62q-60 0 -83 -7t-33 -24q-12 -17 -32 -90h-29q10 116 12 180h20q10 -16 21 -20.5t34 -4.5h395q19 0 28.5 5t21.5 20h21 q2 -89 11 -177z" /></g><g transform="matrix(.022,-0,0,-.022,11.674,15.188)"><path id="x69" d="M135 536q-20 0 -35 15.5t-15 35.5q0 22 15 37t36 15t35.5 -15t14.5 -37q0 -21 -15 -36t-36 -15zM252 0h-220v26q48 5 59 17t11 63v206q0 47 -9 58t-54 18v24q78 12 142 39v-345q0 -51 11.5 -63t59.5 -17v-26z" /></g><g transform="matrix(.022,-0,0,-.022,17.682,15.188)"><path id="x4F" d="M381 665q131 0 226.5 -93t95.5 -239q0 -158 -96 -253t-238 -95q-137 0 -231 95t-94 238q0 142 92.5 244.5t244.5 102.5zM359 629q-89 0 -151 -74.5t-62 -208.5q0 -141 69 -233t175 -92q90 0 150.5 74t60.5 211q0 152 -69 237.5t-173 85.5z" /></g><g transform="matrix(.016,-0,0,-.016,34.425,20.575)"><path id="x1D7D0" d="M453 211h25l-46 -211h-415v23q97 102 151 166q42 49 81 110q51 78 51 148q0 56 -31.5 91.5t-87.5 35.5q-77 0 -122 -90h-28q67 204 223 204q82 0 132 -49.5t50 -133.5q0 -110 -114 -218l-162 -154h140q82 0 107 13q27 13 46 65z" /></g></svg>` with Anatase and Brookite Two Phases: Mechanism for Photocatalytic Activity Enhancement under Visible Light and the Role of Electron. *International Journal of Photoenergy*. 2012;2012:716087.
- [166] Kumar V, Ntwaeaborwa OM, Holsa J, Motaung DE, Swart HC. The role of oxygen and titanium related defects on the emission of TiO₂:Tb³⁺ nano-phosphor for blue lighting applications. *Optical Materials*. 2015;46:510-6.
- [167] Saqib Nu, Adnan R, Shah I. A mini-review on rare earth metal-doped TiO₂ for photocatalytic remediation of wastewater. *Environmental Science and Pollution Research*. 2016;23:15941-51.
- [168] Zhang B, Song Z, Jin J, Bi W, Li H, Chen C, et al. Efficient rare earth co-doped TiO₂ electron transport layer for high-performance perovskite solar cells. *Journal of Colloid and Interface Science*. 2019;553:14-21.
- [169] Chen C, Ma W, Zhao J. Photocatalytic Degradation of Organic Pollutants by Co-Doped TiO₂ Under Visible Light Irradiation. *Current Organic Chemistry*. 2010;14:630-44.
- [170] Cong Y, Zhang J, Chen F, Anpo M, He D. Preparation, Photocatalytic Activity, and Mechanism of Nano-TiO₂ Co-Doped with Nitrogen and Iron (III). *The Journal of Physical Chemistry C*. 2007;111:10618-23.
- [171] Nah Y-C, Paramasivam I, Schmuki P. Doped TiO₂ and TiO₂ Nanotubes: Synthesis and Applications. *ChemPhysChem*. 2010;11:2698-713.
- [172] Li Y, Wang Y, Kong J, Wang J. Synthesis and photocatalytic activity of TiO₂ nanotubes co-doped by erbium ions. *Applied Surface Science*. 2015;328:115-9.
- [173] Di Valentin C, Pacchioni G, Selloni A. Theory of Carbon Doping of Titanium Dioxide. *Chemistry of Materials*. 2005;17:6656-65.
- [174] Sulaiman SNA, Zaky Noh M, Nadia Adnan N, Bidin N, Ab Razak SN. Effects of photocatalytic activity of metal and non-metal doped TiO₂ for Hydrogen production enhancement - A Review. *Journal of Physics: Conference Series*. 2018;1027:012006.
- [175] Basavarajappa PS, Patil SB, Ganganagappa N, Reddy KR, Raghu AV, Reddy CV. Recent progress in metal-doped TiO₂, non-metal doped/codoped TiO₂ and TiO₂ nanostructured hybrids for enhanced photocatalysis. *International Journal of Hydrogen Energy*. 2020;45:7764-78.
- [176] Pan Y, Wen M. Noble metals enhanced catalytic activity of anatase TiO₂ for hydrogen evolution reaction. *International Journal of Hydrogen Energy*. 2018;43:22055-63.

- [177] Kumar CNS, Bauri R, Reddy GS. Phase stability and conductivity of rare earth co-doped nanocrystalline zirconia electrolytes for solid oxide fuel cells. *Journal of Alloys and Compounds*. 2020;833:155100.
- [178] Paßlick C, Johnson JA, Schweizer S. Crystallization studies on rare-earth co-doped fluorozirconate-based glasses. *Journal of Non-Crystalline Solids*. 2013;371-372:33-6.
- [179] Zhou F, Wang H, Zhou S, Liu Y, Yan C. Fabrication of europium-nitrogen co-doped TiO₂/Sepiolite nanocomposites and its improved photocatalytic activity in real wastewater treatment. *Applied Clay Science*. 2020;197:105791.
- [180] Wang X, Zhang Z, Qin J, Shi W, Liu Y, Gao H, et al. Enhanced Photovoltaic Performance of Perovskite Solar Cells Based on Er-Yb Co-doped TiO₂ Nanorod Arrays. *Electrochimica Acta*. 2017;245:839-45.
- [181] Zhang Z, Qin J, Shi W, Liu Y, Zhang Y, Liu Y, et al. Enhanced Power Conversion Efficiency of Perovskite Solar Cells with an Up-Conversion Material of Er³⁺-Yb³⁺-Li⁺ Tri-doped TiO₂. *Nanoscale Research Letters*. 2018;13:147.
- [182] Li S, Wang Z, Yang Y, Li J, Jin C. Enhanced conductivity of anatase TiO₂ nanowires by La and Co co-doping. *Micro & Nano Letters: Institution of Engineering and Technology*; 2020. p. 226-9.
- [183] Li S, Zhang G, Guo D, Yu L, Zhang W. Anodization Fabrication of Highly Ordered TiO₂ Nanotubes. *The Journal of Physical Chemistry C*. 2009;113:12759-65.
- [184] Kasuga T, Hiramatsu M, Hoson A, Sekino T, Niihara K. Formation of Titanium Oxide Nanotube. *Langmuir*. 1998;14:3160-3.
- [185] Zhou W, Liu X, Cui J, Liu D, Li J, Jiang H, et al. Control synthesis of rutile TiO₂ microspheres, nanoflowers, nanotrees and nanobelts via acid-hydrothermal method and their optical properties. *CrystEngComm*. 2011;13:4557-63.
- [186] Li D, Xia Y. Fabrication of Titania Nanofibers by Electrospinning. *Nano Letters*. 2003;3:555-60.
- [187] Yoshida R, Suzuki Y, Yoshikawa S. Syntheses of TiO₂(B) nanowires and TiO₂ anatase nanowires by hydrothermal and post-heat treatments. *Journal of Solid State Chemistry*. 2005;178:2179-85.
- [188] Cao X, Xue X. Heterostructured Ag@TiO₂ Nanoribbons: Synthesis, Characterization, and Photocatalytic Activity. *Science of Advanced Materials*. 2010;2:390-5.
- [189] Khanna S, Utsav, Patel R, Marathe P, Chaudari R, Vora J, et al. Growth of titanium dioxide nanorod over shape memory material using chemical vapor deposition for energy conversion application. *Materials Today: Proceedings*. 2019.
- [190] Gupta VK, Fakhri A, Agarwal S, Bharti AK, Naji M, Tkachev AG. Preparation and characterization of TiO₂ nanofibers by hydrothermal method for removal of Benzodiazepines (Diazepam) from liquids as catalytic ozonation and adsorption processes. *Journal of Molecular Liquids*. 2018;249:1033-8.
- [191] Erdogan N, Ozturk A, Park J. Hydrothermal synthesis of 3D TiO₂ nanostructures using nitric acid: Characterization and evolution mechanism. *Ceramics International*. 2016;42:5985-94.
- [192] Li Y, Fu Y, Zhu M. Green synthesis of 3D tripyramid TiO₂ architectures with assistance of aloe extracts for highly efficient photocatalytic degradation of antibiotic ciprofloxacin. *Applied Catalysis B: Environmental*. 2020;260:118149.
- [193] Ueda M, Uchibayashi Y, Otsuka-Yao-Matsuo S, Okura T. Hydrothermal synthesis of anatase-type TiO₂ films on Ti and Ti-Nb substrates. *Journal of Alloys and Compounds*. 2008;459:369-76.
- [194] Mohamed HH, Mohamed SK. Rutile TiO₂ nanorods/MWCNT composites for enhanced simultaneous photocatalytic oxidation of organic dyes and reduction of metal ions. *Materials Research Express*. 2018;5:015057.
- [195] Jo W-K, Jin Y-J. 2D graphene-assisted low-cost metal (Ag, Cu, Fe, or Ni)-doped TiO₂ nanowire architectures for enhanced hydrogen generation. *Journal of Alloys and Compounds*. 2018;765:106-12.
- [196] Kolen'ko YV, Kovnir KA, Gavrillov AI, Garshev AV, Frantti J, Lebedev OI, et al. Hydrothermal Synthesis and Characterization of Nanorods of Various Titanates and Titanium Dioxide. *The Journal of Physical Chemistry B*. 2006;110:4030-8.

- [197] Rozman N, Tobaldi DM, Cvelbar U, Puliyalil H, Labrincha JA, Legat A, et al. Hydrothermal Synthesis of Rare-Earth Modified Titania: Influence on Phase Composition, Optical Properties, and Photocatalytic Activity. *Materials*. 2019;12:713.
- [198] Liu N, Chen X, Zhang J, Schwank JW. A review on TiO₂-based nanotubes synthesized via hydrothermal method: Formation mechanism, structure modification, and photocatalytic applications. *Catalysis Today*. 2014;225:34-51.
- [199] Chatterjee S, Bhattacharyya K, Ayyub P, Tyagi AK. Photocatalytic Properties of One-Dimensional Nanostructured Titanates. *The Journal of Physical Chemistry C*. 2010;114:9424-30.
- [200] Choi MG, Lee Y-G, Song S-W, Kim KM. Lithium-ion battery anode properties of TiO₂ nanotubes prepared by the hydrothermal synthesis of mixed (anatase and rutile) particles. *Electrochimica Acta*. 2010;55:5975-83.
- [201] Morgan DL, Liu H-W, Frost RL, Waclawik ER. Implications of Precursor Chemistry on the Alkaline Hydrothermal Synthesis of Titania/Titanate Nanostructures. *The Journal of Physical Chemistry C*. 2010;114:101-10.
- [202] Li Y, Zhang M, Guo M, Wang X. Hydrothermal growth of well-aligned TiO₂ nanorod arrays: Dependence of morphology upon hydrothermal reaction conditions. *Rare Metals*. 2010;29:286-91.
- [203] Menzel R, Peiró AM, Durrant JR, Shaffer MSP. Impact of Hydrothermal Processing Conditions on High Aspect Ratio Titanate Nanostructures. *Chemistry of Materials*. 2006;18:6059-68.
- [204] Ali W, Jaffari GH, Khan S, Liu Y. Morphological control of 1D and 3D TiO₂ nanostructures with ammonium hydroxide and TiO₂ compact layer on FTO coated glass in hydrothermal synthesis. *Materials Chemistry and Physics*. 2018;214:48-55.
- [205] Feng H, Zhang M-H, Yu LE. Hydrothermal synthesis and photocatalytic performance of metal-ions doped TiO₂. *Applied Catalysis A: General*. 2012;413-414:238-44.
- [206] Patel SKS, Gajbhiye NS, Date SK. Ferromagnetism of Mn-doped TiO₂ nanorods synthesized by hydrothermal method. *Journal of Alloys and Compounds*. 2011;509:S427-S30.
- [207] Ouyang W, Santiago ARP, Cerdán-Gómez K, Luque R. Chapter 5 - Nanoparticles within functional frameworks and their applications in photo(electro)catalysis. In: Prieto JP, Béjar MG, editors. *Photoactive Inorganic Nanoparticles*; Elsevier; 2019. p. 109-38.
- [208] Das K, Panda SK, Chaudhuri S. Solvent-controlled synthesis of TiO₂ 1D nanostructures: Growth mechanism and characterization. *Journal of Crystal Growth*. 2008;310:3792-9.
- [209] Jiang Z, Yang F, Luo N, Chu BTT, Sun D, Shi H, et al. Solvothermal synthesis of N-doped TiO₂ nanotubes for visible-light-responsive photocatalysis. *Chemical Communications*. 2008:6372-4.
- [210] Arab S, Li D, Kinsinger N, Zaera F, Kisailus D. Solvothermal synthesis of a highly branched Ta-doped TiO₂. *Journal of Materials Research*. 2011;26:2653-9.
- [211] Yan Y, Lee J, Cui X. Enhanced photoelectrochemical properties of Ta-TiO₂ nanotube arrays prepared by magnetron sputtering. *Vacuum*. 2017;138:30-8.
- [212] Pedferri M. Titanium Anodic Oxidation: A Powerful Technique for Tailoring Surfaces Properties for Biomedical Applications. Cham: Springer International Publishing; 2016. p. 515-20.
- [213] Jedi-soltanabadi Z, Pishkar N, Ghoranneviss M. Enhanced physical properties of the anodic TiO₂ nanotubes via proper anodization time. *Journal of Theoretical and Applied Physics*. 2018;12:135-9.
- [214] Fu Y, Mo A. A Review on the Electrochemically Self-organized Titania Nanotube Arrays: Synthesis, Modifications, and Biomedical Applications. *Nanoscale Research Letters*. 2018;13:187.
- [215] Dai X-C, Hou S, Huang M-H, Li Y-B, Li T, Xiao F-X. Electrochemically anodized one-dimensional semiconductors: a fruitful platform for solar energy conversion. *Journal of Physics: Energy*. 2019;1:022002.
- [216] Lee K, Mazare A, Schmuki P. One-Dimensional Titanium Dioxide Nanomaterials: Nanotubes. *Chemical Reviews*. 2014;114:9385-454.

- [217] Beketova D, Motola M, Sopha H, Michalicka J, Cícmancova V, Dvorak F, et al. One-Step Decoration of TiO₂ Nanotubes with Fe₃O₄ Nanoparticles: Synthesis and Photocatalytic and Magnetic Properties. *ACS Applied Nano Materials*. 2020;3:1553-63.
- [218] Li R, Yang J, Xu S, Zhou Y, Wang X, Peng H, et al. Preparation of Gd-Doped TiO₂ Nanotube Arrays by Anodization Method and Its Photocatalytic Activity for Methyl Orange Degradation. *Catalysts*. 2020;10:298.
- [219] Subramanian VR, Sarker S, Yu B, Kar A, Sun X, Dey SK. TiO₂ nanotubes and its composites: Photocatalytic and other photo-driven applications. *Journal of Materials Research*. 2013;28:280-93.
- [220] Liu L, Pan F, Liu C, Huang L, Li W, Lu X. TiO₂ Nanofoam–Nanotube Array for Surface-Enhanced Raman Scattering. *ACS Applied Nano Materials*. 2018;1:6563-6.
- [221] Yodyingyong S, Zhou X, Zhang Q, Triampo D, Xi J, Park K, et al. Enhanced Photovoltaic Performance of Nanostructured Hybrid Solar Cell Using Highly Oriented TiO₂ Nanotubes. *The Journal of Physical Chemistry C*. 2010;114:21851-5.
- [222] Macak JM, Schmuki P. Anodic growth of self-organized anodic TiO₂ nanotubes in viscous electrolytes. *Electrochimica Acta*. 2006;52:1258-64.
- [223] Zhang Q, Ma L, Minghui S, Huang J, Ding M, Deng X, et al. Anodic Oxidation Synthesis of One-Dimensional TiO₂ Nanostructures for Photocatalytic and Field Emission Properties. *Journal of Nanomaterials*. 2014;2014:1-14.
- [224] Fan X, Wan J, Liu E, Sun L, Hu Y, Li H, et al. High-efficiency photoelectrocatalytic hydrogen generation enabled by Ag deposited and Ce doped TiO₂ nanotube arrays. *Ceramics International*. 2015;41:5107-16.
- [225] Nie J, Mo Y, Zheng B, Yuan H, Xiao D. Electrochemical fabrication of lanthanum-doped TiO₂ nanotube array electrode and investigation of its photoelectrochemical capability. *Electrochimica Acta*. 2013;90:589-96.
- [226] Thenmozhi S, Dharmaraj N, Kadirvelu K, Kim HY. Electrospun nanofibers: New generation materials for advanced applications. *Materials Science and Engineering: B*. 2017;217:36-48.
- [227] Ramakrishna SAF, Kazutoshi%A Teo, Wee-Eong%A Lim, Teik-Cheng%A Ma, Zuwei. *An Introduction to Electrospinning and Nanofibers*.
- [228] Contreras-Cáceres R, Cabeza L, Perazzoli G, Díaz A, López-Romero JM, Melguizo C, et al. Electrospun Nanofibers: Recent Applications in Drug Delivery and Cancer Therapy. *Nanomaterials*. 2019;9:656.
- [229] Xue J, Wu T, Dai Y, Xia Y. Electrospinning and Electrospun Nanofibers: Methods, Materials, and Applications. *Chemical Reviews*. 2019;119:5298-415.
- [230] Shi X, Zhou W, Ma D, Ma Q, Bridges D, Ma Y, et al. Electrospinning of Nanofibers and Their Applications for Energy Devices. *Journal of Nanomaterials*. 2015;2015:140716.
- [231] Zelkó R, Lamprou DA, Sebe I. Recent Development of Electrospinning for Drug Delivery. *Pharmaceutics*. 2020;12:5.
- [232] Su Z, Ding J, Wei G. Electrospinning: a facile technique for fabricating polymeric nanofibers doped with carbon nanotubes and metallic nanoparticles for sensor applications. *RSC Advances*. 2014;4:52598-610.
- [233] Ghorani B, Tucker N. Fundamentals of electrospinning as a novel delivery vehicle for bioactive compounds in food nanotechnology. *Food Hydrocolloids*. 2015;51:227-40.
- [234] Fehse M, Cavaliere S, Lippens PE, Savych I, Iadecola A, Monconduit L, et al. Nb-Doped TiO₂ Nanofibers for Lithium Ion Batteries. *The Journal of Physical Chemistry C*. 2013;117:13827-35.
- [235] Sekar AD, Kumar V, Muthukumar H, Gopinath P, Matheswaran M. Electrospinning of Fe-doped ZnO nanoparticles incorporated polyvinyl alcohol nanofibers for its antibacterial treatment and cytotoxic studies. *European Polymer Journal*. 2019;118:27-35.
- [236] Hu Q, Huang B, Li Y, Zhang S, Zhang Y, Hua X, et al. Methanol gas detection of electrospun CeO₂ nanofibers by regulating Ce³⁺/ Ce⁴⁺ mole ratio via Pd doping. *Sensors and Actuators B: Chemical*. 2020;307:127638.

- [237] Liu Y, He J-H, Yu J-y, Zeng H-m. Controlling numbers and sizes of beads in electrospun nanofibers. *Polymer International*. 2008;57:632-6.
- [238] He G, Cai Y, Zhao Y, Wang X, Lai C, Xi M, et al. Electrospun anatase-phase TiO₂ nanofibers with different morphological structures and specific surface areas. *Journal of Colloid and Interface Science*. 2013;398:103-11.
- [239] Someswararao MV, Dubey RS, Subbarao PSV, Singh S. Electrospinning process parameters dependent investigation of TiO₂ nanofibers. *Results in Physics*. 2018;11:223-31.
- [240] Li J, Qiao H, Du Y, Chen C, Li X, Cui J, et al. Electrospinning Synthesis and Photocatalytic Activity of Mesoporous TiO₂ Nanofibers. *The Scientific World Journal*. 2012;2012:154939.
- [241] Zhao J, Hu Z, Jin M, Zhou H, Gu Y, Liu Z, et al. A Facile and Scalable Method to Synthesize Eu³⁺-Doped TiO₂ Porous Nanofibers with Electrospinning. *Science of Advanced Materials*. 2019;11:372-8.
- [242] Mirmohammad Sadeghi S, Vaezi M, Kazemzadeh A, Jamjah R. Morphology enhancement of TiO₂/PVP composite nanofibers based on solution viscosity and processing parameters of electrospinning method. *Journal of Applied Polymer Science*. 2018;135:46337.
- [243] Zhao J, Jia C, Duan H, Sun Z, Wang X, Xie E. Structural and photoluminescence properties of europium-doped titania nanofibers prepared by electrospinning method. *Journal of Alloys and Compounds*. 2008;455:497-500.
- [244] Hoyer P. Formation of a Titanium Dioxide Nanotube Array. *Langmuir*. 1996;12:1411-3.
- [245] Sadeghzadeh Attar A, Sasani Ghamsari M, Hajiesmaeilbaigi F, Mirdamadi S, Katagiri K, Koumoto K. Synthesis and characterization of anatase and rutile TiO₂ nanorods by template-assisted method. *Journal of Materials Science*. 2008;43:5924-9.
- [246] Sander MS, Côté MJ, Gu W, Kile BM, Tripp CP. Template-Assisted Fabrication of Dense, Aligned Arrays of Titania Nanotubes with Well-Controlled Dimensions on Substrates. *Advanced Materials*. 2004;16:2052-7.
- [247] Achoi MF, Asiah MN, Jani NA, Rusop M, Abdullah S. One-Dimensional TiO₂ Nanothorn-Like Structures Assisted TiO₂ Template for High Absorption Hydrophilic Self-Cleaning. *Advanced Materials Research*. 2013;686:18-27.
- [248] Ge M, Li Q, Cao C, Huang J, Li S, Zhang S, et al. One-dimensional TiO₂ Nanotube Photocatalysts for Solar Water Splitting. *Advanced Science*. 2017;4:1600152.
- [249] Cheng L, Kang Y, Tong F. Effect of preparation conditions on characteristics of hollow TiO₂ fibers fabricated by chemical deposition and template method. *Applied Surface Science*. 2012;263:223-9.
- [250] Lee J-H, Leu I-C, Hsu M-C, Chung Y-W, Hon M-H. Fabrication of Aligned TiO₂ One-Dimensional Nanostructured Arrays Using a One-Step Templating Solution Approach. *The Journal of Physical Chemistry B*. 2005;109:13056-9.
- [251] Yuan L, Meng S, Zhou Y, Yue Z. Controlled synthesis of anatase TiO₂ nanotube and nanowire arrays via AAO template-based hydrolysis. *Journal of Materials Chemistry A*. 2013;1:2552-7.
- [252] Bae C, Yoon Y, Yoo H, Han D, Cho J, Lee BH, et al. Controlled Fabrication of Multiwall Anatase TiO₂ Nanotubular Architectures. *Chemistry of Materials*. 2009;21:2574-6.
- [253] Thomas A, Goettmann F, Antonietti M. Hard Templates for Soft Materials: Creating Nanostructured Organic Materials. *Chemistry of Materials*. 2008;20:738-55.
- [254] Hwang K-J, Cho DW, Lee J-W, Im C. Preparation of nanoporous TiO₂ electrodes using different mesostructured silica templates and improvement of the photovoltaic properties of DSSCs. *New Journal of Chemistry*. 2012;36:2094-100.
- [255] Zhao B, Collinson MM. Well-Defined Hierarchical Templates for Multimodal Porous Material Fabrication. *Chemistry of Materials*. 2010;22:4312-9.
- [256] Prakash J, Swart HC, Zhang G, Sun S. Emerging applications of atomic layer deposition for the rational design of novel nanostructures for surface-enhanced Raman scattering. *Journal of Materials Chemistry C*. 2019;7:1447-71.

- [257] Wang X, Li Z, Shi J, Yu Y. One-Dimensional Titanium Dioxide Nanomaterials: Nanowires, Nanorods, and Nanobelts. *Chemical Reviews*. 2014;114:9346-84.
- [258] Nyamukamba P, Okoh O, Heroe H, Taziwa R, Zinya S. Synthetic Methods for Titanium Dioxide Nanoparticles: A Review. 2018.
- [259] Attar A, Mirdamadi S, Hajiesmaeilbaigi F, Sasani Ghamsari M. Growth of TiO₂ Nanorods by Sol–Gel Template Process. *Journal of Materials Science and Technology*. 2007;23.
- [260] Yun J-H, Wang L, Amal R, Ng YH. One-Dimensional TiO₂ Nanostructured Photoanodes: From Dye-Sensitised Solar Cells to Perovskite Solar Cells. *Energies*. 2016;9:1030.
- [261] Taziwa R, Meyer EL, Takata N. Structural and Raman Spectroscopic Characterization of c-TiO₂ Nanotubes Synthesized by Template Assisted Sol-Gel Technique 2017.
- [262] Shi J, Wang X. Growth of Rutile Titanium Dioxide Nanowires by Pulsed Chemical Vapor Deposition. *Crystal Growth & Design*. 2011;11:949-54.
- [263] Yang FH. 2 - Modern metal-organic chemical vapor deposition (MOCVD) reactors and growing nitride-based materials. In: Huang J, Kuo H-C, Shen S-C, editors. *Nitride Semiconductor Light-Emitting Diodes (LEDs)*: Woodhead Publishing; 2014. p. 27-65.
- [264] Wang X, Shi J. Evolution of titanium dioxide one-dimensional nanostructures from surface-reaction-limited pulsed chemical vapor deposition. *Journal of Materials Research*. 2013;28:270-9.
- [265] Pan J, Shen H, Mathur S. One-Dimensional SnO₂ Nanostructures: Synthesis and Applications. *Journal of Nanotechnology*. 2012;2012:917320.
- [266] Zhang T, Fu L. Controllable Chemical Vapor Deposition Growth of Two-Dimensional Heterostructures. *Chem*. 2018;4:671-89.
- [267] Amin SS, Li S-y, Wu X, Ding W, Xu TT. Facile Synthesis and Tensile Behavior of TiO₂ One-Dimensional Nanostructures. *Nanoscale Research Letters*. 2009;5:338.
- [268] Hoa N, Lee Z, Kim E-T. Enhanced Photocatalytic Properties of TiO₂ Nanobelts via In Situ Doping of C and Fe. *Journal of The Electrochemical Society*. 2011;159:K42-K5.
- [269] Dunnill CW, Kafizas A, Parkin IP. CVD Production of Doped Titanium Dioxide Thin Films. *Chemical Vapor Deposition*. 2012;18:89-101.
- [270] Parkin IP. Special Section on the CVD of TiO₂ and Doped TiO₂ Films. *Chemical Vapor Deposition*. 2012;18:87-8.
- [271] Vesna Đ, Bojana M, Miroslav DD. Rare Earth-Doped Anatase TiO₂ Nanoparticles. 2017.
- [272] Reszczyńska J, Grzyb T, Wei Z, Klein M, Kowalska E, Ohtani B, et al. Photocatalytic activity and luminescence properties of RE₃₊–TiO₂ nanocrystals prepared by sol–gel and hydrothermal methods. *Applied Catalysis B: Environmental*. 2016;181:825-37.
- [273] Zong L, Li Q, Zhang J, Wang X, Yang J. Preparation of Pd-loaded La-doped TiO₂ nanotubes and investigation of their photocatalytic activity under visible light. *Journal of Nanoparticle Research*. 2013;15:2042.
- [274] Ma Y-T, Li S-D. Photocatalytic Activity of TiO₂ Nanofibers with Doped La Prepared by Electrospinning Method. *Journal of the Chinese Chemical Society*. 2015;62:380-4.
- [275] Prakash J. Fundamentals and applications of recyclable SERS substrates. *International Reviews in Physical Chemistry*. 2019;38:201-42.
- [276] Venkateswararao A, Ho JKW, So SK, Liu S-W, Wong K-T. Device characteristics and material developments of indoor photovoltaic devices. *Materials Science and Engineering: R: Reports*. 2020;139:100517.
- [277] O'Regan B, Grätzel M. A low-cost, high-efficiency solar cell based on dye-sensitized colloidal TiO₂ films. *Nature*. 1991;353:737-40.
- [278] Prakash J, Singh A, Sathiyam G, Ranjan R, Singh A, Garg A, et al. Progress in tailoring perovskite based solar cells through compositional engineering: Materials properties, photovoltaic performance and critical issues. *Materials Today Energy*. 2018;9:440-86.

- [279] Sathiyar G, Siva G, Sivakumar EKT, Prakash J, Swart HC, Sakthivel P. Synthesis and studies of carbazole-based donor polymer for organic solar cell applications. *Colloid and Polymer Science*. 2018;296:1193-203.
- [280] Sathiyar G, Siva G, Prakash J, Swart HC, Sakthivel P. Design and chemical engineering of carbazole-based donor small molecules for organic solar cell applications. *Journal of Materials Science: Materials in Electronics*. 2018;29:14842-51.
- [281] Hafez H, Lan Z, Li Q, Wu J. High efficiency dye-sensitized solar cell based on novel TiO₂ nanorod/nanoparticle bilayer electrode. *Nanotechnol Sci Appl*. 2010;3:45-51.
- [282] Luitel T, Fernando K, Tatum BS, Alphenaar BW, Zamborini FP. Increased efficiency of dye-sensitized solar cells by addition of rare earth oxide microparticles into a titania acceptor. *Electrochimica Acta*. 2016;211:918-25.
- [283] Chandiran AK, Sauvage F, Casas-Cabanas M, Comte P, Zakeeruddin SM, Graetzel M. Doping a TiO₂ Photoanode with Nb⁵⁺ to Enhance Transparency and Charge Collection Efficiency in Dye-Sensitized Solar Cells. *The Journal of Physical Chemistry C*. 2010;114:15849-56.
- [284] Zhong P, Chen X, Niu B, Li C, Wang Y, Xi H, et al. Niobium doped TiO₂ nanorod arrays as efficient electron transport materials in photovoltaic. *Journal of Power Sources*. 2020;450:227715.
- [285] Zalas M. Gadolinium-modified titanium oxide materials for photoenergy applications: a review. *Journal of Rare Earths*. 2014;32:487-95.
- [286] Huang X, Han S, Huang W, Liu X. Enhancing solar cell efficiency: the search for luminescent materials as spectral converters. *Chemical Society Reviews*. 2013;42:173-201.
- [287] Zhang J, Peng W, Chen Z, Chen H, Han L. Effect of Cerium Doping in the TiO₂ Photoanode on the Electron Transport of Dye-Sensitized Solar Cells. *The Journal of Physical Chemistry C*. 2012;116:19182-90.
- [288] Adachi M, Murata Y, Takao J, Jiu J, Sakamoto M, Wang F. Highly Efficient Dye-Sensitized Solar Cells with a Titania Thin-Film Electrode Composed of a Network Structure of Single-Crystal-like TiO₂ Nanowires Made by the "Oriented Attachment" Mechanism. *Journal of the American Chemical Society*. 2004;126:14943-9.
- [289] Uchida S, Chiba R, Tomiha M, Masaki N, Shirai M. Application of Titania Nanotubes to a Dye-sensitized Solar Cell. *Electrochemistry*. 2002;70:418-20.
- [290] Jiu J, Isoda S, Wang F, Adachi M. Dye-Sensitized Solar Cells Based on a Single-Crystalline TiO₂ Nanorod Film. *The Journal of Physical Chemistry B*. 2006;110:2087-92.
- [291] Tang Y, Wang C, Hu Y, Huang L, Fu J, Yang W. Preparation of anatase TiO₂ nanorods with high aspect ratio for high-performance dye-sensitized solar cells. *Superlattices and Microstructures*. 2016;89:1-6.
- [292] Elzarka A, Liu N, Hwang I, Kamal M, Schmuki P. Large-Diameter TiO₂ Nanotubes Enable Wall Engineering with Conformal Hierarchical Decoration and Blocking Layers for Enhanced Efficiency in Dye-Sensitized Solar Cells (DSSC). *Chemistry – A European Journal*. 2017;23:12995-9.
- [293] Feng X, Shankar K, Paulose M, Grimes CA. Tantalum-Doped Titanium Dioxide Nanowire Arrays for Dye-Sensitized Solar Cells with High Open-Circuit Voltage. *Angewandte Chemie International Edition*. 2009;48:8095-8.
- [294] Yang M, Ding B, Lee J-K. Surface electrochemical properties of niobium-doped titanium dioxide nanorods and their effect on carrier collection efficiency of dye sensitized solar cells. *Journal of Power Sources*. 2014;245:301-7.
- [295] Kouhnavard M, Ahmad Ludin N, Vazifehkhah Ghaffari B, Sopian K, Abdul Karim N, Miyake M. An Efficient Metal-Free Hydrophilic Carbon as a Counter Electrode for Dye-Sensitized Solar Cells. *International Journal of Photoenergy*. 2016;2016:5186762.
- [296] Sathiyar G, Prakash J, Ranjan R, Singh A, Garg A, Gupta RK. Chapter 9 - Recent Progress on Hole-Transporting Materials for Perovskite-Sensitized Solar Cells. In: Bhanvase BA, Pawade VB, Dhoble SJ, Sonawane SH, Ashokkumar M, editors. *Nanomaterials for Green Energy*; Elsevier; 2018. p. 279-324.

- [297] Gao X-X, Ge Q-Q, Xue D-J, Ding J, Ma J-Y, Chen Y-X, et al. Tuning the Fermi-level of TiO₂ mesoporous layer by lanthanum doping towards efficient perovskite solar cells. *Nanoscale*. 2016;8:16881-5.
- [298] Roose B, Gödel KC, Pathak S, Sadhanala A, Baena JPC, Wilts BD, et al. Enhanced Efficiency and Stability of Perovskite Solar Cells Through Nd-Doping of Mesostructured TiO₂. *Advanced Energy Materials*. 2016;6:1501868.
- [299] Kim DH, Han GS, Seong WM, Lee J-W, Kim BJ, Park N-G, et al. Niobium Doping Effects on TiO₂ Mesoscopic Electron Transport Layer-Based Perovskite Solar Cells. *ChemSusChem*. 2015;8:2392-8.
- [300] Li X, Dai S-M, Zhu P, Deng L-L, Xie S-Y, Cui Q, et al. Efficient Perovskite Solar Cells Depending on TiO₂ Nanorod Arrays. *ACS Applied Materials & Interfaces*. 2016;8:21358-65.
- [301] Landman A, Dotan H, Shter GE, Wullenkord M, Houaijia A, Maljusch A, et al. Photoelectrochemical water splitting in separate oxygen and hydrogen cells. *Nature Materials*. 2017;16:646-51.
- [302] Chandrasekaran S, Chung JS, Kim EJ, Hur SH. Advanced Nano-Structured Materials for Photocatalytic Water Splitting. *J Electrochem Sci Technol*. 2016;7:1-12.
- [303] Rüttinger W, Dismukes GC. Synthetic Water-Oxidation Catalysts for Artificial Photosynthetic Water Oxidation. *Chemical Reviews*. 1997;97:1-24.
- [304] Grätzel M. Photoelectrochemical cells. *Nature*. 2001;414:338-44.
- [305] Fu C-F, Wu X, Yang J. Material Design for Photocatalytic Water Splitting from a Theoretical Perspective. *Advanced Materials*. 2018;30:1802106.
- [306] Yu Z, Liu H, Zhu M, Li Y, Li W. Interfacial Charge Transport in 1D TiO₂ Based Photoelectrodes for Photoelectrochemical Water Splitting. *Small*. n/a:1903378.
- [307] Niu F, Wang D, Li F, Liu Y, Shen S, Meyer TJ. Hybrid Photoelectrochemical Water Splitting Systems: From Interface Design to System Assembly. *Advanced Energy Materials*. 2020;10:1900399.
- [308] Cho IS, Chen Z, Forman AJ, Kim DR, Rao PM, Jaramillo TF, et al. Branched TiO₂ Nanorods for Photoelectrochemical Hydrogen Production. *Nano Letters*. 2011;11:4978-84.
- [309] Hernández S, Cauda V, Chiodoni A, Dallorto S, Sacco A, Hidalgo D, et al. Optimization of 1D ZnO@TiO₂ Core-Shell Nanostructures for Enhanced Photoelectrochemical Water Splitting under Solar Light Illumination. *ACS Applied Materials & Interfaces*. 2014;6:12153-67.
- [310] Chen J, Tao HB, Liu B. Unraveling the Intrinsic Structures that Influence the Transport of Charges in TiO₂ Electrodes. *Advanced Energy Materials*. 2017;7:1700886.
- [311] Wen W, Yao J-C, Gu Y-J, Sun T-L, Tian H, Zhou Q-L, et al. Balsam-pear-like rutile/anatase core/shell titania nanorod arrays for photoelectrochemical water splitting. *Nanotechnology*. 2017;28:465602.
- [312] Shaddad MN, Cardenas-Morcoso D, García-Tecedor M, Fabregat-Santiago F, Bisquert J, Al-Mayouf AM, et al. TiO₂ Nanotubes for Solar Water Splitting: Vacuum Annealing and Zr Doping Enhance Water Oxidation Kinetics. *ACS Omega*. 2019;4:16095-102.
- [313] Das C, Roy P, Yang M, Jha H, Schmuki P. Nb doped TiO₂ nanotubes for enhanced photoelectrochemical water-splitting. *Nanoscale*. 2011;3:3094-6.
- [314] Kim M, Kwon C, Eom K, Kim J, Cho E. Electrospun Nb-doped TiO₂ nanofiber support for Pt nanoparticles with high electrocatalytic activity and durability. *Scientific Reports*. 2017;7:44411.
- [315] He S, Meng Y, Wu Q, Yang J, Huang S, Li X, et al. Ta-Doped porous TiO₂ nanorod arrays by substrate-assisted synthesis: efficient photoelectrocatalysts for water oxidation. *Nanoscale*. 2018;10:19367-74.
- [316] He S, Meng Y, Cao Y, Huang S, Yang J, Tong S, et al. Hierarchical Ta-Doped TiO₂ Nanorod Arrays with Improved Charge Separation for Photoelectrochemical Water Oxidation under FTO Side Illumination. *Nanomaterials*. 2018;8:983.
- [317] Hoang S, Guo S, Mullins CB. Coincorporation of N and Ta into TiO₂ Nanowires for Visible Light Driven Photoelectrochemical Water Oxidation. *The Journal of Physical Chemistry C*. 2012;116:23283-90.
- [318] He S, Meng Y, Cao Y, Huang S, Yang J, Tong S, et al. Hierarchical Ta-Doped TiO₂ Nanorod Arrays with Improved Charge Separation for Photoelectrochemical Water Oxidation under FTO Side Illumination. *Nanomaterials*. 2018;8:983.

- [319] Xie S, Zhang Q, Liu G, Wang Y. Photocatalytic and photoelectrocatalytic reduction of CO₂ using heterogeneous catalysts with controlled nanostructures. *Chemical Communications*. 2016;52:35-59.
- [320] Navalón S, Dhakshinamoorthy A, Álvaro M, Garcia H. Photocatalytic CO₂ Reduction using Non-Titanium Metal Oxides and Sulfides. *ChemSusChem*. 2013;6:562-77.
- [321] Liu E, Kang L, Wu F, Sun T, Hu X, Yang Y, et al. Photocatalytic Reduction of CO₂ into Methanol over Ag/TiO₂ Nanocomposites Enhanced by Surface Plasmon Resonance. *Plasmonics*. 2014;9:61-70.
- [322] Habisreutinger SN, Schmidt-Mende L, Stolarczyk JK. Photocatalytic Reduction of CO₂ on TiO₂ and Other Semiconductors. *Angewandte Chemie International Edition*. 2013;52:7372-408.
- [323] Chen Z, Zhang G, Prakash J, Zheng Y, Sun S. Rational Design of Novel Catalysts with Atomic Layer Deposition for the Reduction of Carbon Dioxide. *Advanced Energy Materials*. 2019;9:1900889.
- [324] Xu F, Zhu B, Cheng B, Yu J, Xu J. 1D/2D TiO₂/MoS₂ Hybrid Nanostructures for Enhanced Photocatalytic CO₂ Reduction. *Advanced Optical Materials*. 2018;6:1800911.
- [325] Sim LC, Leong KH, Saravanan P, Ibrahim S. Rapid thermal reduced graphene oxide/Pt-TiO₂ nanotube arrays for enhanced visible-light-driven photocatalytic reduction of CO₂. *Applied Surface Science*. 2015;358:122-9.
- [326] Pan J, Wu X, Wang L, Liu G, Lu GQ, Cheng H-M. Synthesis of anatase TiO₂ rods with dominant reactive {010} facets for the photoreduction of CO₂ to CH₄ and use in dye-sensitized solar cells. *Chemical Communications*. 2011;47:8361-3.
- [327] Ye L, Mao J, Peng T, Zan L, Zhang Y. Opposite photocatalytic activity orders of low-index facets of anatase TiO₂ for liquid phase dye degradation and gaseous phase CO₂ photoreduction. *Physical Chemistry Chemical Physics*. 2014;16:15675-80.
- [328] Cheng J, Zhang M, Wu G, Wang X, Zhou J, Cen K. Photoelectrocatalytic Reduction of CO₂ into Chemicals Using Pt-Modified Reduced Graphene Oxide Combined with Pt-Modified TiO₂ Nanotubes. *Environmental Science & Technology*. 2014;48:7076-84.
- [329] Lee YY, Jung HS, Kang YT. A review: Effect of nanostructures on photocatalytic CO₂ conversion over metal oxides and compound semiconductors. *Journal of CO₂ Utilization*. 2017;20:163-77.
- [330] Shehzad N, Tahir M, Johari K, Murugesan T, Hussain M. A critical review on TiO₂ based photocatalytic CO₂ reduction system: Strategies to improve efficiency. *Journal of CO₂ Utilization*. 2018;26:98-122.
- [331] Fu J, Cao S, Yu J, Low J, Lei Y. Enhanced photocatalytic CO₂-reduction activity of electrospun mesoporous TiO₂ nanofibers by solvothermal treatment. *Dalton Transactions*. 2014;43:9158-65.
- [332] Sarkar A, Gracia-Espino E, Wågberg T, Shchukarev A, Mohl M, Rautio A-R, et al. Photocatalytic reduction of CO₂ with H₂O over modified TiO₂ nanofibers: Understanding the reduction pathway. *Nano Research*. 2016;9:1956-68.
- [333] Matějová L, Kočí K, Reli M, Čapek L, Hospodková A, Peikertová P, et al. Preparation, characterization and photocatalytic properties of cerium doped TiO₂: On the effect of Ce loading on the photocatalytic reduction of carbon dioxide. *Applied Catalysis B: Environmental*. 2014;152-153:172-83.
- [334] Tahir M, Amin NS. Advances in visible light responsive titanium oxide-based photocatalysts for CO₂ conversion to hydrocarbon fuels. *Energy Conversion and Management*. 2013;76:194-214.
- [335] Camarillo R, Rizaldos D, Jiménez C, Martínez F, Rincón J. Enhancing the photocatalytic reduction of CO₂ with undoped and Cu-doped TiO₂ nanofibers synthesized in supercritical medium. *The Journal of Supercritical Fluids*. 2019;147:70-80.
- [336] Luo D, Bi Y, Kan W, Zhang N, Hong S. Copper and cerium co-doped titanium dioxide on catalytic photo reduction of carbon dioxide with water: Experimental and theoretical studies. *Journal of Molecular Structure*. 2011;994:325-31.
- [337] vianna nogueira M, Lustosa G, Kobayakawa Y, Kogler W, Ruiz M, Monteiro Filho E, et al. Nb-Doped TiO₂ Photocatalysts Used to Reduction of CO₂ to Methanol. *Advances in Materials Science and Engineering*. 2018;2018:1-8.

- [338] Tahir B, Tahir M, Saidina Amin NA. Photocatalytic Carbon Dioxide and Methane Reduction to Fuels over La-Promoted Titanium Dioxide Nanocatalyst. *Chemical Engineering Transactions*. 2017;56.
- [339] Fu Z, Zhong Y, Yu Y, Long L, Xiao M, Han D, et al. TiO₂(2)-Doped CeO₂ Nanorod Catalyst for Direct Conversion of CO₂ and CH₃OH to Dimethyl Carbonate: Catalytic Performance and Kinetic Study. *ACS omega*. 2018;3:198-207.
- [340] Wang Y, Li B, Zhang C, Cui L, Kang S, Li X, et al. Ordered mesoporous CeO₂-TiO₂ composites: Highly efficient photocatalysts for the reduction of CO₂ with H₂O under simulated solar irradiation. *Applied Catalysis B: Environmental*. 2013;130-131:277-84.
- [341] Liu J, Liu B, Ren Y, Yuan Y, Zhao H, Yang H, et al. Hydrogenated nanotubes/nanowires assembled from TiO₂ nanoflakes with exposed {111} facets: excellent photo-catalytic CO₂ reduction activity and charge separation mechanism between (111) and $\bar{1}\bar{1}\bar{1}$ polar surfaces. *Journal of Materials Chemistry A*. 2019;7:14761-75.
- [342] Roy P, Srivastava SK. Nanostructured anode materials for lithium ion batteries. *Journal of Materials Chemistry A*. 2015;3:2454-84.
- [343] Liu B, Jia Y, Yuan C, Wang L, Gao X, Yin S, et al. Safety issues and mechanisms of lithium-ion battery cell upon mechanical abusive loading: A review. *Energy Storage Materials*. 2020;24:85-112.
- [344] Ding Y, Hu L, He D, Peng Y, Niu Y, Li Z, et al. Design of multishell microsphere of transition metal oxides/carbon composites for lithium ion battery. *Chemical Engineering Journal*. 2020;380:122489.
- [345] Gan Q, Wu B, Qin N, Chen J, Luo W, Xiao D, et al. Sandwich-like dual carbon layers coated NiO hollow spheres with superior lithium storage performances. *Electrochimica Acta*. 2020;343:136121.
- [346] Gao X, Sun X, Jiang Z, Wang Q, Gao N, Li H, et al. Introducing nanodiamond into TiO₂-based anode for improving the performance of lithium-ion batteries. *New Journal of Chemistry*. 2019;43:3907-12.
- [347] Guo H, Zhou J, Li Q, Li Y, Zong W, Zhu J, et al. Emerging Dual-Channel Transition-Metal-Oxide Quasiaerogels by Self-Embedded Templating. *Advanced Functional Materials*. 2020;30:2000024.
- [348] Wu HB, Chen JS, Hng HH, Lou XW. Nanostructured metal oxide-based materials as advanced anodes for lithium-ion batteries. *Nanoscale*. 2012;4:2526-42.
- [349] Zhang W-M, Wu X-L, Hu J-S, Guo Y-G, Wan L-J. Carbon Coated Fe₃O₄ Nanospindles as a Superior Anode Material for Lithium-Ion Batteries. *Advanced Functional Materials*. 2008;18:3941-6.
- [350] Wang S, Qu D, Jiang Y, Xiong WS, Sang HQ, He RX, et al. Three-Dimensional Branched TiO₂ Architectures in Controllable Bloom for Advanced Lithium-Ion Batteries. *ACS Appl Mater Interfaces*. 2016;8:20040-7.
- [351] Madian M, Eychmüller A, Giebel L. Current Advances in TiO₂-Based Nanostructure Electrodes for High Performance Lithium Ion Batteries. *Batteries*. 2018;4:7.
- [352] Gardecka AJ, Lübke M, Armer CF, Ning D, Reddy MV, Williams AS, et al. Nb-doped rutile titanium dioxide nanorods for lithium-ion batteries. *Solid State Sciences*. 2018;83:115-21.
- [353] Wu M, Zhang G, Wu M, Prakash J, Sun S. Rational design of multifunctional air electrodes for rechargeable Zn–Air batteries: Recent progress and future perspectives. *Energy Storage Materials*. 2019;21:253-86.
- [354] Jeong J-H, Jung D-w, Shin EW, Oh E-S. Boron-doped TiO₂ anode materials for high-rate lithium ion batteries. *Journal of Alloys and Compounds*. 2014;604:226-32.
- [355] Chattopadhyay S, Maiti S, Das I, Mahanty S, De G. Electrospun TiO₂-rGO Composite Nanofibers with Ordered Mesopores by Molecular Level Assembly: A High Performance Anode Material for Lithium-Ion Batteries. *Advanced Materials Interfaces*. 2016;3:1600761.
- [356] An Y, Zhang Z, Fei H, Xiong S, Ji B, Feng J. Ultrafine TiO₂ Confined in Porous-Nitrogen-Doped Carbon from Metal-Organic Frameworks for High-Performance Lithium Sulfur Batteries. *ACS Appl Mater Interfaces*. 2017;9:12400-7.
- [357] Xu H, Zeng M, Li J, Li F. Cr-Doped TiO₂ Core–Shell Nanospheres with Enhanced Photocatalytic Activity and Lithium Storage Capacity. *Nano*. 2016;11:1650006.

- [358] Ming H, Li X, Su L, Liu M, Jin L, Bu L, et al. One step synthesis of C&N co-doped mesoporous TiO₂ with enhanced performance in a lithium-ion battery. *RSC Adv.* 2013;3:3836-9.
- [359] Liu Y, Gao X, Hong Z, Shi W. Formation of uniform nitrogen-doped C/Ni/TiO₂ hollow spindles toward long cycle life lithium-ion batteries. *Journal of Materials Chemistry A.* 2016;4:8983-8.
- [360] Tan L, Pan L, Cao C, Wang B, Li L. Nitrogen-doped carbon coated TiO₂ nanocomposites as anode material to improve cycle life for lithium-ion batteries. *Journal of Power Sources.* 2014;253:193-200.
- [361] Park S-J, Kim Y-J, Lee H. Synthesis of carbon-coated TiO₂ nanotubes for high-power lithium-ion batteries. *Journal of Power Sources.* 2011;196:5133-7.
- [362] Tan L, Cao C, Yang H, Wang B, Li L. Nitrogen-doped carbon coated anatase TiO₂ anode material for lithium-ion batteries. *Materials Letters.* 2013;109:195-8.
- [363] Kang K-Y, Lee Y-G, Kim S, Seo SR, Kim J-C, Kim KM. Electrochemical properties of carbon-coated TiO₂ nanotubes as a lithium battery anode material. *Materials Chemistry and Physics.* 2012;137:169-76.
- [364] Goriparti S, Miele E, Prato M, Scarpellini A, Marras S, Monaco S, et al. Direct Synthesis of Carbon-Doped TiO₂-Bronze Nanowires as Anode Materials for High Performance Lithium-Ion Batteries. *ACS Appl Mater Interfaces.* 2015;7:25139-46.
- [365] Jiao S, Lian G, Jing L, Xu Z, Wang Q, Cui D, et al. Sn-Doped Rutile TiO₂ Hollow Nanocrystals with Enhanced Lithium-Ion Batteries Performance. *ACS Omega.* 2018;3:1329-37.
- [366] Kashale AA, Rasal AS, Kamble GP, Ingole VH, Dwivedi PK, Rajoba SJ, et al. Biosynthesized Co-doped TiO₂ nanoparticles based anode for lithium-ion battery application and investigating the influence of dopant concentrations on its performance. *Composites Part B: Engineering.* 2019;167:44-50.
- [367] Wang Y, Smarsly BM, Djerdj I. Niobium Doped TiO₂ with Mesoporosity and Its Application for Lithium Insertion. *Chemistry of Materials.* 2010;22:6624-31.
- [368] Bi Z, Paranthaman MP, Guo B, Unocic RR, Meyer Iii HM, Bridges CA, et al. High performance Cr, N-codoped mesoporous TiO₂ microspheres for lithium-ion batteries. *J Mater Chem A.* 2014;2:1818-24.
- [369] Zhang W, Gong Y, Mellott NP, Liu D, Li J. Synthesis of nickel doped anatase titanate as high performance anode materials for lithium ion batteries. *Journal of Power Sources.* 2015;276:39-45.
- [370] Zhang W, Zhou W, Wright JH, Kim YN, Liu D, Xiao X. Mn-doped TiO₂ nanosheet-based spheres as anode materials for lithium-ion batteries with high performance at elevated temperatures. *ACS Appl Mater Interfaces.* 2014;6:7292-300.
- [371] Thi TV, Rai AK, Gim J, Kim S, Kim J. Effect of Mo⁶⁺ doping on electrochemical performance of anatase TiO₂ as a high performance anode material for secondary lithium-ion batteries. *Journal of Alloys and Compounds.* 2014;598:16-22.
- [372] Zhou H, Lv P, Xia X, Zhang J, Yu J, Pang Z, et al. MoS₂ nanograins doped TiO₂ nanofibers as intensified anodes for lithium ion batteries. *Materials Letters.* 2018;218:47-51.
- [373] Bai X, Li T, Qi Y-X, Wang Y-X, Yin L-W, Li H, et al. One-step fabricating nitrogen-doped TiO₂ nanoparticles coated with carbon to achieve excellent high-rate lithium storage performance. *Electrochimica Acta.* 2016;187:389-96.
- [374] Hasegawa G, Sato T, Kanamori K, Nakanishi K, Abe T. Synthesis and electrochemical performance of hierarchically porous N-doped TiO₂ for Li-ion batteries. *New Journal of Chemistry.* 2014;38:1380.
- [375] Jiao W, Li N, Wang L, Wen L, Li F, Liu G, et al. High-rate lithium storage of anatase TiO₂ crystals doped with both nitrogen and sulfur. *Chem Commun (Camb).* 2013;49:3461-3.
- [376] Li Y, Wang Z, Lv X-J. N-doped TiO₂ nanotubes/N-doped graphene nanosheets composites as high performance anode materials in lithium-ion battery. *Journal of Materials Chemistry A.* 2014;2:15473.
- [377] Ren M, Xu H, Li F, Liu W, Gao C, Su L, et al. Sugarapple-like N-doped TiO₂@carbon core-shell spheres as high-rate and long-life anode materials for lithium-ion batteries. *Journal of Power Sources.* 2017;353:237-44.
- [378] Li Y, Wang Z, Zhao D, Zhang L. Gd doped single-crystalline Li₄Ti₅O₁₂/TiO₂ nanosheets composites as superior anode material in lithium ion batteries. *Electrochimica Acta.* 2015;182:368-75.

- [379] Abhilash KP, Christopher Selvin P, Nalini B, Jose R, Vijayaraghavan R, Chowdari BVR, et al. Investigations on the influence of Sm³⁺ ion on the nano TiO₂ matrix as the anode material for lithium ion batteries. *Journal of Alloys and Compounds*. 2017;710:205-15.
- [380] Zhang J, Zhang J, Ren H, Yu L, Wu Z, Zhang Z. High rate capability and long cycle stability of TiO₂-δ-La composite nanotubes as anode material for lithium ion batteries. *Journal of Alloys and Compounds*. 2014;609:178-84.
- [381] Zhu M, Huang Y, Huang Y, Meng W, Gong Q, Li G, et al. An electrochromic supercapacitor and its hybrid derivatives: quantifiably determining their electrical energy storage by an optical measurement. *Journal of Materials Chemistry A*. 2015;3:21321-7.
- [382] Liu N, Ma W, Tao J, Zhang X, Su J, Li L, et al. Cable-type supercapacitors of three-dimensional cotton thread based multi-grade nanostructures for wearable energy storage. *Adv Mater*. 2013;25:4925-31.
- [383] Lu X, Wang G, Zhai T, Yu M, Gan J, Tong Y, et al. Hydrogenated TiO₂ nanotube arrays for supercapacitors. *Nano Lett*. 2012;12:1690-6.
- [384] Wu L, Li C, Song Y, Zhang K, Zhang J, Li P, et al. What happens if anodic TiO₂ nanotubes are soaked in H₃PO₄ at room temperature for a long time? *Electrochemistry Communications*. 2019;105:106501.
- [385] Lv Y, Du W, Ren Y, Cai Z, Yu K, Zhang C, et al. An integrated electrochromic supercapacitor based on nanostructured Er-containing titania using an Er(III)-doped polyoxotitanate cage. *Inorganic Chemistry Frontiers*. 2016;3:1119-23.
- [386] Reszczyńska J, Grzyb T, Sobczak JW, Lisowski W, Gazda M, Ohtani B, et al. Lanthanide co-doped TiO₂: the effect of metal type and amount on surface properties and photocatalytic activity. *Applied surface science*. 2014;307:333-45.
- [387] Obregón S, Kubacka A, Fernández-García M, Colón G. High-performance Er³⁺-TiO₂ system: Dual up-conversion and electronic role of the lanthanide. *Journal of catalysis*. 2013;299:298-306.
- [388] Mao X, Yan B, Wang J, Shen J. Up-conversion fluorescence characteristics and mechanism of Er³⁺-doped TiO₂ thin films. *Vacuum*. 2014;102:38-42.
- [389] Salhi R, Deschanvres J-L. Efficient green and red up-conversion emissions in Er/Yb co-doped TiO₂ nanopowders prepared by hydrothermal-assisted sol-gel process. *Journal of Luminescence*. 2016;176:250-9.
- [390] Zhang Z, Qin J, Shi W, Liu Y, Zhang Y, Liu Y, et al. Enhanced power conversion efficiency of perovskite solar cells with an up-conversion material of Er³⁺-Yb³⁺-Li⁺ tri-doped TiO₂. *Nanoscale research letters*. 2018;13:1-8.
- [391] Liu W, Zhang H, Wang H-g, Zhang M, Guo M. Titanium mesh supported TiO₂ nanowire arrays/upconversion luminescence Er³⁺-Yb³⁺ codoped TiO₂ nanoparticles novel composites for flexible dye-sensitized solar cells. *Applied Surface Science*. 2017;422:304-15.
- [392] Huang H, Liang X, Wang Z, Wang P, Zheng Z, Liu Y, et al. Bi₂₀Ti₃₂O₃₂ Nanoparticles Doped with Yb³⁺ and Er³⁺ as UV, Visible, and Near-Infrared Responsive Photocatalysts. *ACS Applied Nano Materials*. 2019;2:5381-8.
- [393] Navas J, Sánchez-Coronilla A, Aguilar T, Desireé M, Hernández NC, Alcántara R, et al. Thermo-selective Tm^xTi_{1-x}O_{2-x/2} nanoparticles: from Tm-doped anatase TiO₂ to a rutile/pyrochlore Tm₂Ti₂O₇ mixture. An experimental and theoretical study with a photocatalytic application. *Nanoscale*. 2014;6:12740-57.
- [394] Desiré M, Navas J, Aguilar T, Sánchez-Coronilla A, Fernández-Lorenzo C, Alcántara R, et al. Tm-doped TiO₂ and Tm₂Ti₂O₇ pyrochlore nanoparticles: enhancing the photocatalytic activity of rutile with a pyrochlore phase. *Beilstein J Nanotechnol*. 2015;6:605-16.
- [395] Qin W, Zhang D, Zhao D, Wang L, Zheng K. Near-infrared photocatalysis based on YF₃: Yb³⁺, Tm³⁺/TiO₂ core/shell nanoparticles. *Chemical communications*. 2010;46:2304-6.
- [396] Zhang H, Wang T, Yang Z, Liu Y, Zhao J, Li Q, et al. Synthesis and photocatalytic activity of δ-doped hexagonal NaYF₄: Yb, Tm@TiO₂/RGO nanocrystals. *CrystEngComm*. 2019;21:1019-25.

- [397] Jarosz-Duda A, O'Callaghan P, Kuncewicz J, Łabuz P, Macyk W. Enhanced UV Light Emission by Core-Shell Upconverting Particles Powering up TiO₂ Photocatalysis in Near-Infrared Light. *Catalysts*. 2020;10:232.
- [398] Wang L, Xia C, Yang T, Wang H, Liu N, Liang C. Spindle-like porous N-doped TiO₂ encapsulated (Ca, Y) F₂: Yb³⁺, Tm³⁺ as the efficient photocatalyst near-infrared range. *Nanotechnology*. 2019;31:025601.
- [399] Parnicka P, Grzyb T, Mikolajczyk A, Wang K, Kowalska E, Steinfeldt N, et al. Experimental and theoretical investigations of the influence of carbon on a Ho³⁺-TiO₂ photocatalyst with Vis response. *Journal of colloid and interface science*. 2019;549:212-24.
- [400] Xu X, Sun Y, Zhang Q, Cai H, Li Q, Zhou S. Synthesis and photocatalytic activity of plasmon-enhanced core-shell upconversion luminescent photocatalytic Ag@ SiO₂@ YF₃: Ho³⁺@ TiO₂ nanocomposites. *Optical Materials*. 2019;94:444-53.
- [401] Parnicka P, Mazierski P, Grzyb T, Wei Z, Kowalska E, Ohtani B, et al. Preparation and photocatalytic activity of Nd-modified TiO₂ photocatalysts: Insight into the excitation mechanism under visible light. *Journal of catalysis*. 2017;353:211-22.
- [402] Dihingia P, Rai S. Synthesis of TiO₂ nanoparticles and spectroscopic upconversion luminescence of Nd³⁺-doped TiO₂-SiO₂ composite glass. *Journal of luminescence*. 2012;132:1243-51.
- [403] Lakshminarayana G, Yang H, Teng Y, Qiu J. Spectral analysis of Pr³⁺-, Sm³⁺-and Dy³⁺-doped transparent GeO₂-BaO-TiO₂ glass ceramics. *Journal of luminescence*. 2009;129:59-68.
- [404] Kaur N, Singh M, Moumen A, Duina G, Comini E. 1D Titanium Dioxide: Achievements in Chemical Sensing. *Materials*. 2020;13:2974.
- [405] Liu H, Ding D, Ning C, Li Z. Wide-range hydrogen sensing with Nb-doped TiO₂nanotubes. *Nanotechnology*. 2011;23:015502.
- [406] Tshabalala ZP, Shingange K, Dhonge BP, Ntwaeaborwa OM, Mhlongo GH, Motaung DE. Fabrication of ultra-high sensitive and selective CH₄ room temperature gas sensing of TiO₂ nanorods: Detailed study on the annealing temperature. *Sensors and Actuators B: Chemical*. 2017;238:402-19.
- [407] Li Z, Yao Z, Haidry AA, Plecenik T, Xie L, Sun L, et al. Resistive-type hydrogen gas sensor based on TiO₂: A review. *International Journal of Hydrogen Energy*. 2018;43:21114-32.
- [408] Zarifi MH, Farsinezhad S, Abdolrazzaghi M, Daneshmand M, Shankar K. Selective microwave sensors exploiting the interaction of analytes with trap states in TiO₂ nanotube arrays. *Nanoscale*. 2016;8:7466-73.
- [409] Tshabalala ZP, Motaung DE, Swart HC. Structural transformation and enhanced gas sensing characteristics of TiO₂ nanostructures induced by annealing. *Physica B: Condensed Matter*. 2018;535:227-31.
- [410] Mor GK, Carvalho MA, Varghese OK, Pishko MV, Grimes CA. A room-temperature TiO₂-nanotube hydrogen sensor able to self-clean photoactively from environmental contamination. *Journal of Materials Research*. 2011;19:628-34.
- [411] Comini E. Metal oxide nanowire chemical sensors: innovation and quality of life. *Materials Today*. 2016;19:559-67.
- [412] Kaur N, Singh M, Comini E. One-Dimensional Nanostructured Oxide Chemoresistive Sensors. *Langmuir*. 2020;36:6326-44.
- [413] Galstyan V, Comini E, Faglia G, Sberveglieri G. TiO₂ Nanotubes: Recent Advances in Synthesis and Gas Sensing Properties. *Sensors*. 2013;13:14813-38.
- [414] Şennik E, Alev O, Öztürk ZZ. The effect of Pd on the H₂ and VOC sensing properties of TiO₂ nanorods. *Sensors and Actuators B: Chemical*. 2016;229:692-700.
- [415] Zhou M, Liu Y, Wu B, Zhang X. Different crystalline phases of aligned TiO₂ nanowires and their ethanol gas sensing properties. *Physica E: Low-dimensional Systems and Nanostructures*. 2019;114:113601.

- [416] Wang H, Sun Q, Yao Y, Li Y, Wang J, Chen L. A micro sensor based on TiO₂ nanorod arrays for the detection of oxygen at room temperature. *Ceramics International*. 2016;42:8565-71.
- [417] Tong X, Shen W, Chen X. Enhanced H₂S sensing performance of cobalt doped free-standing TiO₂ nanotube array film and theoretical simulation based on density functional theory. *Applied Surface Science*. 2019;469:414-22.
- [418] Li G, Zhang X, Lu H, Yan C, Chen K, Lu H, et al. Ethanol sensing properties and reduced sensor resistance using porous Nb₂O₅-TiO₂ n-n junction nanofibers. *Sensors and Actuators B: Chemical*. 2019;283:602-12.
- [419] Ren S, Liu W. One-step photochemical deposition of PdAu alloyed nanoparticles on TiO₂ nanowires for ultra-sensitive H₂ detection. *Journal of Materials Chemistry A*. 2016;4:2236-45.
- [420] Gopala Krishnan V, Elango P, Ganesan V. Surface characterization and gas sensing performance of yttrium doped TiO₂ nanofilms prepared by automated nebulizer spray pyrolysis (ANSP). *Journal of Materials Science: Materials in Electronics*. 2018;29:392-401.
- [421] Nithya N, Bhoopathi G, Magesh G, Balasundaram ON. Synthesis and characterization of yttrium doped titania nanoparticles for gas sensing activity. *Materials Science in Semiconductor Processing*. 2019;99:14-22.
- [422] Seeley Z, Choi YJ, Bose S. Citrate–nitrate synthesis of nano-structured titanium dioxide ceramics for gas sensors. *Sensors and Actuators B: Chemical*. 2009;140:98-103.
- [423] Jing Z, Ling B, Yu Y, Qi W, Zhang S. Preparation and gas sensing activity of La and Y co-doped titania nanoparticles. *Journal of Sol-Gel Science and Technology*. 2015;73:112-7.
- [424] Eltermann M, Utt K, Lange S, Jaaniso R. Sm³⁺ doped TiO₂ as optical oxygen sensor material. *Optical Materials*. 2016;51:24-30.
- [425] Kiisk V, Jaaniso R. Chapter Nine - Rare earth–doped oxide materials for photoluminescence-based gas sensors. In: Jaaniso R, Tan OK, editors. *Semiconductor Gas Sensors (Second Edition)*: Woodhead Publishing; 2020. p. 271-305.
- [426] Miranda-Muñoz JM, Geng D, Calvo ME, Lozano G, Míguez H. Flexible nanophosphor films doped with Mie resonators for enhanced out-coupling of the emission. *Journal of Materials Chemistry C*. 2019;7:267-74.
- [427] Li J-G, Wang X, Watanabe K, Ishigaki T. Phase Structure and Luminescence Properties of Eu³⁺-Doped TiO₂ Nanocrystals Synthesized by Ar/O₂ Radio Frequency Thermal Plasma Oxidation of Liquid Precursor Mists. *The Journal of Physical Chemistry B*. 2006;110:1121-7.
- [428] Xu X, Wen S, Mao Q, Feng Y. N-Anchoring in Rare Earth-Doped Amorphous TiO₂ as a Route to Broadband Down-Conversion Phosphor. *ACS Applied Materials & Interfaces*. 2018;10:39238-44.
- [429] Łysień M, Fiączyk K, Tomala R, Granek F, Stręk W. Synthesis and luminescence of Eu³⁺ doped nanocrystalline TiO₂ spheres. *Journal of Rare Earths*. 2019;37:1121-5.
- [430] Kunti AK, Sharma SK. Structural and spectral properties of red light emitting Eu³⁺ activated TiO₂ nanophosphor for white LED application. *Ceramics International*. 2017;43:9838-45.
- [431] Zhu P, Zhu H, Qin W, Dantas BH, Sun W, Tan C-K, et al. Narrow-linewidth red-emission Eu³⁺-doped TiO₂ spheres for light-emitting diodes. *Journal of Applied Physics*. 2016;119:124305.
- [432] Chang M, Song Y, Zhang H, Sheng Y, Zheng K, Zhou X, et al. Hydrothermal assisted sol–gel synthesis and multisite luminescent properties of anatase TiO₂:Eu³⁺ nanorods. *RSC Advances*. 2015;5:59314-9.
- [433] Su B, Wang S, Yang W, Wang Y, Huang L, Popat KC, et al. Synthesis of Eu-modified luminescent Titania nanotube arrays and effect of voltage on morphological, structural and spectroscopic properties. *Materials Science in Semiconductor Processing*. 2020;113:105026.
- [434] Sandoval S, Yang J, Alfaro JG, Liberman A, Makale M, Chiang CE, et al. Europium-Doped TiO₂ Hollow Nanoshells: Two-Photon Imaging of Cell Binding. *Chemistry of Materials*. 2012;24:4222-30.
- [435] Tachikawa T, Majima T. Single-Molecule Fluorescence Imaging of TiO₂ Photocatalytic Reactions. *Langmuir*. 2009;25:7791-802.

- [436] Drew K, Girishkumar G, Vinodgopal K, Kamat PV. Boosting Fuel Cell Performance with a Semiconductor Photocatalyst: TiO₂/Pt–Ru Hybrid Catalyst for Methanol Oxidation. *The Journal of Physical Chemistry B*. 2005;109:11851-7.
- [437] Choi H, Kim J, Lee G, Tak Y. Nb-doped TiO₂ support with enhanced durability as a cathode for polymer electrolyte membrane fuel cells. *Nanotechnology*. 2019;31:03LT1.
- [438] Zhang B, Li B, Gao S, Li Y, Cao R, Cheng J, et al. Y-doped TiO₂ coating with superior bioactivity and antibacterial property prepared via plasma electrolytic oxidation. *Materials & Design*. 2020;192:108758.
- [439] Gunpath UF, Le H, Lawton K, Besinis A, Tredwin C, Handy RD. Antibacterial properties of silver nanoparticles grown in situ and anchored to titanium dioxide nanotubes on titanium implant against *Staphylococcus aureus*. *Nanotoxicology*. 2020;14:97-110.
- [440] Kim S-G, Dhandole LK, Seo Y-S, Chung H-S, Chae W-S, Cho M, et al. Active composite photocatalyst synthesized from inactive Rh & Sb doped TiO₂ nanorods: Enhanced degradation of organic pollutants & antibacterial activity under visible light irradiation. *Applied Catalysis A: General*. 2018;564:43-55.
- [441] Zhang X, Zhang G, Chai M, Yao X, Chen W, Chu PK. Synergistic antibacterial activity of physical-chemical multi-mechanism by TiO₂ nanorod arrays for safe biofilm eradication on implant. *Bioactive Materials*. 2021;6:12-25.
- [442] Yousefi M, Gholamian F, Ghanbari D, Salavati-Niasari M. Polymeric nanocomposite materials: Preparation and characterization of star-shaped PbS nanocrystals and their influence on the thermal stability of acrylonitrile–butadiene–styrene (ABS) copolymer. *Polyhedron*. 2011;30:1055-60.
- [443] Prakash J, Tripathi A, Khan SA, Pivin JC, Singh F, Tripathi J, et al. Ion beam induced interface mixing of Ni on PTFE bilayer system studied by quadrupole mass analysis and electron spectroscopy for chemical analysis. *Vacuum*. 2010;84:1275-9.

Table 1: List of various RE doped 1D TiO₂ NSs including their synthesis methods, improved important properties and applications in various fields of energy and environments.

RE Dopant	1D TiO₂ NSs	Synthesis methods of RE doping in 1D TiO₂ NSs	Improved optoelectronic and structural properties due to RE doping	Mechanism of action/ application	Ref.
La ³⁺	NTs, NRs	Hydrothermal Method	La doping decreases the crystallite size and increases the surface defects.	Reduced recombination rate of electron hole pair and Enhanced Photodegradation of Formic acid was seen.	[122]
La ³⁺	NRs	Hydrothermal Method	Charge carrier density and optoelectronic properties were enhanced.	Increased efficiency of DSSCs upto 21% as compared to undoped.	[126]
Ce ³⁺	NTs	Hydrothermal Method	Highly oriented NTs were formed. With absorption upto 600nm.	Ce-TiO ₂ NTs show higher photodegradation of MB dye and also be useful in waste water treatment.	[129]
Ce ³⁺	NTs	Hydrothermal Method	Highly oriented and show visible light absorption.	Glyphosate photodegradation rate was enhanced due to reduced charge carrier recombination.	[130]
Eu ³⁺	NRs	Hydrothermal Method	Acidic and alkaline conditions have great effect on morphologies.	Luminiscent properties were dependent on morphologies NRs show highest luminescent property.	[134]
La ³⁺ , Sm ³⁺ , Eu ³⁺ and Er ³⁺	NRs	Hydrothermal Method, Electrostatic incorporation	Enhanced photo catalytic activity	Eu-TiO ₂ NRs are the best for degrading MO, Lignin can also be photo degraded effectively at room temperature	[85]
La ³⁺	NTs	Sol Gel and Hydrothermal Method	Absorption spectra shows a shift to higher wavelength	Higher Photo activity for MO degradation	[61]
Eu ³⁺ and Ce ³⁺	NWs	Hydrothermal Method	Single Crystallinity, NWs growth along [001] direction	Decompose organic toluidine blue-O dye under UV irradiation	[135]
La ³⁺ , Ce ³⁺ and Nd ³⁺	NFs	Electrospinning	Inhibits the TiO ₂ Phase Transformation	Rhodamine 6G (R6G) dye degradation under UV light Nd ³⁺ -doped TiO ₂ show highest photoactivity	[110]
La ³⁺ , Eu ³⁺ and Er ³⁺	NFs	Electrospinning	Provide Thermal stability to phase transformation	Enhanced Luminescent property	[141]
Ce ³⁺	NRs	Hydrothermal Method	Diameter of NRs increased with increasing concentration of dopant. Also morphology	Higher amount of dye adsorbed on NRs surface show higher DSSC application.	[39]

			changes from NRs to NTs by etching the sample for 4hr.		
Nb ³⁺	NRs	Microwave assisted method	Surface states and interface distance of Nb doped NRs was modified.	Energy conversion efficiency of NRs DSSSc was enhanced by 70% which was due to enhanced electron injection and reduction in electron hole pair recombination.	[294]
Er ³⁺	NRs	Hydrothermal Method	Er ³⁺ doping enhances the electron density. And also show broad absorption in Near IR region.	Enhancement in photocurrent density and power conversion efficiency was observed because of absorption of NIR.	[149]
Er ³⁺ and Yb ³⁺ co-doped	NRs	Hydrothermal Method	Fabrication of NRs show faster electron transfer and reduced recombination of charge carriers.	Fabricated solar cells show upto 7% high power conversion efficiency.	[180]
Er ³⁺ -Yb ³⁺ -Li ⁺ tri-doped	NRs	Hydrothermal Method	The tri doped TiO ₂ NRs show enhanced up conversion emission.	The power conversion efficiency was increased upto 19% ,	[181]
Yb ³⁺ , Er ³⁺ co-doped	Inverted pyramidal NRs	Hydrothermal Method	Inverted pyramidal morphology enhanced the light utilization. And exhibit reduced electron recombination.	Increased the sunlight utilization because of light absorption in near IR region.	[94]
Mg ²⁺ and Er ³⁺ co-doped	NRs	Hydrothermal Method	Increases the charge injection efficiency and enhanced open circuit voltage of solar cells. Also absorb light in near IR region.	Enhancement in power conversion efficiency by 17% and utilization of sunlight was observed.	[77]
Gd ³⁺	NRs	Hydrothermal Method	Highly oriented NRs with high optical and electronic property were formed.	Gd doped NRs show reduced charge carrier recombination and optimum photoconversion efficiency of 0.64%.	[89]
La ³⁺	NTs	Ion exchange Method	NTs Morphology retained during dehydration process.	TiO ₂ - δ -La composite nanotubes show high electrochemical potential as anode in Li ion Battery.	[380]
Eu ³⁺	NRs	Hydrothermal Method	Spindal shape NRs was prepared.	Luminescent decay show multiple sites of dopant were present in crystal lattice.	[432]
Eu ³⁺	NTs	Anodization Method	NTs diameter decreases with anodizing voltage and thickness increases.	NTs with high dopant concentration an large diameter show wide and gap and strong PL due to which it can be used as potential material for biosensor and photocatalytic applications.	[433]

La ³⁺	NTs	Hydrothermal Method	Doped NTs have large surface area.	Pd deposited La doped NTs show enhanced photoactivity against propylene removal.	[273]
La ³⁺	NFs	Electrospinning	Doped NFs show inhibition in phase transfer.	La doped NFs show enhanced photodegradation against MB dye.	[274]
Dy ³⁺	NBs	Hydrothermal Method	Dopant concentration affects the morphology and absorption spectra.	Dy/TNBs show enhanced activity in UV light. Degradation efficiency of MB Increased.	[162]
Nd ³⁺	NRs	Solvothermal Method	Doped NRs show reduction in recombination of charge carriers.	Incident-photon-to-current conversion efficiency (IPCE) got enhanced and absorb more of visible light.	[93]
La ³⁺	NRs	Hydrothermal Method	After doping expansion along one direction was observed.	La doped NRs were good material for nonlinear optical properties.	[128]
Eu ³⁺	NFs	Electrospinning	Randomly oriented doped NFs show red shift in absorption spectra.	Show strong luminescence and stable thermal behavior.	[136]
Eu ³⁺	NTs	Hydrothermal Method	Doped NTs were formed by rolling up of sheet.	Enhanced PL intensity which increase as concentration of dopant increases.	[137]
Eu ³⁺	NFs	Electrospinning	NFs with uniform size and diameter were formed.	NFs composed of Ti ⁴⁺ and Eu ³⁺ species. Reduction in Ti ⁴⁺ , decreased as the dopant concentration increases.	[138]
Eu ³⁺	NTs	Template Assisted Method	Highly oriented NTs with uniform size show Red emission.	TiO ₂ :Eu ³⁺ NTs show red emission at 612 nm due to the 5D ₀ →7F ₂ transition	[140]
Eu ³⁺	NBs	Hydrothermal Method	Crystallinity, morphology and PL of TiO ₂ :Eu ³⁺ -nanobelts vary with the annealing temperature.	At 500°C annealing Temperature the doped NBs show Red emission PL spectra.	[96]
Er ³⁺	NFs	Electrospinning	As annealing temperature increases then TiO ₂ phase changes from anatase to rutile.	Strong PL emission was seen in doped NFs. Because of Green emission it act as potential material in Nanodevices.	[145]

Er ³⁺	NRs	Electrospinning	Red shift in absorption spectra was seen due to doping.	Because of Transition of 4f electrons of Er ³⁺ high degradation rate of MB was observed.	[146]
Er ³⁺	NFs	Electrospinning	Er ³⁺ doped TiO ₂ NFs morphology depend upon the collector speed and the flow rate.	Er ³⁺ -TiO ₂ nanofibers absorb light in visible region because doping decreases the band gap and shift absorption to higher wavelength.	[148]
Gd ³⁺	NTs	Hydrothermal Method	Doping shift the absorption to visible light.	Rhodamine B degradation was increased and also photocatalytic efficiency was increased by 1.78 times.	[150]
Gd ³⁺	NTs	Anodization Method	Growth direction grown along the (101) direction of NTs show enhanced photactivity.	Hydrophilic and photocatalytic activity of the TiO ₂ NTs got enhanced and show higher photodegradation rate of MO.	[218]
Sm ³⁺	NTs	Chemical Processing	Doped TNT show enhancement in fluorescence spectra.	UV light emission was seen due to energy transfer from band-to-band excitation of TiO ₂ to the Sm ³⁺ ion.	[153]
Pr ³⁺	NRs (Biphasic)	Hydrothermal Method	Uniform well aligned NRs show high absorption and reduce the electron hole pair recombination.	NRs grown on activated carbon fibers show visible light absorption and it is reusable and have high photodegradation rate.	[156]
Yb ³⁺	NFs	Solution Method	Yb-TiO ₂ NRs and ACFs enhance toluene adsorption.	Increased the quantum efficiency and photo degradation of Toluene.	[159]
Dy ³⁺	NTs	Anodic oxidation method	Dy doped NTs have high stability and activity.	Dy doped TNTs increased photodegradation of MO dye upto 72%.	[161]
Ho ³⁺	NWs	Hydrothermal Method	Ho doping inhibits the growth of crystallite and phase transformation.	Small size, large surface area and charge imbalance of Ho/TiO ₂ NWs increased the photocatalytic activity.	[164]
Er ³⁺	NTs	Ion doping Method	Er doped TNTs show absorption of light of IR region.	Photo-degradation rate of the Er ³⁺ TNTs of MB increased upto 95.2%.	[172]
Ce ³⁺	NTs	Anodic Oxidation Method	Ag-Ce/TiO ₂ NTs show high visible light absorption and reduced electron hole pair recombination.	Dispersed Ag NPs enhance visible light absorption. This composite show water splitting under both UV and visible light irradiation.	[224]

La ³⁺	NTs	Anodization Method	Highly ordered La doped TNTs show red shift in absorption spectra and also promote phase transformation.	La/TNTs show enhanced photoconversion efficiency. And show enhanced photo degradation of p-nitrophenol.	[225]
Eu ³⁺	NFs	Electrospinning	Highly oriented NFs were formed.	PL spectra show enhanced emission due to intraband 4f transitions.	[243]
Er-, Yb-, Ho-, Tb-, Gd-, Pr	NTs	Anodic oxidation Method	Band gap of doped sample decreased due to formation of new states below the CB.	Ho/TNTs show best photodegradation of Toluene due to formation of ROS.	[97]
Eu ³⁺ and N codoped	NTs	Hydrothermal Method	Codoped TNTs show high activity due to synergetic effect of Eu and N.	Real textile dye water was treated with 70% efficiency.	[179]
La ³⁺ and Co	NWs	Solvothermal Method	La doping reduces the band gap and electron hole pair recombination.	Enhanced conductivity and electrical properties make it efficient semiconductor to be used in nanodevices.	[181]
Eu ³⁺	NFs	Electrospinning	High crystallinity anatase TiO ₂ NFs were formed.	Magnetic properties show ordered structure, ferromagnetic property first increases then decreases as temperature rises.	[239]
Ce and N doped	1D photonic crystal	Sol Gel	Crystallite size decreases and morphology got enhanced with doping.	Red shift was observed with doping and also vivid color were also obtained with Ce doping.	[84]